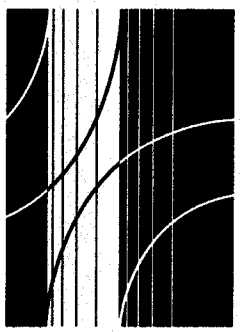

Joint Transportation Research Program

JTRP

FHWA/IN/JTRP-2000/22

Final Report

SEISMIC DESIGN OF DEEP FOUNDATIONS

Antonio Bobet
Rodrigo Salgado
Dimitrios Loukidis

September 2001

Indiana Department of Transportation

Purdue University

Final Report

SEISMIC DESIGN OF DEEP FOUNDATIONS

FHWA/IN/JTRP-2000/22

by

Antonio Bobet
Assistant Professor

Rodrigo Salgado
Associate Professor

Dimitrios Loukidis
Graduate Research Assistant

Purdue University
School of Civil Engineering

Joint Transportation Research Program
Project No. C-36-36GG
File No. 6-14-33

Prepared in Cooperation with the
Indiana Department of Transportation and the
U.S. Department of Transportation
Federal Highway Administration

Purdue University
West Lafayette, Indiana 47907
September 2001

TECHNICAL REPORT STANDARD TITLE PAGE

1. Report No.	2. Government Accession No.	3. Recipient's Catalog No.
FHWA/IN/JTRP-2000/22		

4. Title and Subtitle	5. Report Date
Seismic Design of Deep Foundations	September 2001
	6. Performing Organization Code

7. Author(s)	8. Performing Organization Report No.
Antonio Bobet, Rodrigo Salgado, and Dimitri Loukidis	FHWA/IN/JTRP-2000/22

9. Performing Organization Name and Address	10. Work Unit No.
Joint Transportation Research Program 1284 Civil Engineering Building Purdue University West Lafayette, Indiana 47907-1284	
	11. Contract or Grant No. SPR-2410

12. Sponsoring Agency Name and Address	13. Type of Report and Period Covered
Indiana Department of Transportation State Office Building 100 North Senate Avenue Indianapolis, IN 46204	Final Report
	14. Sponsoring Agency Code

15. Supplementary Notes

Prepared in cooperation with the Indiana Department of Transportation and Federal Highway Administration.

16. Abstract

Detailed investigations of pile foundations affected by earthquakes around the world since the 1960's indicate that pile foundations are susceptible to damage to such a degree that the serviceability and integrity of the superstructure may be affected. Although numerous cases of seismically damaged piles are reported, the detailed mechanisms causing the damage are not yet fully understood. As a consequence, an effective seismic design of pile foundations has not been yet established in practice.

Many road bridge structures supported on piles exist in southern Indiana. This is a region where the risk of occurrence of a dangerous earthquake is high due to its proximity to two major seismic sources: (1) the New Madrid Seismic Zone (NMSZ); and (2) the Wabash Valley Fault System (WVFS). The present study is a first step towards the assessment of potential earthquake-induced damage to pile foundations in southern Indiana. Credible earthquake magnitudes for each of the two potential seismic sources, NMSZ and WVFS, are assessed for a return period of 1000 years. SHAKE analyses are performed at nine selected sites in southwestern Indiana to estimate the potential of ground shaking and liquefaction susceptibility. The soil profile and soil properties at each site are obtained from the archives of the Indiana Department of Transportation. The amplitude of the rock outcrop motion is estimated using attenuation relationships appropriate to the region, and estimated values are compared with predictions from USGS. SHAKE analyses are performed for two earthquake scenarios: (1) a NMSZ earthquake; and (2) a WVFS earthquake. Two sets of input motions are considered for each scenario. The liquefaction potential at those nine sites is assessed based on the Seed et al. (1975) method.

Data from a total of 59 real cases of earthquake-induced damage to piles have been gathered through an extensive literature survey. The collected and compiled data have been used to identify the causes and types of pile damage, and the severity of damage. Based on the survey, damage is usually located near the pile head, at the interfaces between soft and stiff layers, and between liquefiable and non-liquefiable layers. Large inertial loads from the superstructure can cause crushing of the head of concrete piles. Imposed deformations due to the response of the surrounding soil can produce small to large cracks on concrete piles depending on the soil profile. In contrast, large inertial loads, liquefaction and lateral spreading can cause wide cracks. Few cases of steel piles are found in the literature. Steel casing seems to improve the performance of concrete piles. Numerical simulations of a concrete pile at a selected road bridge site with and without steel casing are used to investigate the effect of steel casing on the performance of concrete piles.

Results from this work suggest that major credible seismic events can generate accelerations high enough to produce damage to concrete piles in southern Indiana. The potential of liquefaction and lateral spreading increase the likelihood of damage in both concrete and steel piles; this may pose a special risk to those bridges crossing the Wabash and Ohio rivers. However, further examination and analysis is required for existing bridge structures, as well as for future bridges. Existing structures may be retrofitted by placing a steel jacket on the upper portion of the piles or by installing additional steel encased concrete piles, or large diameter concrete piles.

17. Key Words	18. Distribution Statement
Pile foundation, peak ground acceleration, liquefaction, lateral spreading, pile damage, steel casing.	No restrictions. This document is available to the public through the National Technical Information Service, Springfield, VA 22161

19. Security Classif. (of this report)	20. Security Classif. (of this page)	21. No. of Pages	22. Price
Unclassified	Unclassified	99	

Form DOT F 1700.7 (8-69)

TABLE OF CONTENTS

LIST OF TABLES

LIST OF FIGURES

CHAPTER 1: IMPLEMENTATION REPORT

Many road bridges in Southern Indiana are supported on pile foundations. Most of the bridges are located on rivers and valleys where recent thick loose alluvial deposits can be found. Piles are used to safely transmit the loads from the piers and abutments to stiffer soil layers at depth. Southern Indiana is close to the New Madrid seismic zone and the Wabash Valley fault system, both active seismic sources capable of generating large earthquakes. Ground shaking produced by these events is capable to produce damage to pile foundations, as observed after recent earthquakes in Japan and in other parts of the world. These observations suggest that pile foundations are highly susceptible to significant damage from seismically induced loads. Damage to the deep foundation may affect the serviceability as well as the safety of the superstructure; it can even cause complete failure during an aftershock or in future seismic events. To design seismic resistant pile foundations, the causes and mechanisms of damage and the parameters controlling the pile behavior must be identified and analyzed. Such information is not currently available.

The present study is a first step towards the assessment of potential damage to pile foundations located in Southern Indiana due to a credible earthquake. Results of this work point to the need for further research. The first task has been the evaluation of the seismicity of Indiana. The region where the earthquake hazard is significant is the southwestern tip of the State, laying between the Ohio and Wabash rivers. This part of Indiana is close to the major seismic source in central United States, the New Madrid seismic zone, which is capable of generating destructive earthquakes. Also, southwestern Indiana is located next to the Wabash Valley fault system, which has produced moderate magnitude earthquakes in the last decades, but is also capable of generating larger seismic events, as evidenced by traces of paleoliquefaction found in natural soil deposits.

One-dimensional wave propagation analyses are performed at nine selected sites. Results from this investigation are used to evaluate the magnitude of ground acceleration and to examine the effect of specific soil conditions on the seismic motion. The computer program SHAKE is used for the response analyses. The rock outcrop motion amplitude is estimated using attenuation relationships appropriate to the local conditions. The soil properties are

extracted from data provided by the Indiana Department of Transportation. The results suggest a typical average value for the peak ground surface acceleration of 0.33g and 0.17g for a Wabash Valley fault system and New Madrid seismic zone event, respectively. The estimated peak accelerations, which have a 10% probability of being exceeded in 100years, are higher than the values considered in design. Moreover, the analyses show that there is potential of liquefaction at sites containing loose granular soils. The scatter of the computed accelerations, the sensitivity of the ground response to soil profile conditions, and the uncertainty of the soil properties and earthquake characteristics, indicate that each project should be treated and analyzed separately in terms of imposed seismic loads.

Information concerning real cases of pile damage during past major earthquakes, such as the Niigata, 1964, and the Kobe, 1995 earthquakes in Japan, has been gathered through an extensive literature survey. The collected data includes pile type and pile characteristics, type of superstructure, soil profile conditions, peak ground acceleration, type and cause of damage for each case. This data is summarized in Table 4.1 and can be used as a reference for sites in Southern Indiana with similar pile and soil characteristics. Based on this data, four causes of damage are identified: (1) inertia loads from the superstructure; (2) deformation imposed by ground response; (3) liquefaction; and (4) lateral spreading. In most of the cases damage tends to concentrate near the pile head and at the interfaces between very soft and stiff layers and between liquefiable and non-liquefiable layers. Concrete piles are more susceptible to heavy (wide cracks) and severe (concrete crushing) damage, especially in cases of large inertial loads and in cases of liquefaction/lateral spreading. Heavy damage reduces the strength and stiffness of deep foundations and repairs are required. Structures supported by severely damaged piles may suffer settlement and tilting. Steel piles can resist earthquake loads more efficiently and steel casing seems to improve the behavior of concrete piles by reducing the potential of cracking. This has been corroborated by both available data and numerical analyses of steel casing concrete piles at one of the selected road bridge sites. Large diameter piles prevent heavy and severe damage in cases without liquefaction and lateral spreading. The potential of liquefaction and lateral spreading increase the likelihood of damage in both concrete and steel piles.

Results from the present study suggest that large ground accelerations in Southern Indiana can be generated by a major seismic event. These accelerations are high enough to produce damage to concrete piles. Based on this observation, further examination and analysis are required for each important bridge located in Southern Indiana as well as for future projects. Emphasis must be given to the effects of liquefaction and lateral spreading, and to the differences of stiffness between adjacent soil layers. Based on the compiled data from real cases of pile damage, excavation and placement of a steel jacket at the upper portion of the pile, or the introduction of additional steel encased concrete piles or large diameter concrete piles can be considered as possible retrofitting techniques for deficient pile foundations. However, a detailed study of the behavior of steel encased concrete piles for a typical soil and earthquake in Southern Indiana is strongly suggested. The current practice of using steel H-piles in Indiana is found to be appropriate to minimize damage during an earthquake. This is based on a limited number of cases found in the literature. While this study endorses the practice, it also finds it advisable to conduct a detailed investigation to confirm this observation.

CHAPTER 2: INTRODUCTION

Observations from recent earthquakes have shown that pile foundations are susceptible to significant damage when subjected to loads induced by large seismic events. The Hyogoken-Nambu earthquake in 1995 had a decisive impact on the city of Kobe, Japan, where most of the infrastructure, including road and railway bridges, suffered severe damage. Investigations of the foundations of the damaged bridges revealed that there was a large percentage of pile foundations affected by the earthquake. The extent of the damage was amplified by the liquefaction of alluvial deposits and reclaimed land, where many of the structures were sited, and by lateral spreading.

During subsequent years, large efforts have been made by earthquake engineers and researches to record, identify, and analyze the pile damage from the Kobe earthquake to better understand the failure mechanisms and to develop mitigation techniques to preserve the integrity of civil engineering structures during major earthquakes. In some cases, although the superstructure appeared to be intact, concrete piles were cracked, especially near the pile head. This type of damage decreases the structure's capability to sustain future earthquakes, even if it has not an effect on the serviceability of the structure.

The southwestern tip of Indiana is close to the New Madrid seismic zone, which generated the large earthquakes of 1811-1812. Moreover, there are several faults extending along the Wabash Valley that are active. These faults produced large earthquakes in prehistoric times, as suggested by paleoliquefaction features in the soil deposits in the region. The seismic activity of the Mississippi Valley is small compared to that of California, where the reoccurrence of large events is of the order of tens of years. In the central United States, the scarcity of seismic data and low earthquake reoccurrence could raise questions about the reliability of related seismological studies and could question the need of further research and action concerning earthquake hazard mitigation. However, there is evidence suggesting that this intra-plate tectonic environment produced and is capable of producing major seismic events.

Most of the fatalities and economic loss in modern times are produced by earthquakes because of the lack of prevention and post-earthquake mitigation measures. Recent examples are the Kobe 1995 earthquake and the Turkey, Athens, and Taiwan 1999 earthquakes. The largest seismic event reported during historic times in the area of Kobe was the Fushimi earthquake, which occurred in 1596 and had a magnitude approaching M = 7. Since then the area of Kobe has been seismically quiescent. Therefore, the strong ground motions were underestimated, as reflected in the Japanese seismic code, which had been used for most of the buildings and infrastructure in the area of Kobe. The accelerations recorded during the 1995 earthquake with magnitude M_{JMA} = 7.2 were unexpected and surprising (Ishihara, 1997). The Athens 1999 earthquake was triggered by a fault a few kilometers from the urban area, which was considered nearly inactive. In addition, its contribution to the seismic hazard evaluation was almost neglected. This past experience, which shows an underestimation of the consequences from a strong earthquake, together with evidence, from numerous seismological studies of the New Madrid and Wabash Valley, that shows the potential for a major earthquake, indicates the need for an increased awareness and prevention against a credible earthquake.

In the present study, an initial evaluation of the damage potential of pile foundations located in Southern Indiana due to a seismic event is presented. The data recorded worldwide about the performance of deep foundations during past earthquakes is used to identify the causes and mechanism of pile damage. A classification of the causes, types and severity of damage is proposed based on the collected and compiled data obtained from technical publications. The ground acceleration for specific sites in southern Indiana seismicity of the specific region is assessed according to the potential seismic sources, credible earthquake magnitudes and strong ground motion characteristics. Information concerning the soil deposits is extracted from geologic maps and boring logs from the Indiana Department of Transportation. To achieve a deeper understating of the response of the soil deposits under the expected ground motion, nine sites located in the Southwestern tip of Indiana are selected. Seven of the sites are road bridge sites and the other two sites are inside Evansville. Ground accelerations and liquefaction potential are estimated for the selected sites by one-dimensional wave propagation analyses using SHAKE. The analyses are combined with the conclusions from the literature survey to estimate the effect of an earthquake to deep

foundations in Southern Indiana. Additionally, simple numerical simulations for a single pile at one of the road bridge sites are performed using finite element methods. The pile is a concrete pile with or without retrofitting with different thickness of steel casing. Comparisons between the concrete and retrofitted piles are used to evaluate the strengthening effects of the steel casing.

This report is divided in another four chapters. Chapter 3 is about the seismicity of the southwestern tip of Indiana, the strong ground motion and the response of the typical soil deposits in the region. Chapter 4 presents the information on cases of damaged pile foundations during earthquakes found in the literature. In chapter 5, the collected information is compiled and conclusions are presented. Finally, chapter 6 consists of the recommendations.

CHAPTER 3: THE SEISMICITY OF SOUTHERN INDIANA

During an earthquake, stresses are developed in the pile due to inertial loads applied by the superstructure to the pile head, as well as due to the response and deformation of the surrounding soil. Both inertial loads and soil deformation are directly related to the acceleration developed during the seismic event at the pile foundation site. The amplitude of the seismic accelerations at the ground surface depends on the earthquake magnitude, the distance from the seismic source and the properties of the soil deposit. In this chapter, seismic sources and credible earthquake magnitudes are identified. In this study, the one-dimensional wave propagation code SHAKE is used to assess the acceleration at the ground surface and at depth. The amplitude of the input motion is determined based on ground motion attenuation relationships for Central and Eastern North America.

Seismic sources and credible earthquake magnitude

The southern part of the state of Indiana between the Wabash and Ohio rivers is relatively close to the New Madrid Seismic Zone, the major seismic sources in Central and Eastern North America. This part of the state is located on a tectonic feature called the Southern Indiana rift arm, which constitutes an extension of the Reelfoot Rift, hosting the New Madrid Seismic Zone. The present study is focused on this particular area of Indiana where the seismic hazard appears to be significantly higher than in the rest of the state. History has shown that few earthquakes of small to moderate magnitude have occurred in this region.

The southwestern part of Indiana is located at about 300km to 360km from the New Madrid Seismic Zone (NMSZ). The last significant seismic events produced by the New Madrid seismic zone were the 1811 and 1812 earthquakes, in the Central Mississippi Valley, of body-wave magnitude m_b from 7.2 to 7.4, corresponding to surface-wave magnitudes M_s ranging form 8.5 to 8.8 (Nuttli, 1982; Nuttli and Hermann, 1984). These events caused significant structural damage at large distances form the epicenter (earthquake intensity based on the Modified Mercalli scale larger than XVIII) and are among the major historical seismic events worldwide (Figure 3.1).

Several small-to-moderate seismic events have occurred in the vicinity of the Wabash Valley fault system since the 19th century, including the Southern Illinois, 1968, and the Southeastern Illinois, 1987, earthquakes with magnitudes M_s=5.3 (M_w=5.6) and M_s=5.0 (M_w=5.4), respectively (Wheeler and Johnston, 1992). The epicenter of the 1968 earthquake was located 80km from Evansville. Extensive evidence of paleoliquefaction found in the alluvial deposits of the southern Indiana and Illinois suggest that earthquakes originating from the Wabash Valley fault system of moment magnitude up to M_w=7.5 took place in prehistoric times (Obermeier, 1998). Figure 3.2 shows areas where traces of paleoliquefaction have been found by the Central United States Earthquake Consortium (CUSEC).

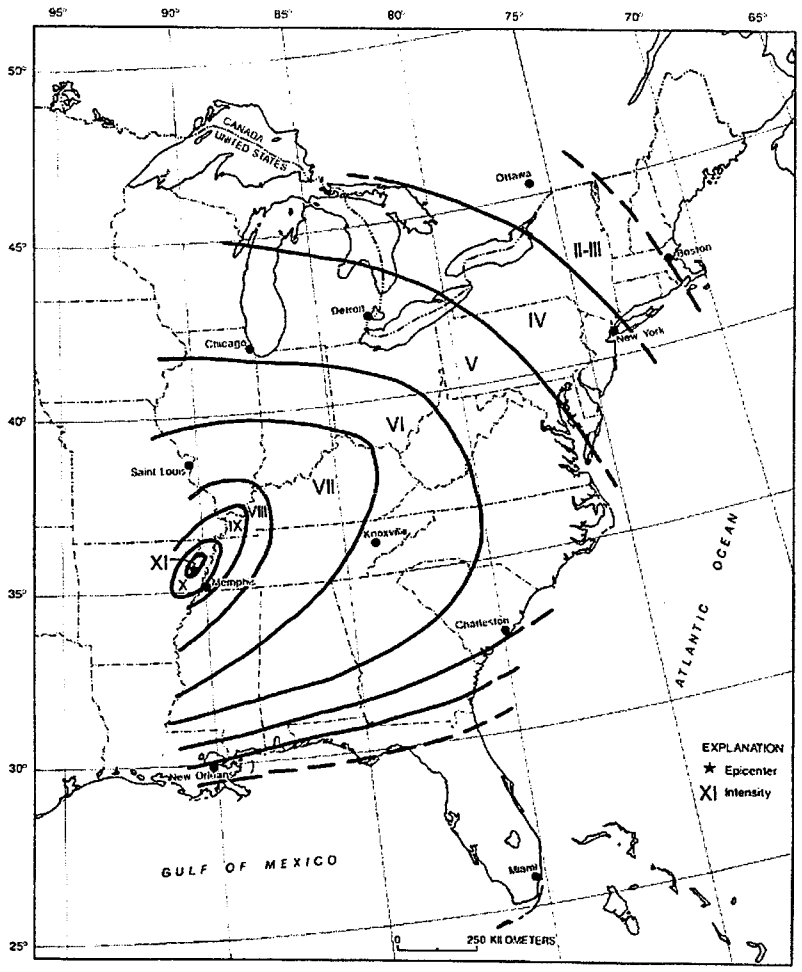

Figure 3.1. Intensity distribution for the New Madrid, 1811-1812 earthquakes (after Stover and Coffman, USGS Paper 1527).

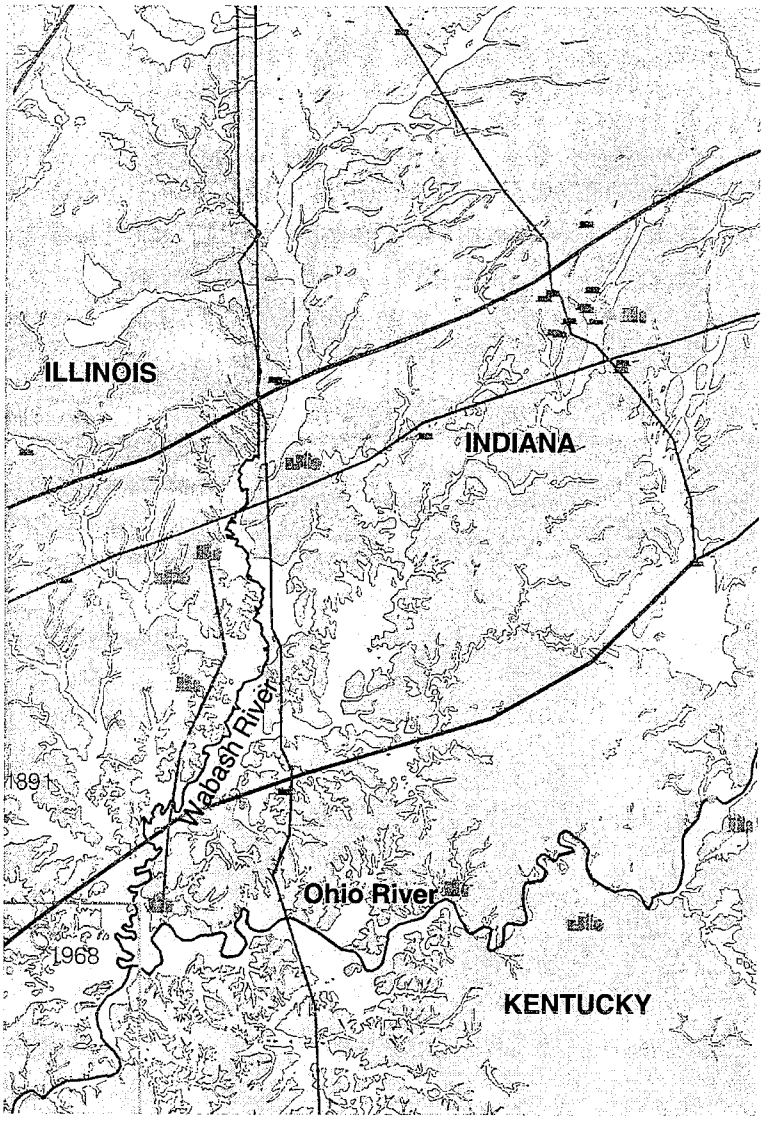

Figure 3.2. Map showing areas with evidence of paleoliquefaction (in light gray) by CUSEC.

It can be noticed that the deposits liquefied by these earthquakes lay mainly along the valleys of the Ohio, Wabash and Patoka rivers, where recent and loose fluvial deposits of granular soils are predominant.

The recent seismic activity in the vicinity of the Mississippi Embayment is scarce and limited compared to the activity in the West Coast; it appears that the area is experiencing a

seismically quiet period. However, this is a typical characteristic of intra-plate seismic zones. Although the recurrence of large events in the intra-plate area is small, very large earthquakes may be produced. This has occurred in the past as evidenced by seismological and geological data.

Besides the hazard severity, Central and Eastern North America (CENA) earthquakes differ in numerous aspects from West North America (WNA) earthquakes, as outlined by Nuttli (1982). According to Nuttli, the fact that in CENA the earthquake generating faults scarcely rupture the ground surface results in ground motions characterized by lower amplitudes in the lower frequencies, compared to WNA earthquakes. As an example, ground motion recorded during the recent CENA earthquake, the Saguenay, Canada, 1988, earthquake of moment magnitude M_w=5.9, has predominant period of 0.15-0.19sec at an epicentral distance of 100 to 150km, while the expected period, based on data from WNA earthquakes, is approximately 0.4sec (Kayabali, 1993). The focal depth of earthquakes occurring in the Mississippi is relatively large, especially in the case of large events. A larger focal depth results in smaller ground accelerations at the ground surface. The most significant difference between WNA and CENA earthquakes is that the energy transmitted form the source in CENA dissipates at a much lower rate than in WNA. This is probably due to the fact that the crust in the region in relatively unfractured. One of the main characteristics of the major New Madrid earthquakes in 1811-1812 was that architectural damage was observed at locations several hundreds of kilometers away from the source area, and the earthquake was felt in the Atlantic coast.

In this study, two potential seismic sources are considered: (1) the Wabash Valley Fault System (WVFS); and (2) the New Madrid Seismic Zone (NMSZ) (Figure 3.3). Magnitude-reoccurrence relationships developed by Kayabali, (1993) yielded values of the earthquake magnitude m_b for 1000yr reoccurrence of 6.9 for the Wabash Valley and 7.4 for the New Madrid seismic zone. The earthquake recurrence model of Green et al. (1988) gives m_b=6.25 and m_b=6.8, for WVFZ and NMSZ, respectively. USGS assumes that the return period of events with m_b greater than 6.5 is 2600 years; this coincides with the prediction of Green et al. for the same return period. However, seismological data indicates that the rate of increase of the magnitude with increasing return period is significantly smaller for return periods larger

than 1000years. Thus, the dependence of earthquake magnitude on the reoccurrence rate for major events is low and the differences in the earthquake magnitude estimation for large seismic events are small.

Two scenarios are considered with a 10% probability of exceedance in 100 years (i.e. a return period of 1000years): (1) WVFZ earthquake with m_b=6.5; and (2) NMSZ earthquake with m_b=7.2. This takes into account the fact that most bridges are designed for a return period of 1000 years. Both earthquake magnitudes may be considered unexpectedly large compared to magnitudes observed in other, more active regions in North America and in the rest of the world. However, the New Madrid seismic zone and its adjacent fault system, such as the one extending along the Wabash river produced and may produce in the future earthquakes of magnitudes very close to the above values. Obermeier (1998), based on paleoliquefaction evidence, estimated that two earthquakes with magnitudes M_w greater than 7 occurred in the Wabash Valley. Similar studies were taken into account by USGS for the construction of the 1996 seismic hazard maps. However, there is no agreement as to the accuracy of paleoseismic analysis in predicting the earthquake magnitude.

The surface wave-magnitude M_s can be extracted from the body-wave magnitude m_b and vice-versa by the relationships developed by Nuttli (1980) for Central and Eastern United States earthquakes.

$$M_s = 1.64 \cdot m_b - 3.16 \quad (m_b \geq 5.59) \tag{3.1a}$$

$$M_s = 1.02 \cdot m_b + 0.30 \quad (m_b < 5.59) \tag{3.1b}$$

The surface-wave magnitude M_s can be converted to moment magnitude M_w based on the relationship by Johnston (1989):

$$M_w = 4.355 - 0.268 \cdot M_s + 0.094 \cdot M_s^2 \tag{3.2}$$

Equation (3.2) is valid for M_w>4.5. It must be noted that the difference between the values of M_s and M_w is small, and is smaller than the difference between m_b and M_s.

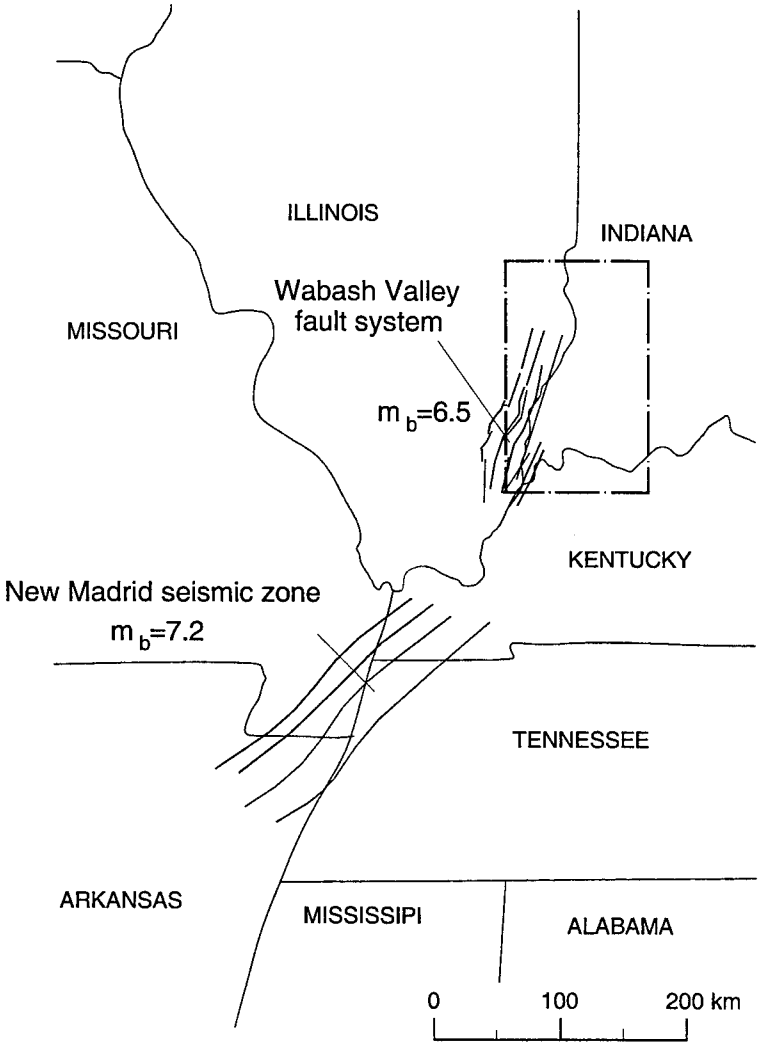

Figure 3.3. Map showing seismic sources and earthquake magnitudes considered in the study.

It is common that seismological studies related to CNA refer to body-wave earthquake magnitude m_b rather than surface-wave M_s or moment magnitude M_w. Thus, equations 3.1 are useful in cases where ground motion parameters, such as peak ground acceleration (PGA)), predominant period and the number of major motion cycles needed for the assessment of the liquefaction potential, must be extracted from empirical relationships, which are usually given in terms of M_s and M_w.

Strong ground motion attenuation.

Attenuation relationships provide the amplitude of ground motion (usually acceleration) as a function of the distance R from the source, the earthquake magnitude, and in some cases the local site conditions. Numerous attenuation relationships for Central and Eastern North America have been proposed during recent years. Due to the lack of recorded data from large earthquakes in the region, most of the attenuation relationships proposed are based on theoretical models adjusted to the seismotectonic environment of CENA and to the strong ground motion data obtained from small to moderate earthquakes in the region.

The Nuttli and Hermann (1984) attenuation relationships are some of the older and more widely used (Greene et al., 1992; Kayabali, 1993), due to the fact that they were developed and addressed specifically for Mississippi Valley earthquakes. Nuttli and Hermann took also into account the large New Madrid earthquakes of the 19th century by considering empirical relationships between the earthquake intensity, strong ground motion acceleration, and magnitude for the determination of the shape of the curves. According to Nuttli and Hermann attenuation relationships, the peak horizontal ground acceleration (PHGA) for a Mississippi Valley earthquake is estimated as

$$\log PHGA = 0.57 + 0.50 \cdot m_b - 0.83 \cdot \log(R^2 + h^2)^{1/2} - 0.00069 \cdot R \qquad (3.3)$$

where R is the epicentral distance in km, h is the focal depth in km, PHGA in cm/sec^2 and $m_b \geq 4.5$. Nuttli and Hermann, (1984), provide also an estimation of the minimum focal depth h_{min} for CNA earthquakes

$$\log h_{\min}(km) = -1.73 + 0.456 \cdot m_b \qquad (3.4)$$

with $m_b \geq 4.5$. It has to be noted that, in the Nuttli and Hermann attenuation relationships, the ground motion does not depend on the local site conditions or on the site geology. According to Nuttli and Hermann most of the data used for the correlations were recoded at soil sites. For ground motion at rock sites, the values from equation (3.3) must be adjusted appropriately.

Campbell (1981) developed attenuation relationships for Central North America with focus on near field strong ground motion.

$$PHGA=0.0142\cdot e^{0.79\cdot Ms}(R+0.0286\cdot e^{0.778\cdot Ms})^{-0.862}\cdot e^{-\gamma R} \quad (3.5a)$$

$$\text{with} \qquad \gamma=-(0.023-0.0048M_s+0.00028M_s^2)\cdot R) \quad (3.5b)$$

where PHGA is the peak horizontal ground acceleration in multiples of "g" (gravity acceleration) and R is the distance from the fault in km. The relationships are based mainly on empirical data and are independent of the focal depth. The estimated peak ground acceleration applies to general site conditions. However, according to Campbell (1981), data from soft soil sites were excluded from the study.

Atkinson and Boore worked for a number of years on the development of attenuation relationships for Central and Eastern North America (CENA). In 1987, they proposed the following attenuation relationships for ground acceleration.

$$\log(PHGA)=3.763+0.3354\cdot(M_w-6)-0.02473\cdot(M_w-6)^2+C_1\cdot R_{hyp}-\log(R_{hyp}) \quad (3.6a)$$

$$\text{with} \qquad C_1=(-0.003885+0.001042\cdot(M_w-6)-0.00009169\cdot(M_w-6)^2) \quad (3.6b)$$

where the hypocentral distance R_{hyp} is in km and the PHGA in cm/sec^2. This relationship is valid for earthquake magnitudes M_w between 4.5 and 7.5, and applies to strong motions at hard rock sites. During recent years, they proposed simpler relationships for motion at hard-rock sites

$$\log(PHGA)=3.65+0.42(M_w-6)-0.03(M_w-6)^2-0.00281R_{hyp}-\log(R_{hyp}), \text{ (Atkinson\&Boore, 1990)} \quad (3.7)$$

$$\log(PHGA)=3.79+0.30(M_w-6)-0.054\cdot(M_w-6)^2-0.00135R_{hyp}-\log(R_{hyp}), \text{ (Atkinson\&Boore, 1995)} \quad (3.8)$$

$$\ln(PHGA)=1.84+0.686(M_w-6)-0.123(M_w-6)^2-0.0031R_{hyp}-\ln(R_{hyp}), \text{ (Atkinson\&Boore, 1995)} \quad (3.9)$$

where the hypocentral distance R_{hyp} is in km and the PHGA in cm/sec^2.

Seismic hazard maps by USGS, such as the map shown in Figure 3.4, indicate the distribution of PHGA for firm rock ground conditions. This seismic hazard analysis for the

Central and Eastern North America was performed using the probabilistic approach and the attenuation relationships of Toro et al (1993).

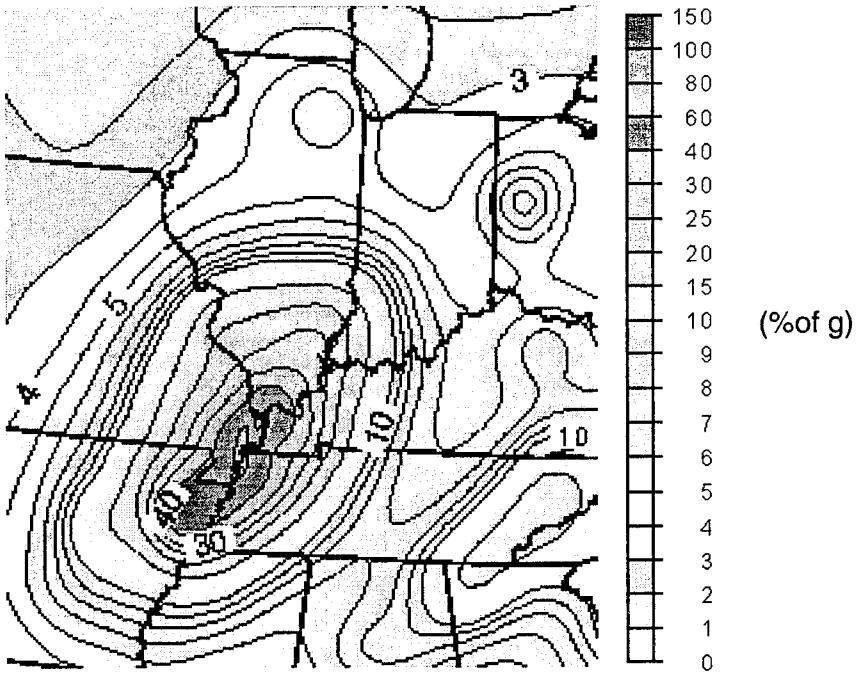

Figure 3.4. Enlarged portion of the seismic hazard map by USGS (1996) showing peak ground horizontal acceleration with 10% exceedance in a 100 year period.

Response of soil deposits and liquefaction susceptibility

The bedrock formations in the specific area consist mainly of limestone, shale, and sandstone and are covered by thick soil deposits of alluvial and lacustrine origin. Near the Wabash and Ohio rivers, soil deposits are composed of alluvial sands and silts, as well as by outwash deposits of sand and gravel. In other areas, windblown silt and lacustrine deposits of clays predominate. The thickness of these soil deposits at some locations reaches 46m (150ft). Some bridge structures, supported by pile foundations, are sitting on soil deposits of this nature.

Nine sites in southern Indiana are selected for this study to examine the particular effect of local site conditions on the ground motion and also, to estimate the potential of liquefaction of

the loose granular soils that are present in the region (Figure 3.5). Seven sites are road bridge sites crossing rivers and ditches, and the other two sites are located inside Evansville,

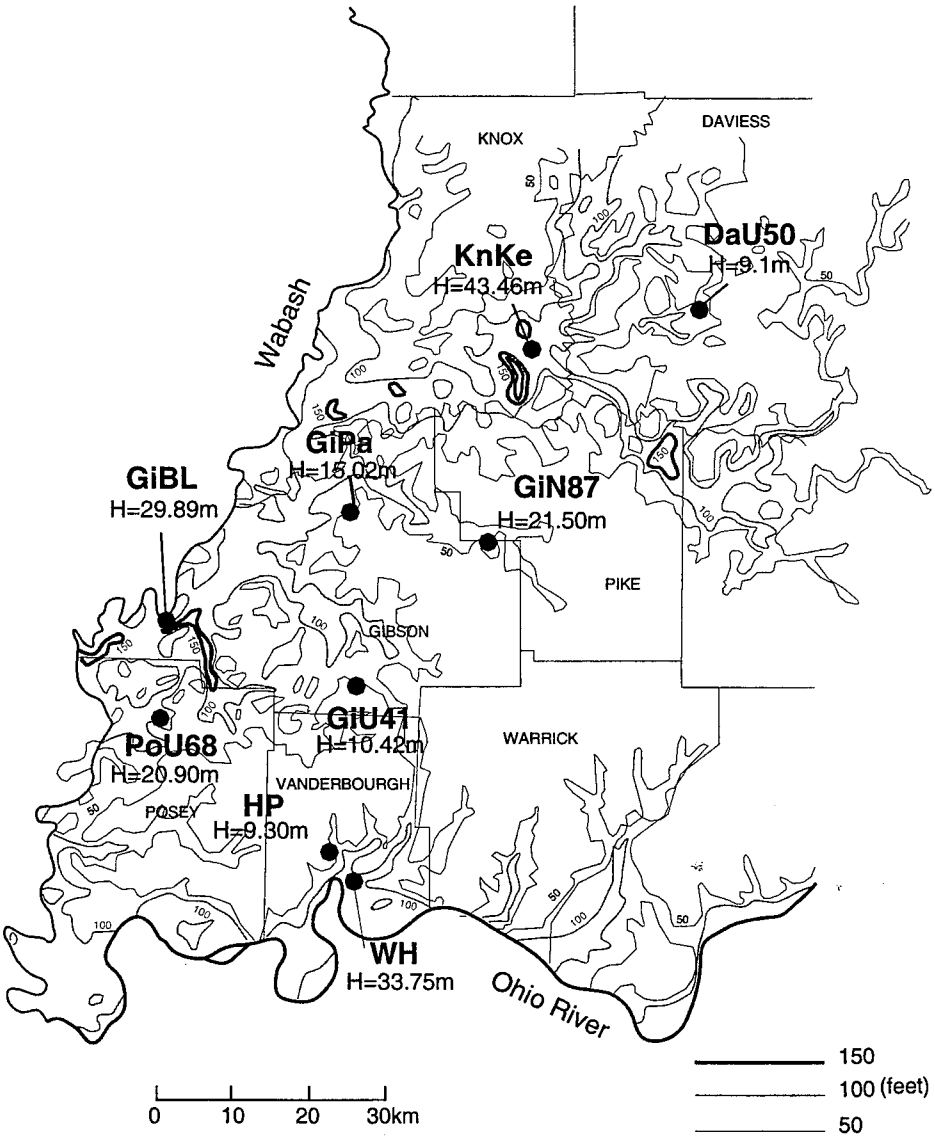

Figure 3.5. Map showing the location of selected sites and the thickness of soil deposits.

next to the Ohio River (WH and HP sites in Figure 3.5). The thickness of the soil deposits for the nine sites ranges from 9 to 43m (Figure 3.5). The evaluation of the site response and liquefaction susceptibility are performed using a deterministic approach. The calculations are repeated for two scenarios: (1) an earthquake occurring at the New Madrid Seismic Zone

with magnitude m_b= 7.2; (2) an earthquake occurring at the Wabash Valley fault system with magnitude m_b= 6.5. This magnitude values have a 10% probability of being exceeded in 100 years. To determine the distance from the source for the WVFS scenario, the representative linear source was assumed to be close to the epicenters of the 1958 and 1968 Southeastern Illinois earthquakes (Gordon, 1988) and to the epicenters of the large earthquakes (M_w>7) that took place in prehistoric times (Obermeier, 1998). The distance between the two potential sources and the selected sites ranges from 19 to 61km for a WVFS earthquake and from 300 to 400km for a NMSZ earthquake.

SHAKE analyses have been performed at each site to obtain the soil response at each location. SHAKE executes a one-dimensional wave propagation analysis using the equivalent linear method. The equivalent linear method computes the ground response taking into account the non-linearity of the soil behavior. This is achieved by assuming values for the secant shear modulus and the damping ratio that are consistent with the level of shear strain developed in the soil deposit during the earthquake. The input motion is usually assigned to the bedrock or to the rock outcrop; in the second case, the code performs deconvolution in order to compute the motion at the bedrock from the rock outcrop motion. Different attenuation relationships are used to calculate the amplitude of the rock acceleration for the two different scenarios. For the WVFS scenario, the Atkinson and Boore, 1997, attenuation relationships are used, while the Nuttli and Herrmann (1984) attenuation relationships, the most representative for an earthquake occurring in Central North America, are used to determine the amplitude of the input acceleration for the NMSZ earthquake scenario. The reason that the Nuttli and Hermann relationships are not considered for the WVFS scenario, is that the behavior of the soil profile is highly non-linear when the bedrock acceleration is high. In cases of highly non-linear response, the acceleration at the ground surface is sensitive to the local site conditions. For the WVFS earthquake scenario, the bedrock and rock accelerations are high due to the proximity of the sites to the seismic source (epicentral distance less than 65km). Thus, in the case of a WVFS earthquake, it would be better to use relationships referring to rock sites rather than general relationships as the Nuttli and Hermann (1984) relationships. The Atkinson and Boore (1997) relationships are among the most recent ones and are related specifically to Eastern North America. The Dahle et al. (1990) relationships were obtained from data from past large intra-plate

earthquakes, but these earthquakes occurred in regions other than CENA. The Toro et al. (1994) and Hwang and Huo (1999) attenuation relationships give acceleration amplitudes that are usually high. Nevertheless, the differences between the acceleration values form the above attenuation relationships are small for the range of distances encountered in the WVFS earthquake scenario.

The rate of energy dissipation with distance from the source is smaller for Central North America (CAN) earthquakes than for ENA earthquakes, as suggested by observations from the 1811-1812 major seismic events. This effect becomes more predominant at large epicentral distances (R>100km). The Nuttli and Hermann (1994) attenuation relationships take into account the lower rate of attenuation in CNA and predict PHGA higher than the other attenuation relationships that would apply to CENA, for distances larger than 100km. Results of a study about the influence of local site conditions on the attenuation relationships for the western part of the United States by Seed et al. (1976) show that the difference between acceleration recorded on rock and acceleration on deep cohesionless soils (these soils are predominant in the central Mississippi Valley, where most of the Nuttli and Hermann data was obtained), is small for acceleration amplitudes smaller than 0.1g. Thus, the Nuttli and Hermann relationships may be used without the introduction of significant errors.

Table 3.1 shows the rock outcrop peak acceleration values for each earthquake scenario, and the values extracted from the USGS map on firm rock sites, and for 10% probability to be exceeded in 100 years. Although the chosen magnitude for a NMSZ earthquake is larger than that of a WVFS earthquake, the peak acceleration produced by a WVFS earthquake is larger due to the proximity of the seismic source to the selected sites. Thus, an earthquake occurring in WVFS is more critical for the southern part of Indiana. The PHGA for a Wabash Valley Fault System earthquake can be up to 4.8 times higher than the PHGA for a NMSZ earthquake, especially for sites that are closer to the Wabash Valley, as the GiBL and PoUS68 sites (Figure 3.5). For sites at larger distances form the WVFS, as the sites in Evansville (EvanHP and EvanWH), the difference is smaller but still significant (0.19g and 0.09g for WVFS and NMSZ events, respectively). The PHGA values for a WVFS earthquake (critical seismic event) are close to the values predicted by USGS for the same return period

(100 years), with differences ranging from 3% to 27%. In most of the cases, the peak ground accelerations at rock sites predicted by USGS are smaller than the values estimated for the WVFS scenario. This tendency is expected due to the fact that the USGS predictions are obtained using the probabilistic approach instead of the deterministic approach considered in this study. Moreover USGS used the Toro et al. (1993) relationships, which apply to the Central and Eastern North America.

	WVFS earthquake		NMSZ earthquake		
Site	**Distance from seismic source (km)**	**Rock outcrop peak acc. (g) - A&B (1997)**	**Distance from seismic source (km)**	**Rock outcrop peak acc. (g) - N&H (1984)**	**Rock outcrop peak acc. (g) - USGS (1996)**
DaU50	61	0.16	380	0.06	0.14
KnoxKe	45	0.21	367	0.06	0.16
GiPa	33	0.27	342	0.07	0.19
GiN87	52	0.19	338	0.07	0.16
GiBL	19	0.36	321	0.07	0.23
GiU41	43	0.22	315	0.08	0.19
PoUS68	23	0.33	306	0.08	0.24
EvanHP	53	0.19	300	0.08	0.19
EvanWH	53	0.19	300	0.08	0.19

Table 3.1. Assumed rock outcrop PHGA of the two earthquake scenarios and comparison with values estimated by USGS.

The above PHGA values, for each earthquake scenario, are used for the determination of the input acceleration amplitude for the SHAKE analyses. The input acceleration time histories are scaled appropriately in order to have peak values equal those appearing in Table 3.1. Analyses are performed with two sets of input acceleration for each earthquake scenario because differences on the frequency content of the input motion result in differences in the amplitude of the soil profile response. Results from two different sets of input motion provide a better indication of the ground response. For the WVFS earthquake scenario, acceleration time histories are taken from strong motion data of Cape Medicino, M_w= 7.1, 1992, and Saguenay, M_w= 5.9, 1988, earthquakes recorded at distances 36km and 60km from the source, respectively. For the NMSZ scenario, acceleration recorded during the Kern County 1952 earthquake of magnitude M_w= 7.4 and Saguenay 1988 earthquake of magnitude M_w= 5.9, recorded at distances from the source 110km and 200km, respectively, are used as input motion. The Saguenay earthquake occurred in Quebec, Canada, which is inside the

Central and Eastern North America area. Unfortunately, the available strong ground motion data for CENA is limited to the data recorded during the Saguenay earthquake. Thus, the second set of input motion is taken from records of California earthquakes (Kern County, 1952, and Cape Medocino, 1992). These earthquakes have large magnitudes and are consistent with the magnitudes assumed for the WVFS and NMSZ scenarios. However, the relatively small magnitude of the Saguenay earthquake results in a difference in the predominant period. Therefore, the Saguenay acceleration time histories are scaled with respect to time to achieve predominant periods of motion of 0.2sec and 0.63sec, for the WVFS and NMSZ earthquakes, respectively. These values are close to the predominant periods of the Kern County and Cape Medocino earthquake records and are consistent with the observations of the predominant period of CENA earthquakes by Kayabali (1993).

The soil properties required to perform site response analyses (shear wave velocity V_s and soil density) are taken from SPT data and other experimental data obtained from the Indiana Department of Transportation (INDOT). For the two sites located in Evansville (EvanWH and EvanHP), soil properties are taken from Kayabali (1993). At sites where borings ended before reaching bedrock, the record has been extrapolated to the bedrock depth taking into account information from maps of quaternary geology. In many cases, N_{SPT} blowcounts indicate very loose deposits. The Imai and Tonouchi (1982) equations correlate shear wave velocity V_s with blowcounts N_{SPT}. For all soil types except clayey soils the following equation is used:

$$V_s = 97 \cdot N_{SPT}^{0.314} \qquad \text{(m/sec)} \qquad (3.10)$$

while for soils characterized as clay or silty clay, the relationship is:

$$V_s = 114 \cdot N_{SPT}^{0.217} \qquad \text{(m/sec)} \qquad (3.11)$$

In addition, shear modulus reduction and damping ratio curves by Ishibashi and Zhang (1993), which take into account the dependence of soil dynamic behavior on both the plasticity index and the effective stress, are used.

Figures 3.6 to 3.23 and Tables 3.2 and 3.3 show the results from the SHAKE analyses. Peak ground horizontal accelerations can be as large as 0.49g and 0.20g for the Wabash Valley Fault System earthquake and for the New Madrid Seismic Zone earthquake, respectively.

Generally, the amplification factor is greater for the NMSZ event because the effects of non-linearity and damping are less significant for relatively low-amplitude ground motion. From the profile of peak acceleration with depth, the potential of liquefaction initiation is assessed from Seed et al. (1985). The actual cyclic stress ratio (CSR) and the critical cyclic stress ratio required to initiate liquefaction (CSR) are plotted only for those sites with soil profile containing liquefiable soils (i.e. sandy materials).

California input motion records

	Event from Wabash Valley fault system				Event from New Madrid seismic zone			
Site	**Rock outcrop peak acc. (g)**	**Bedr. peak acc. (g)**	**Surf. peak acc. (g)**	**Amplif. factor**	**Rock outcrop peak acc. (g)**	**Bedr. peak acc. (g)**	**Surf. peak acc. (g)**	**Amplif. factor**
DaU50	0.16	0.15	0.32	2.13	0.06	0.05	0.14	2.80
KnoxKe	0.21	0.18	0.33	1.83	0.06	0.06	0.16	2.67
GiPa	0.27	0.22	0.45	2.05	0.07	0.07	0.12	1.71
GiN87	0.19	0.16	0.22	1.38	0.07	0.07	0.14	2.00
GiBL	0.36	0.28	0.38	1.36	0.07	0.07	0.13	1.86
GiU41	0.22	0.20	0.34	1.70	0.08	0.09	0.15	1.67
PoUS68	0.33	0.28	0.50	1.79	0.08	0.08	0.16	2.00
EvanHP	0.19	0.18	0.36	2.00	0.08	0.08	0.13	1.63
EvanWH	0.19	0.19	0.18	0.95	0.08	0.08	0.10	1.25

Table 3.2. Resulting peak accelerations at bedrock, at the ground surface, and amplification factor from California earthquake records.

Saguenay input records

	Event from Wabash Valley fault system				Event from New Madrid seismic zone			
Site	**Rock outcrop peak acc. (g)**	**Bedr. peak acc. (g)**	**Surf. peak acc. (g)**	**Amplif. factor**	**Rock outcrop peak acc. (g)**	**Bedr. peak acc. (g)**	**Surf. peak acc. (g)**	**Amplif. factor**
DaU50	0.16	0.14	0.28	2.00	0.06	0.06	0.22	3.67
KnoxKe	0.21	0.16	0.28	1.75	0.06	0.05	0.15	3.00
GiPa	0.27	0.25	0.42	1.68	0.07	0.06	0.18	3.00
GiN87	0.19	0.18	0.14	0.78	0.07	0.07	0.10	1.43
GiBL	0.36	0.30	0.40	1.33	0.07	0.06	0.16	2.67
GiU41	0.22	0.22	0.34	1.55	0.08	0.07	0.23	3.29
PoUS68	0.33	0.28	0.53	1.89	0.08	0.06	0.17	2.83
EvanHP	0.19	0.18	0.34	1.89	0.08	0.07	0.25	3.57
EvanWH	0.19	0.17	0.12	0.71	0.08	0.08	0.07	0.88

Table 3.3. Resulting peak accelerations at bedrock, at the ground surface, and amplification factor from the Saguenay, Canada earthquake records.

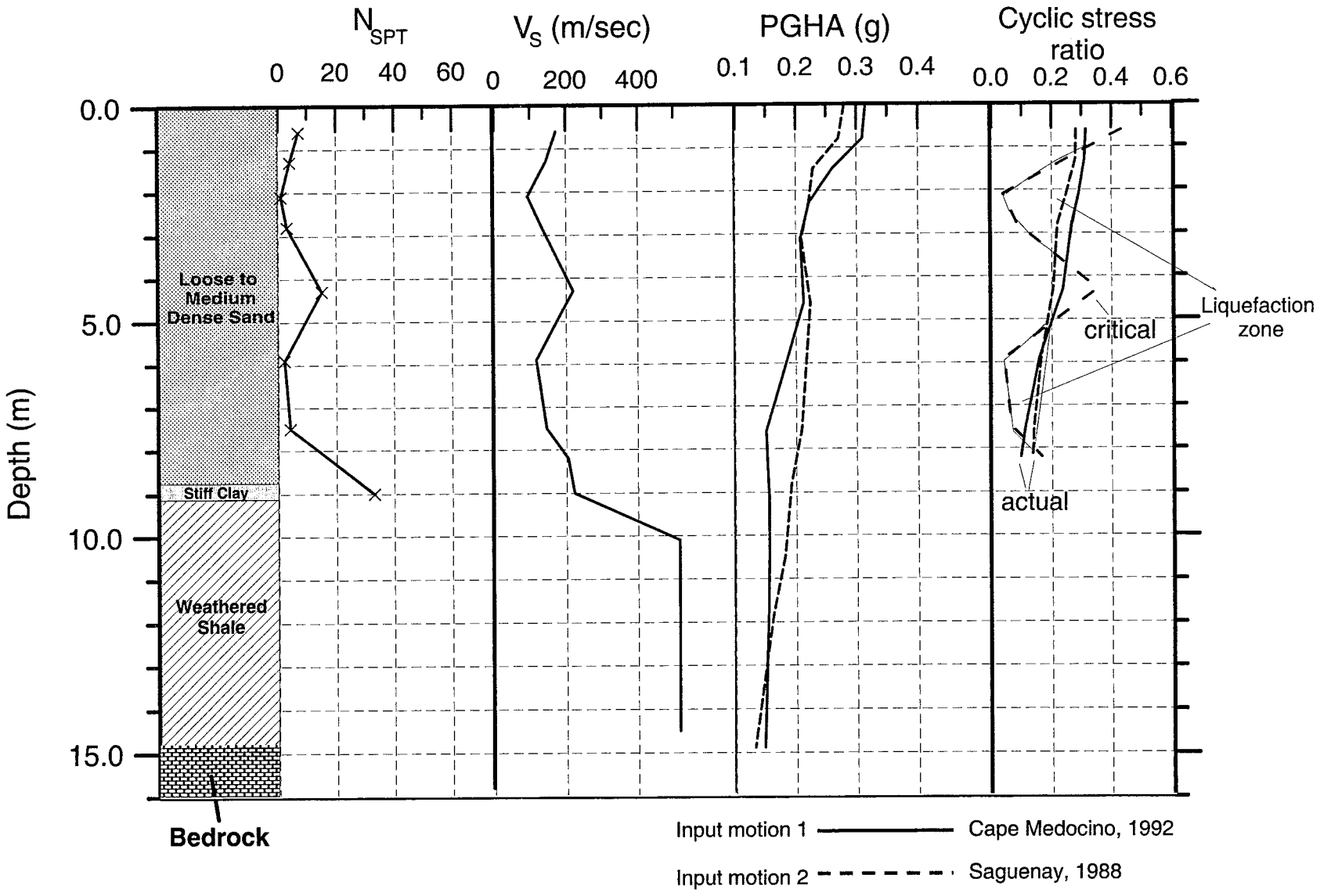

Figure 3.6. Blowcount number (N_{SPT}), shear wave velocity (V_S), peak ground horizontal acceleration (PGHA), and cyclic stress ratio vs. depth at the site DaU50, for a WVFS seismic event.

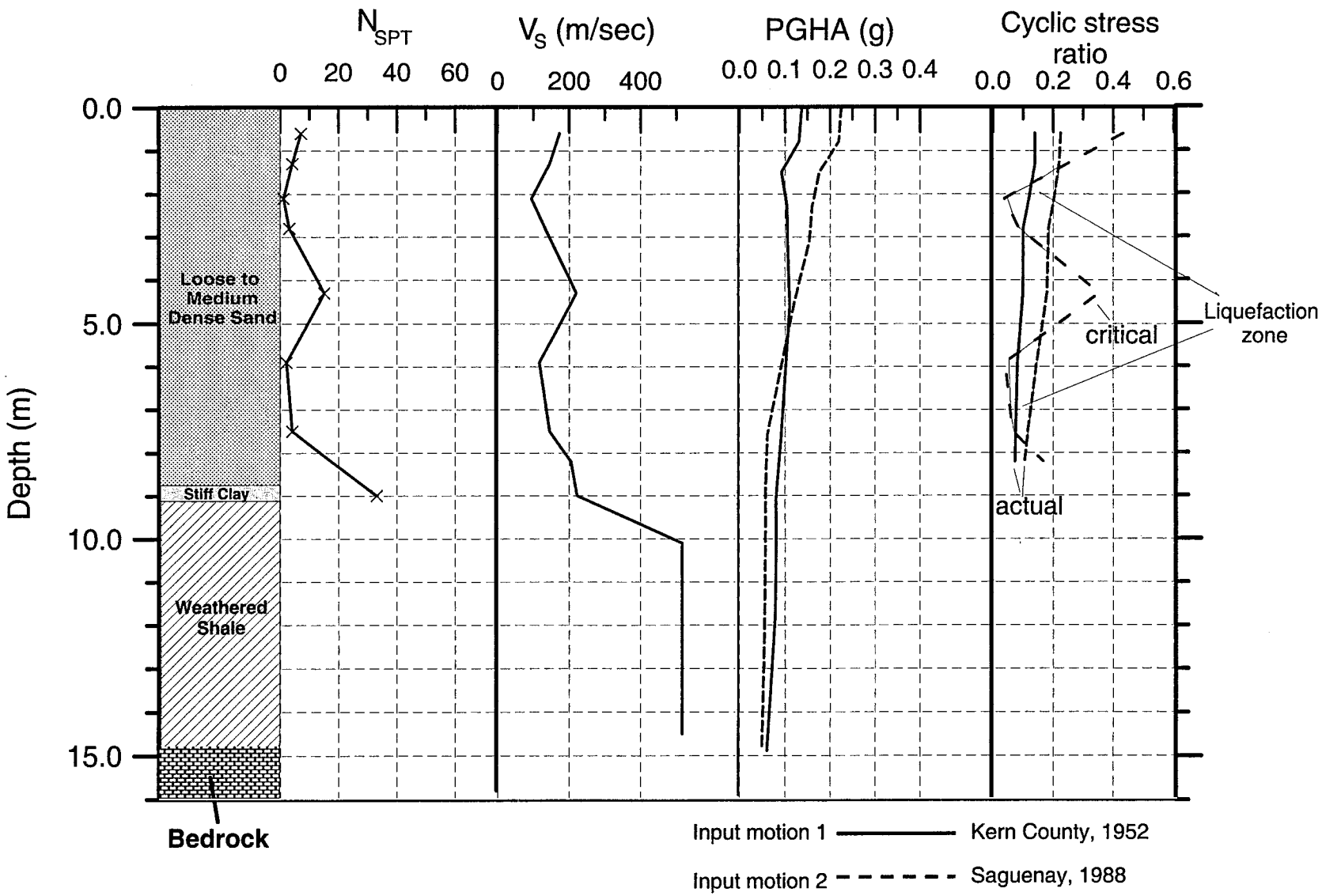

Figure 3.7 Blowcount number (N_{SPT}), shear wave velocity (V_S), peak ground horizontal acceleration (PGHA), and cyclic stress ratio vs. depth at the site DaU50, for a NMSZ seismic event.

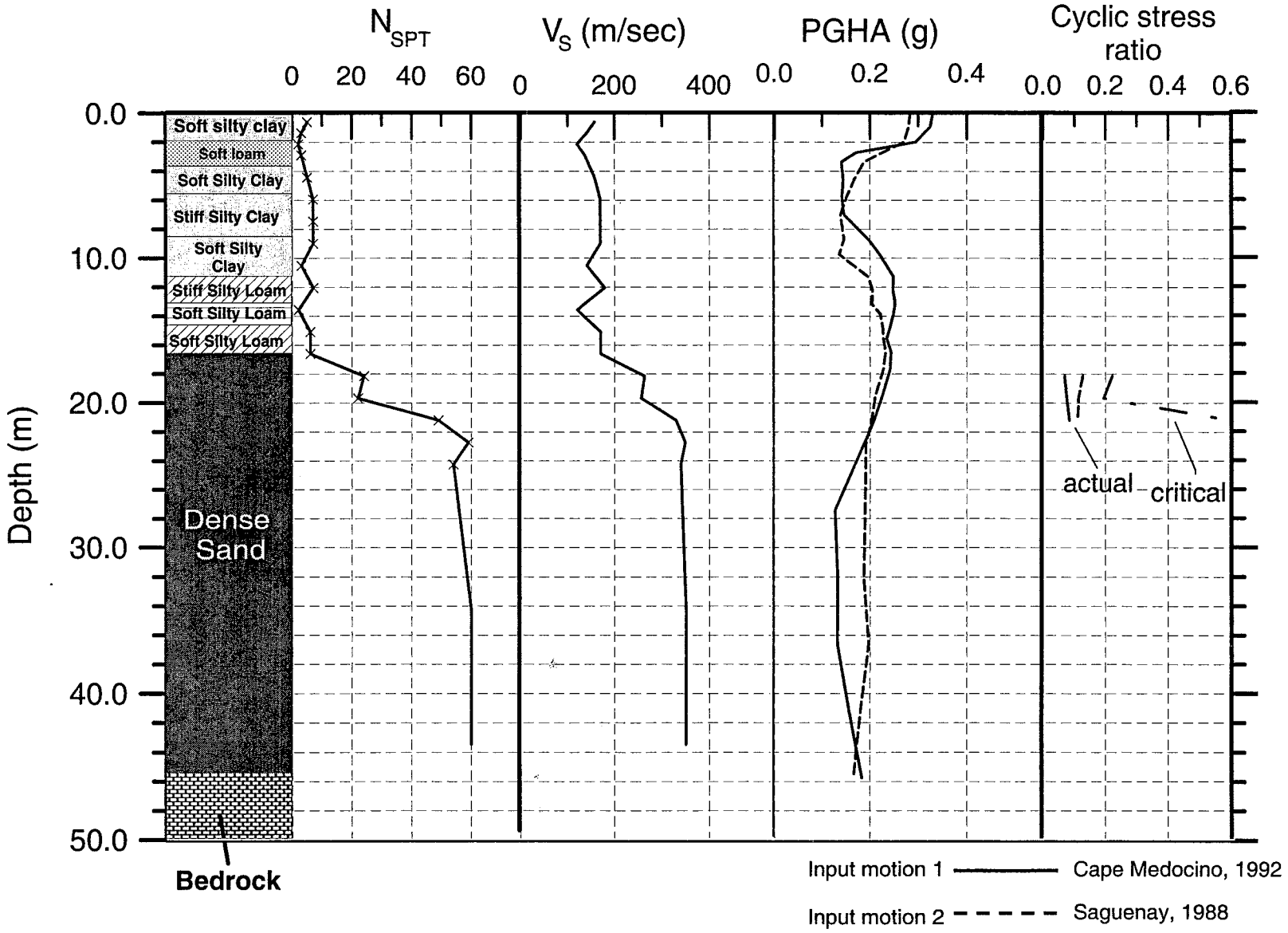

Figure 3.8. Blowcount number (N_{SPT}), shear wave velocity (V_S), peak ground horizontal acceleration, and cyclic stress ratio vs. depth at the site KnoKe, for a WVFS seismic event.

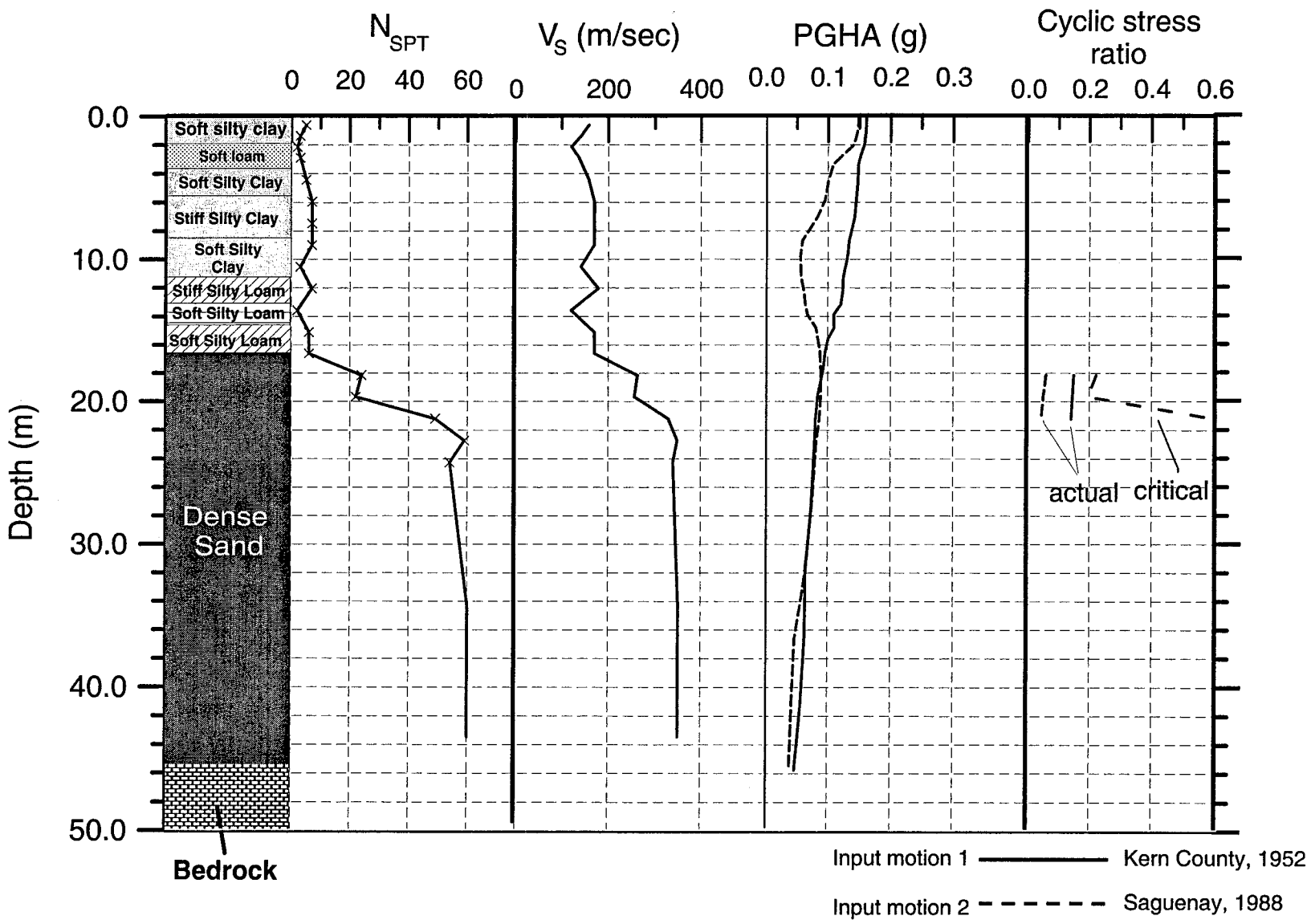

Figure 3.9. Blowcount number (N_{SPT}), shear wave velocity (V_S), peak ground horizontal acceleration (PGHA), and cyclic stress ratio vs. depth at the site KnoKe, for a NMSZ seismic event.

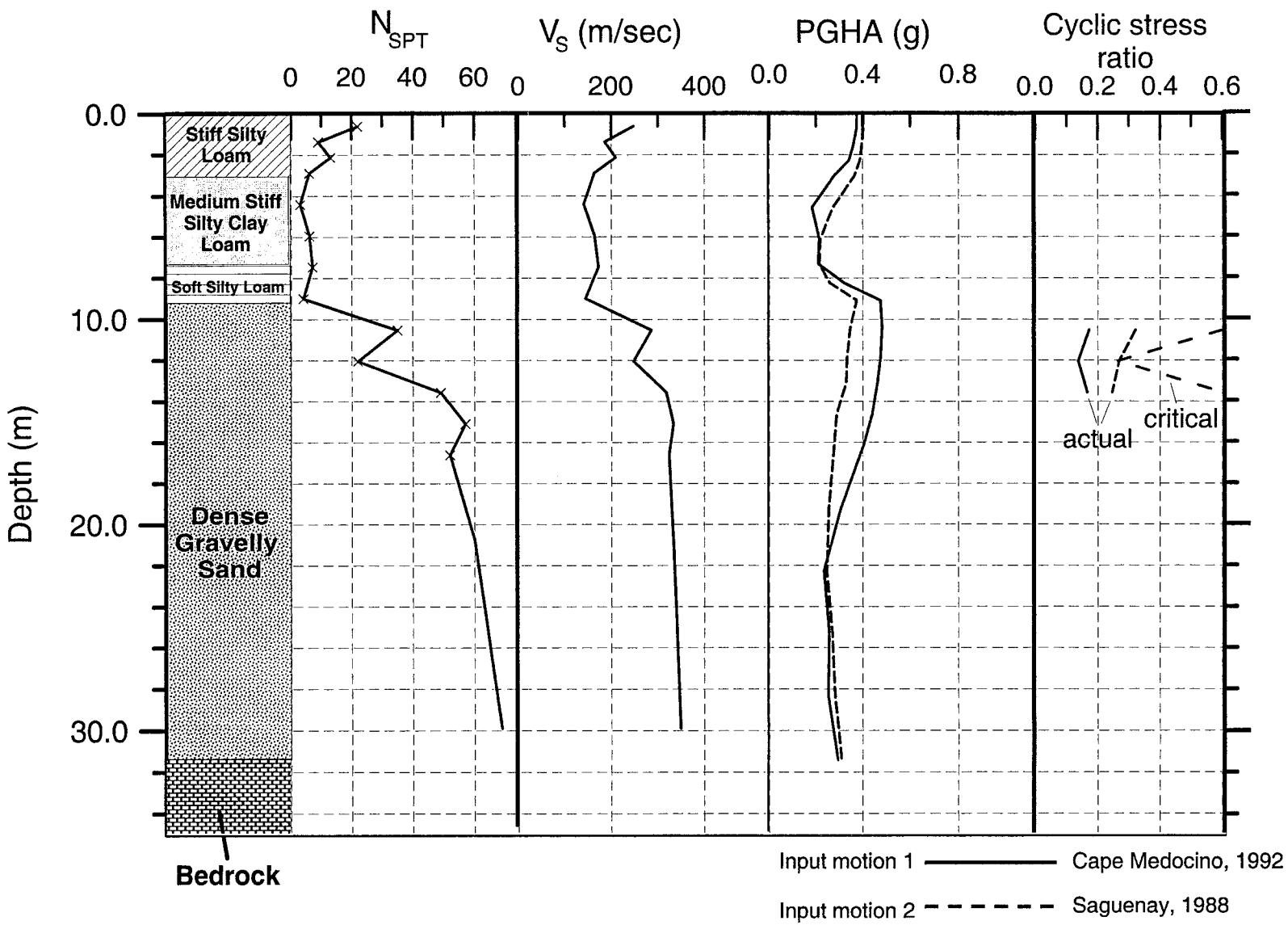

Figure 3.10. Blowcount number (N_{SPT}), shear wave velocity (V_S), peak ground horizontal acceleration (PGHA), and cyclic stress ratio vs. depth at the site GiBL, for a WVFS seismic event.

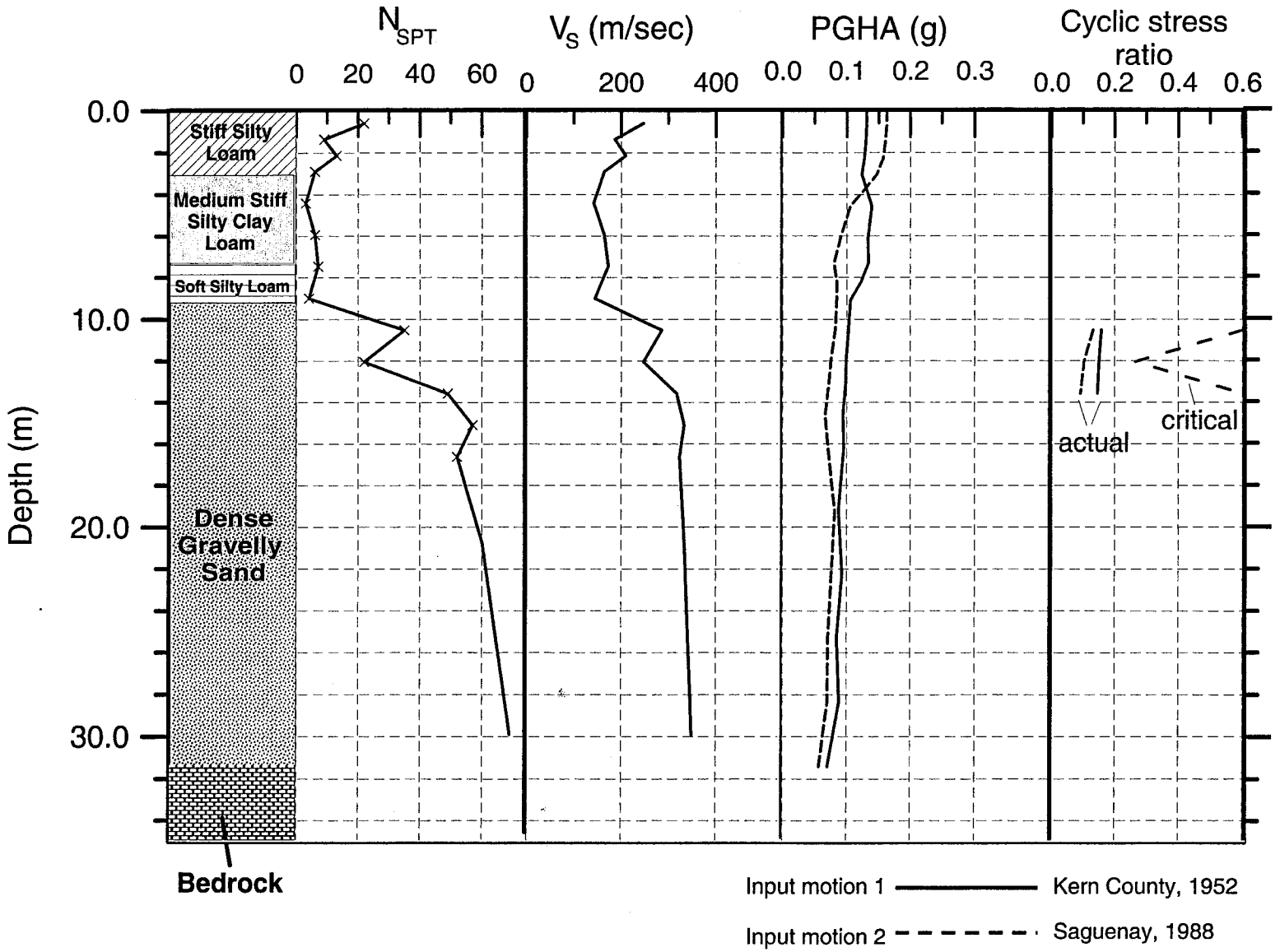

Figure 3.11. Blowcount number (N_{SPT}), shear wave velocity (V_S), peak ground horizontal acceleration (PGHA), and cyclic stress ratio vs. depth at the site GiBL, for a NMSZ seismic event.

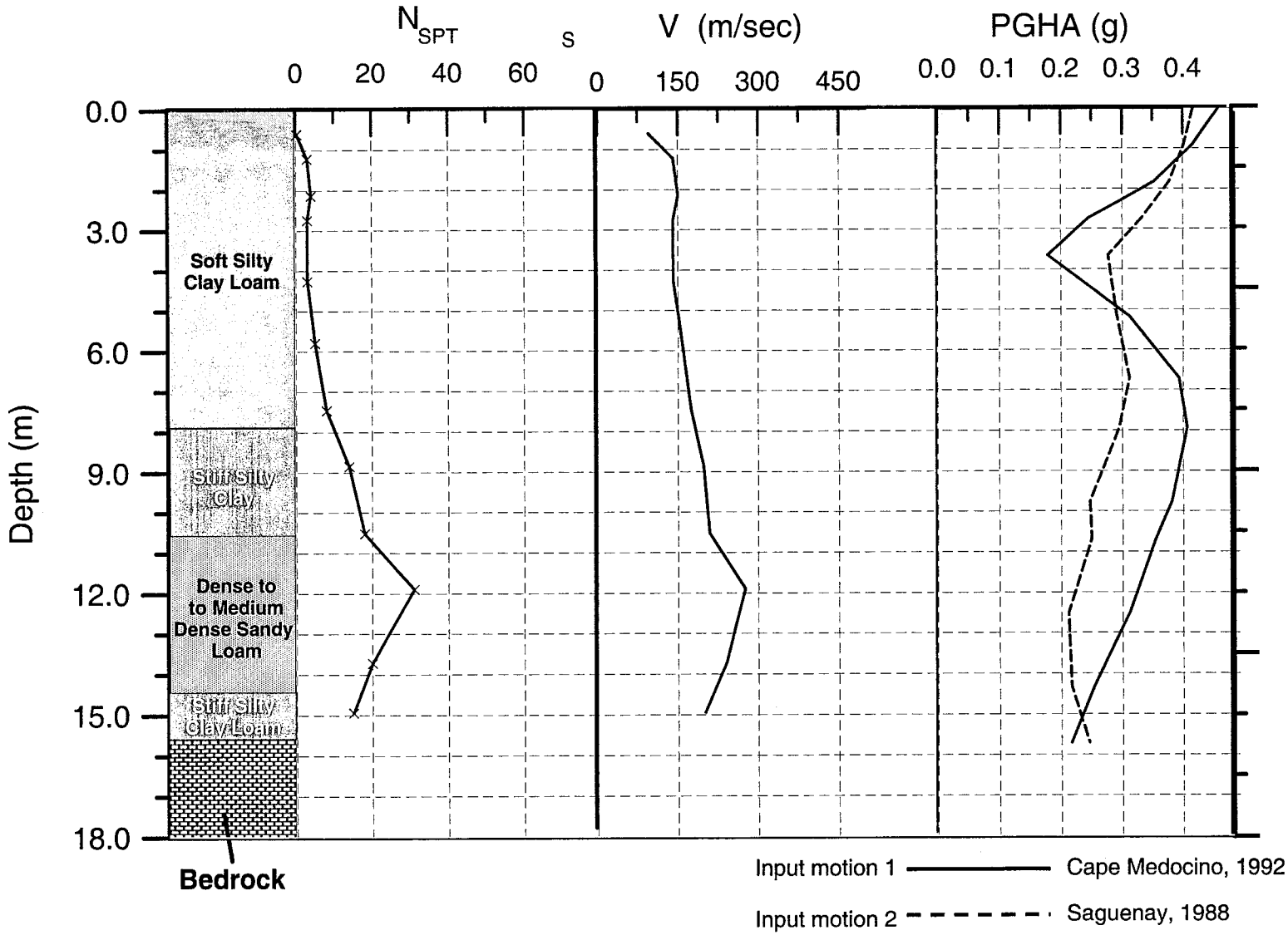

Figure 3.12. Blowcount number (N_{SPT}), shear wave velocity (V_S), peak ground horizontal acceleration (PGHA), and cyclic stress ratio vs. depth at the site GiPa, for a WVFS seismic event.

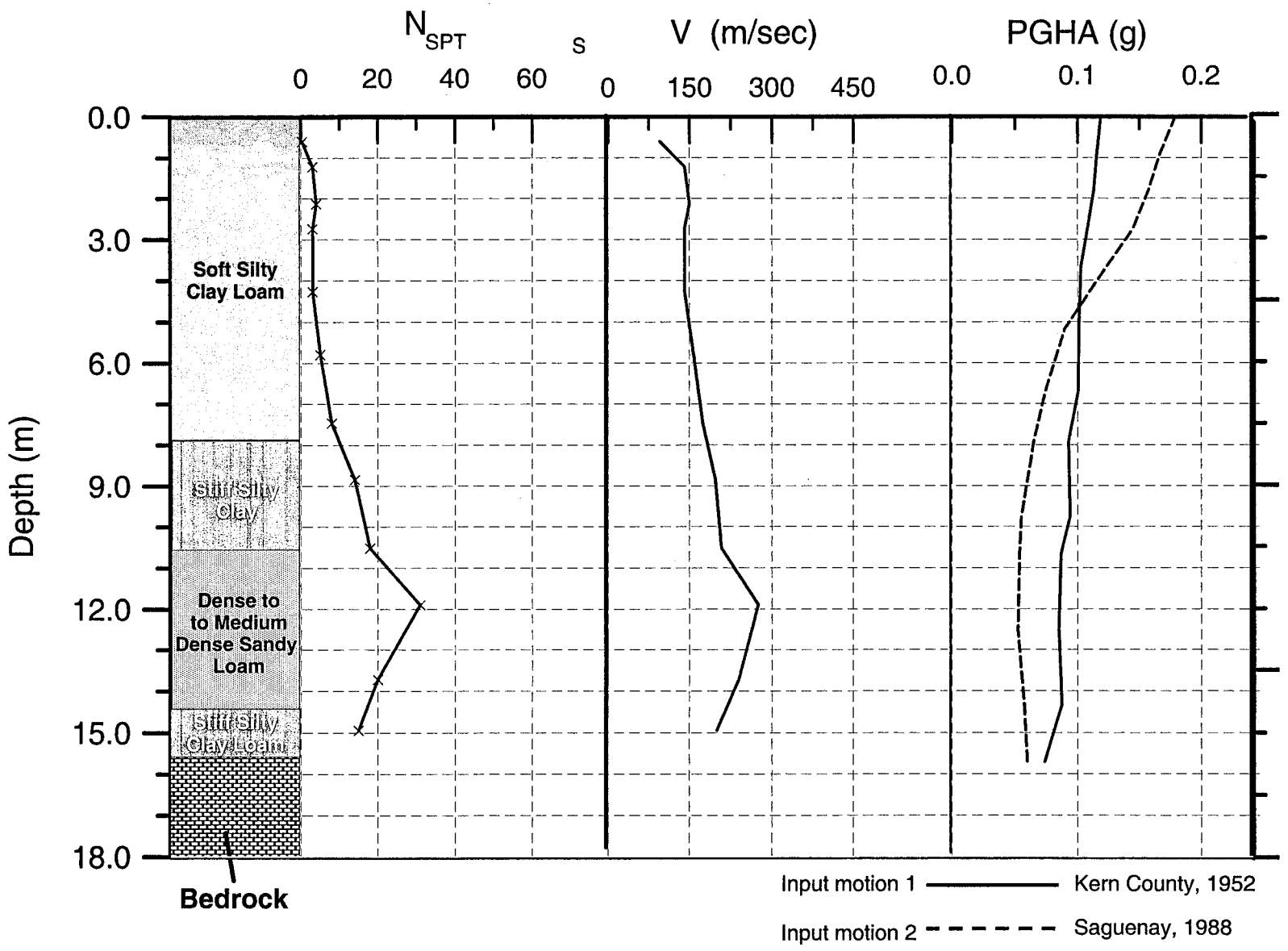

Figure 3.13. Blowcount number (N_{SPT}), shear wave velocity (V_S), peak ground horizontal acceleration (PGHA), and cyclic stress ratio vs. depth at the site GiPa, for a NMSZ seismic event.

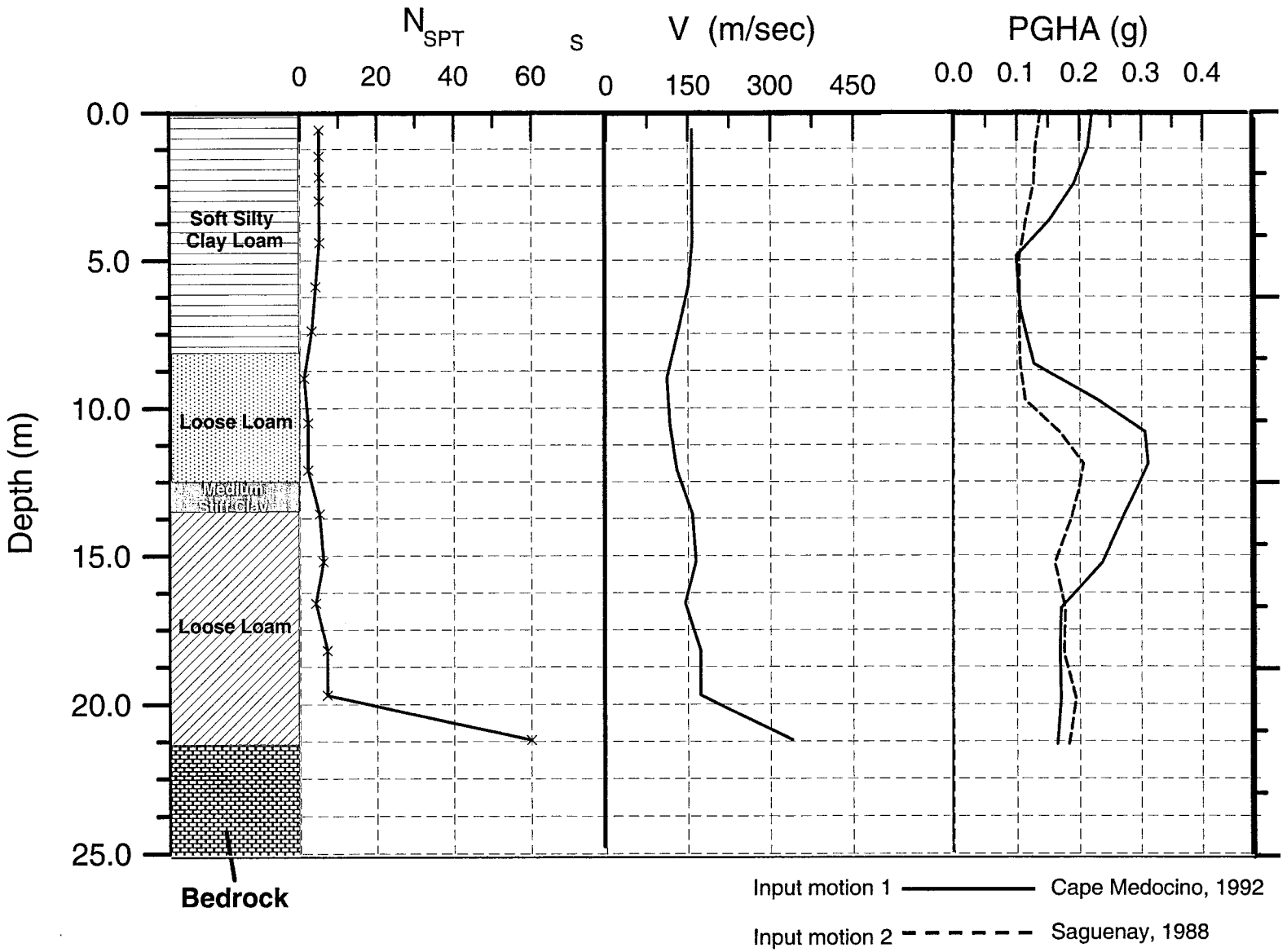

Figure 3.14. Blowcount number (N_{SPT}), shear wave velocity (V_S), peak ground horizontal acceleration (PGHA), and cyclic stress ratio vs. depth at the site GiN87, for a WVFS seismic event.

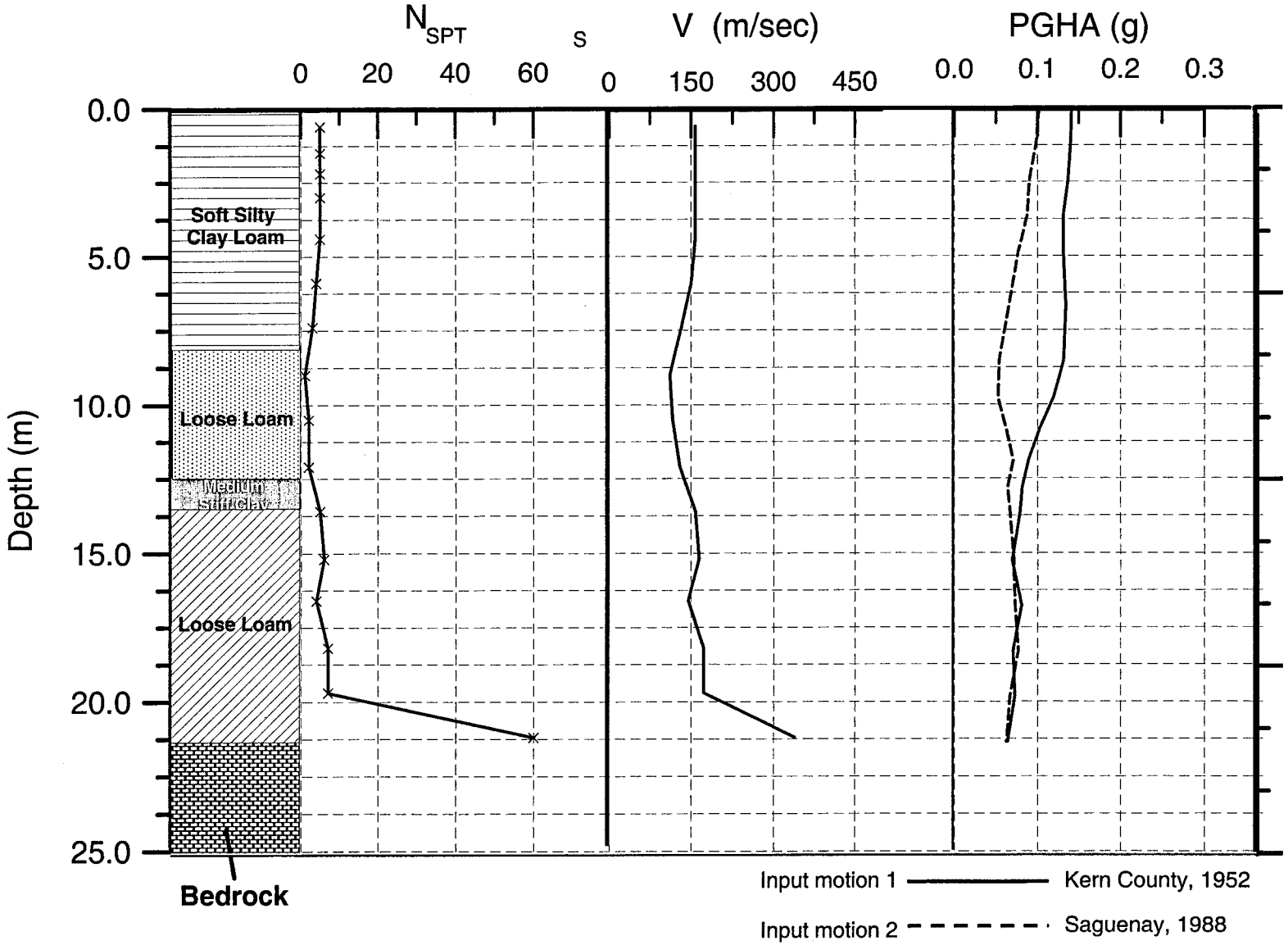

Figure 3.15 Blowcount number (N_{SPT}), shear wave velocity (V_S), peak ground horizontal acceleration (PGHA), and cyclic stress ratio vs. depth at the site GiN87, for a NMSZ seismic event.

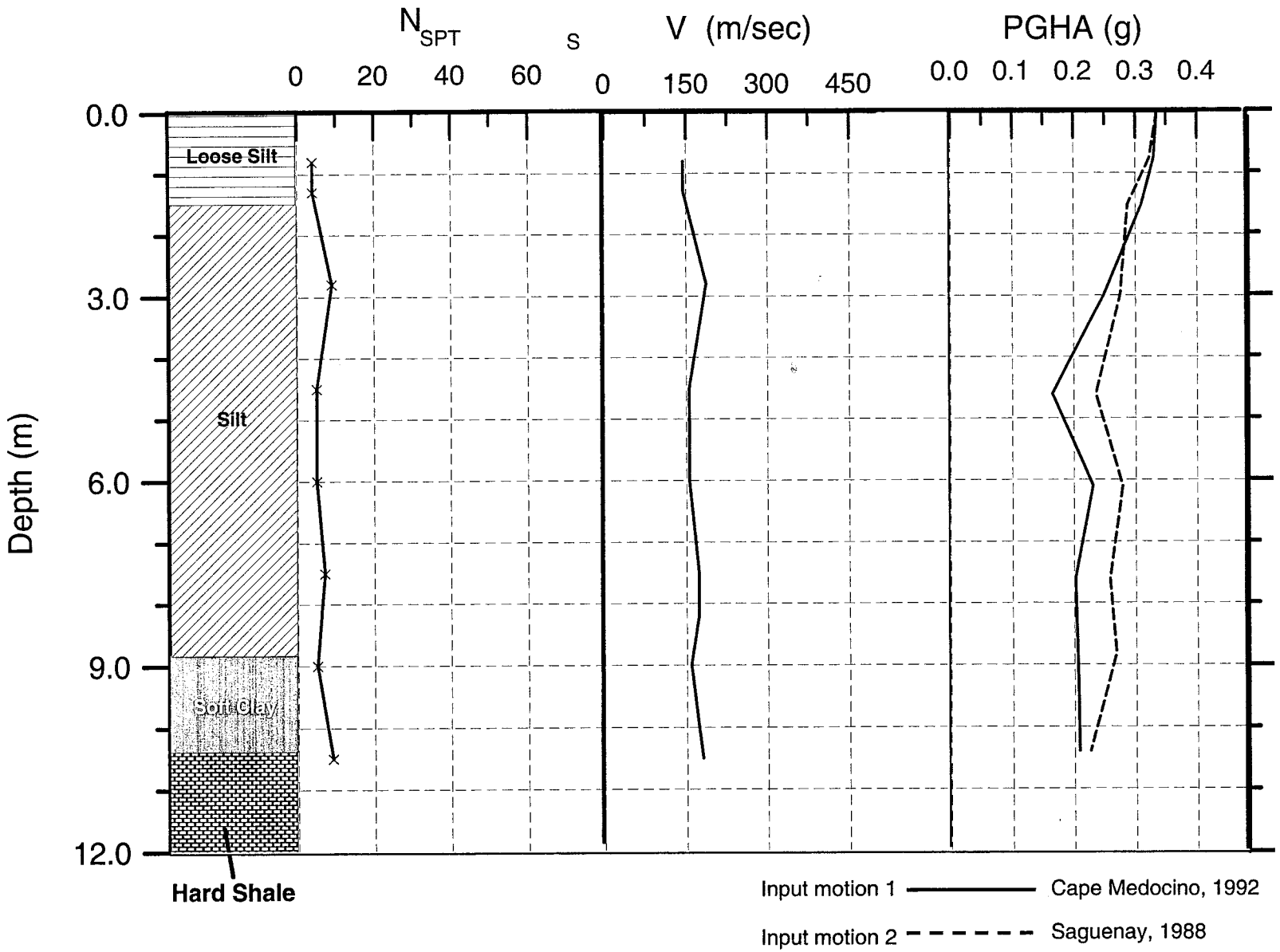

Figure 3.16. Blowcount number (N_{SPT}), shear wave velocity (V_S), peak ground horizontal acceleration (PGHA), and cyclic stress ratio vs. depth at the site GiU41, for a WVFS seismic event.

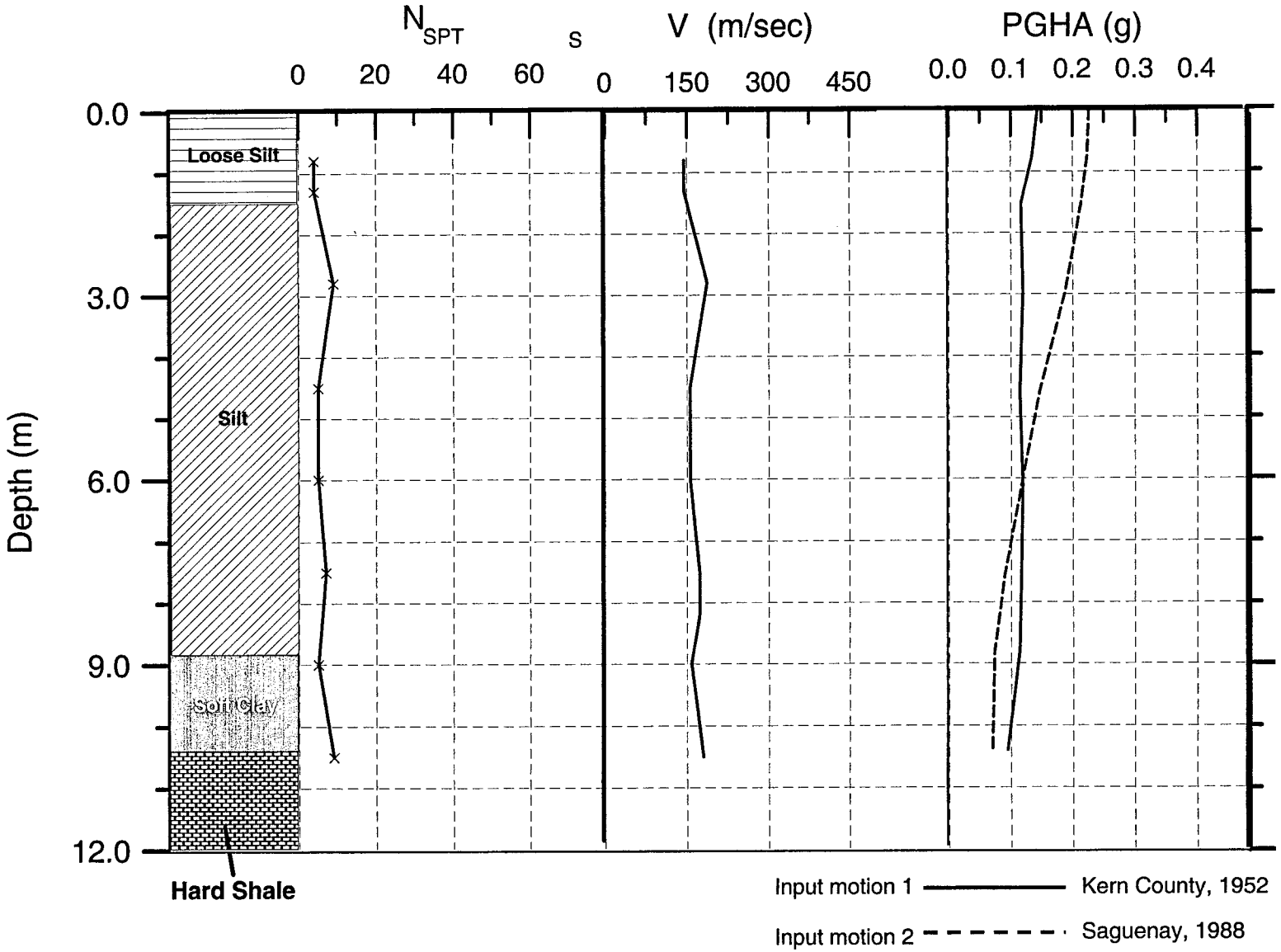

Figure 3.17. Blowcount number (N_{SPT}), shear wave velocity (V_S), peak ground horizontal acceleration (PGHA), and cyclic stress ratio vs. depth at the site GiU41, for a NMSZ seismic event.

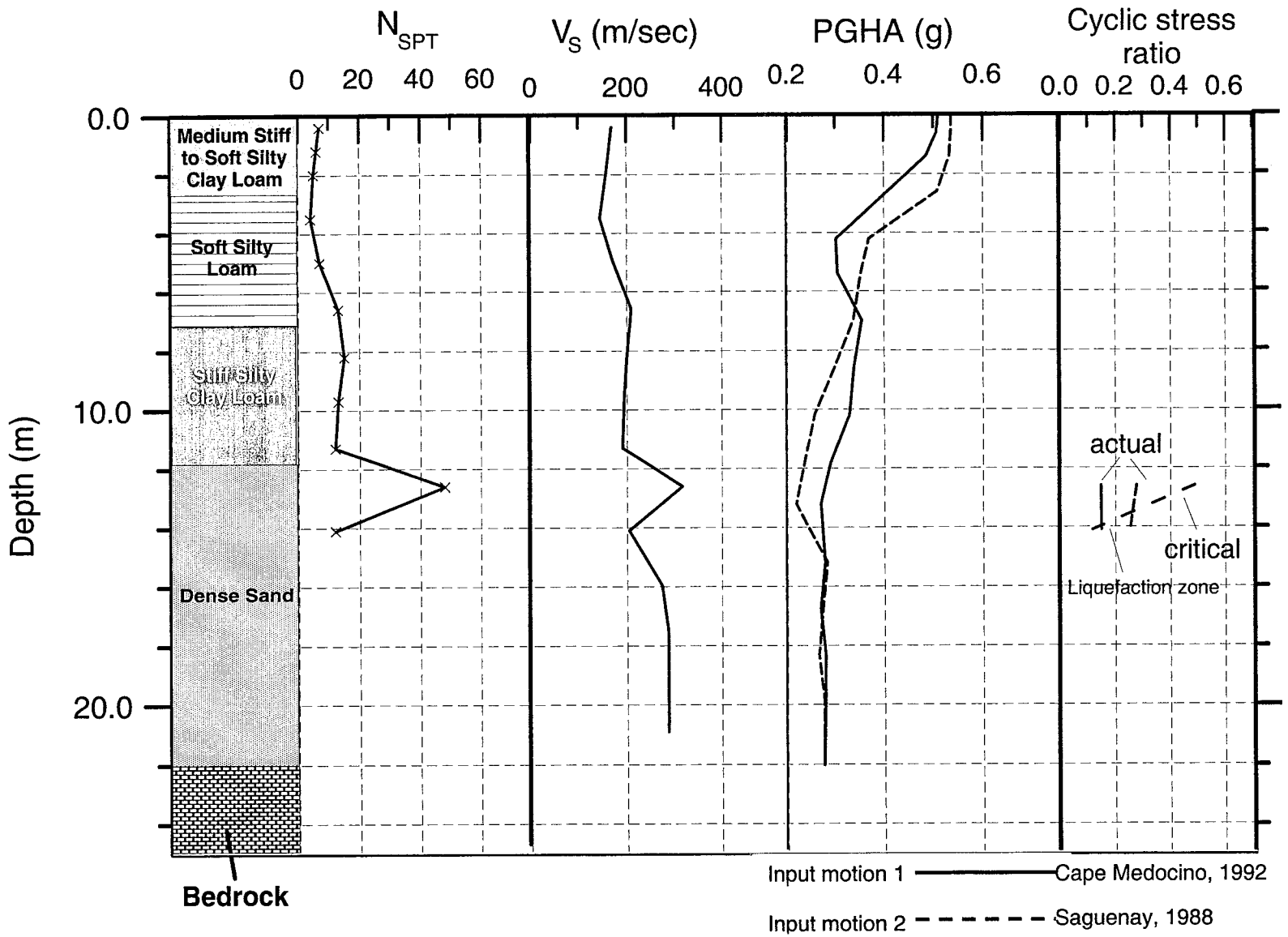

Figure 3.18. Blowcount number (N_{SPT}), shear wave velocity (V_S), peak ground horizontal acceleration (PGHA), and cyclic stress ratio vs. depth at the site PoU68, for a WVFS seismic event.

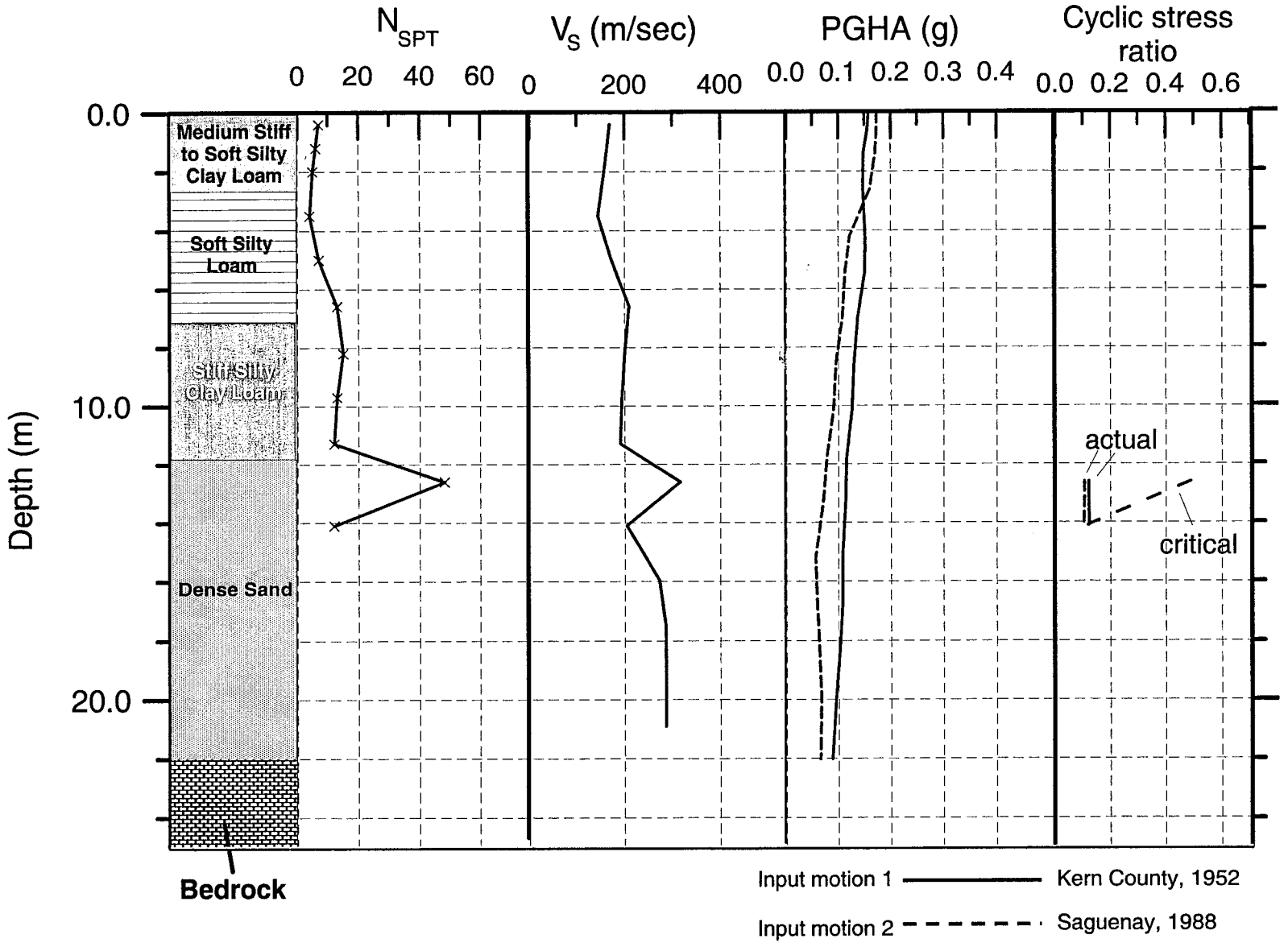

Figure 3.19. Blowcount number (N_{SPT}), shear wave velocity (V_S), peak ground horizontal acceleration (PGHA), and cyclic stress ratio vs. depth at the site PoU68, for a NMSZ seismic event.

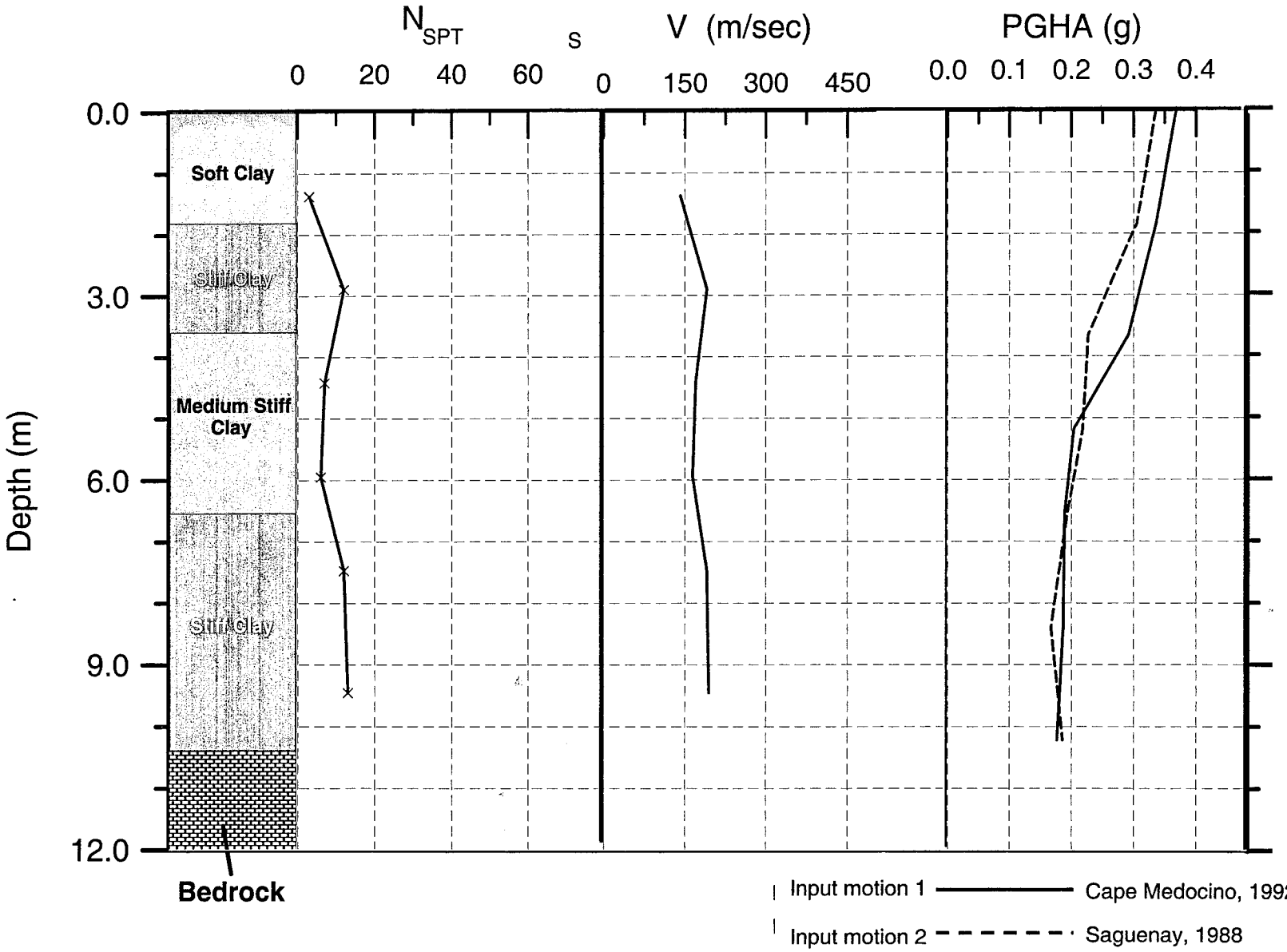

Figure 3.20. Blowcount number (N_{SPT}), shear wave velocity (V_S), peak ground horizontal acceleration (PGHA), and cyclic stress ratio vs. depth at the site EvanHP, for a WVFS seismic event.

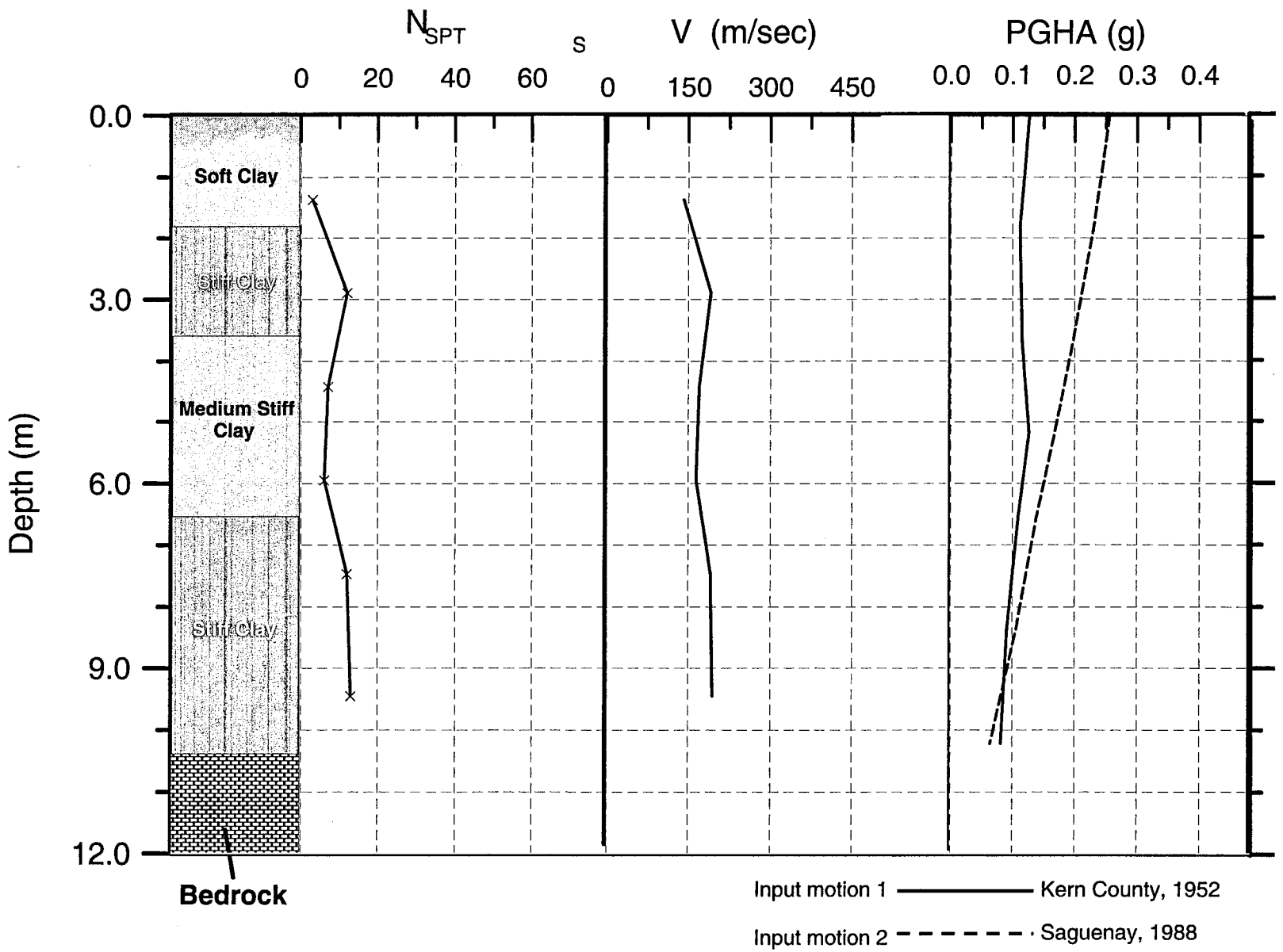

Figure 3.21. Blowcount number (N_{SPT}), shear wave velocity (V_S), peak ground horizontal acceleration (PGHA), and cyclic stress ratio vs. depth at the site EvanHP, for a NMSZ seismic event.

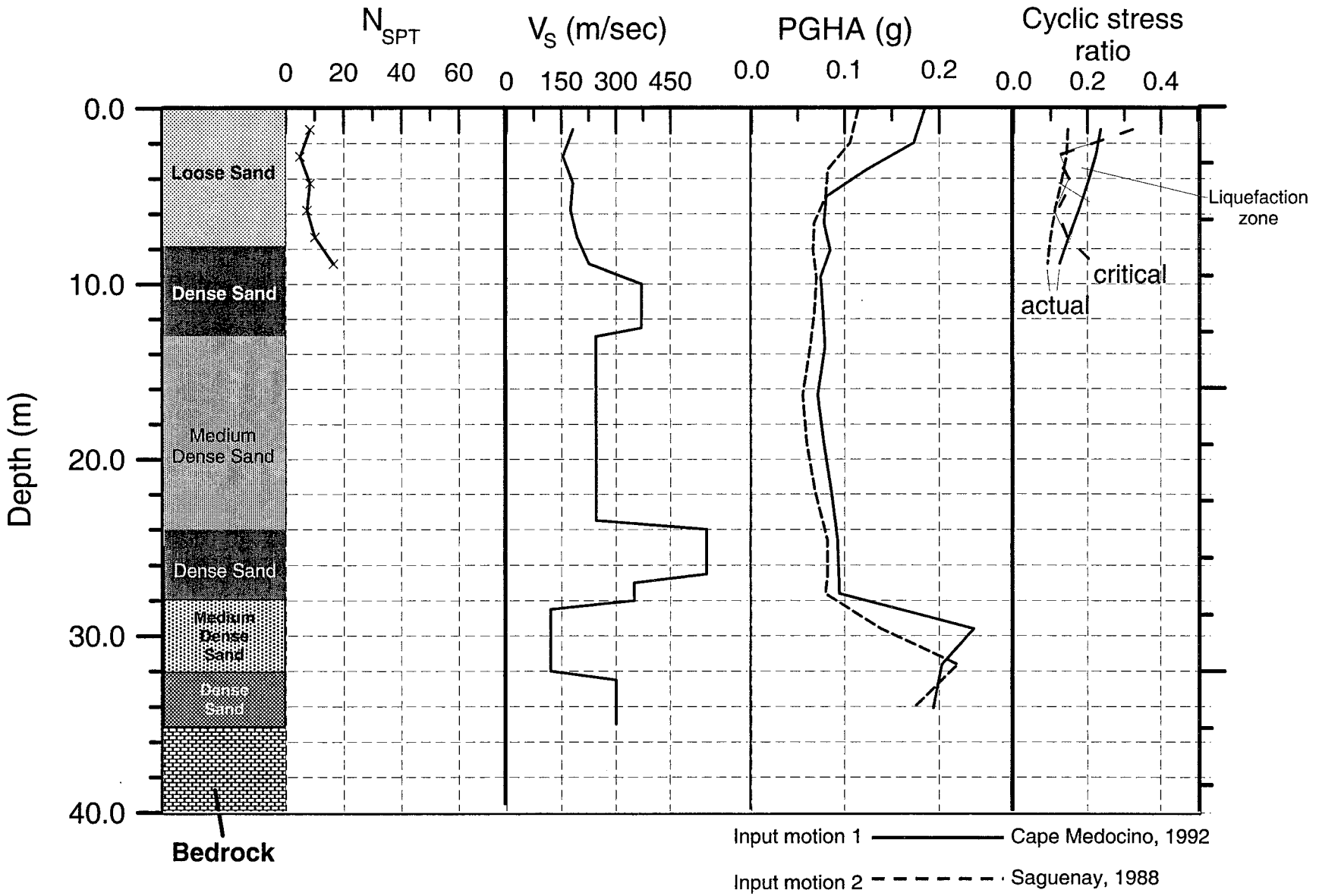

Figure 3.22. Blowcount number (N_{SPT}), shear wave velocity (V_S), peak ground horizontal acceleration (PGHA), and cyclic stress ratio vs. depth at the site EvanWH, for a WVFS seismic event.

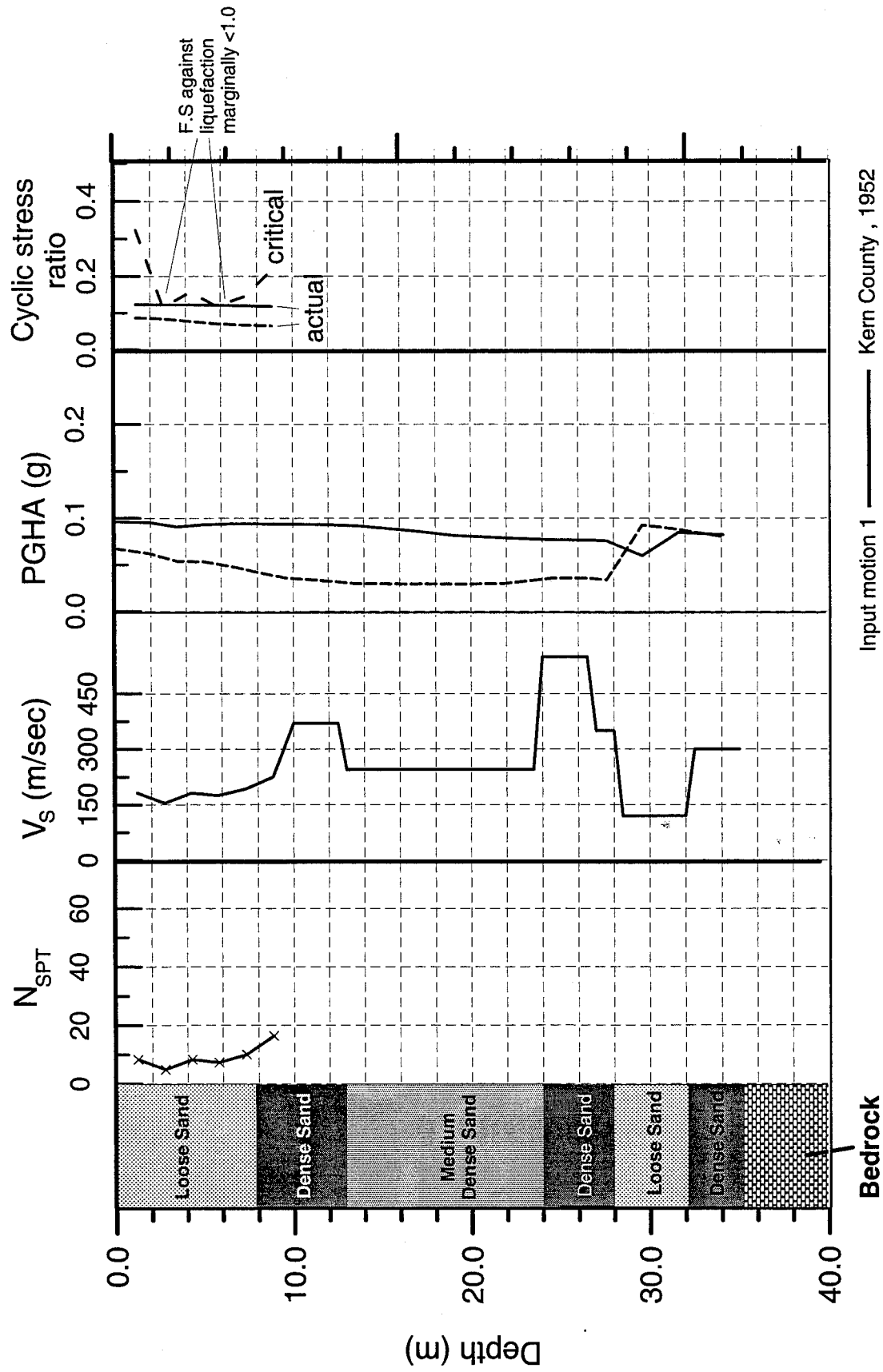

Figure 3.23. Blowcount number (N_{SPT}), shear wave velocity (V_S), peak ground horizontal acceleration (PGHA), and cyclic stress ratio vs. depth at the site EvanWH, for a NMSZ seismic event.

CHAPTER 4: SOIL-PILE INTERACTION AND PILE DAMAGE DUE TO EARTHQUAKE LOADS

Piles are widely used to support heavy and large-scale structures, such as bridges, on soft and deep soil deposits. Their primary function is to provide adequate support against the vertical loads coming from the superstructure. The fact that until recent years the behavior of pile foundations upon seismic loading was not sufficiently understood led to the damage and failure of piles during major earthquakes around the globe, and especially in Japan. Observation of extensive damage on piles, especially in cases of liquefied soil deposits, has led to an increasing need for understanding the failure mechanisms and retrofitting existing foundations and for improving pile design in future projects.

Mizuno (1987) was one of the first researchers who gathered and compiled data of damage to piles during past earthquakes in Japan: Niigata (1964), Tokachi-Oki (1968), Miyagiken-Oki (1978), Urakawa-Oki (1983) and Nihonkai-Chubu (1983). Numerous additional cases of pile foundations that suffered damage during major seismic events can be found in the literature, especially after the Hyogoken-Nambu, 1995, earthquake. In the present study, data concerning pile damage have been collected through an extensive literature survey of actual cases. The collected data include information about pile type, site geometry, soil properties (in the form of N_{SPT} blowcounts), peak ground acceleration at the pile foundation site, as well as information about the type and severity of pile damage. The data is summarized in Table 4.1. and the cases examined are presented in this chapter.

Niigata earthquake, 1964

The Niigata earthquake, in Japan, was one of the first earthquakes that indicated how large the impact of liquefaction could be to civil engineering structures. The city of Niigata sits on primarily sandy soil deposits with thickness in the range of 20 to 30m. This soil formation is very loose with N_{SPT} blowcounts scarcely exceeding 5 down to 10m depth. During the earthquake, there was extensive liquefaction in the saturated loose sand layer. Additionally, the slight inclination of the boundary between liquefied and non-liquefied layers resulted in the development of lateral spreading. Due to liquefaction, the peak acceleration at the ground surface in most parts of the city did not exceed 0.19g.

Steel pipe piles supporting the pier of a road bridge deformed permanently. The diameter of the piles was 0.6m and the steel thickness ranged from 9 to 16mm. The piles were 25m long, with their lower part embedded in the dense sand layer (N_{SPT}>30). The rest of the pile body was surrounded by a medium dense sand layer with N_{SPT} around 10. The residual bending, probably due to local buckling, occurred at 6m from the pile tip, at the boundary between the medium dense and the dense sand layer. The permanent displacement of the pile head was 2m (Tazoh et al., 1987). [case 1 in table 4.1].

Precast concrete piles (PC) with diameter D=0.6m and length of 10m suffered severe damage. The upper part of the piles, in a range of 3.1-3.5m below the cap, was intact without any sign of cracking. At 3.1-3.5m the concrete was heavily crushed and rebars were exposed. Below this depth, horizontal cracks extending across the entire cross-section appeared every 30cm, even at the lower part of pile that was embedded 2m into the denser sand layer. These cracks had an average width of about 0.7-1.2mm. Concrete crushing and rebar exposure occurred also near the interface between the bearing substratum and the sand layer (Tazoh et al., 1987). [case 2 in table 4.1]

Concrete piles (D=0.3m and L=10m) which were supporting a two-story building crushed and flanked out at 2.2m above the bearing stratum and 3.1-3.5m below the footing slabs. Between these depths several circular cracks (5-10cracks/2meters) appeared with a width ranging from 0.7-1.2mm. The damage was caused by liquefaction and lateral spreading of the loose sand layer (Mizuno, 1987; Tazoh et al., 1987). [case 9]

In the case of the NHK building, the pile damage was discovered after some restoration work started much later, in 1980. From a total of 204 PC piles, 74 were investigated; it was found that all of them were similarly damaged. The concrete was crushed at 2.5 to 3.5m from the pile top and 2-3m from the bottom (Figure 4.1). The damage at the bottom was located slightly above the boundary between the loose sand and the bearing stratum. Due to lateral spreading, the ground in the neighborhood of the building moved horizontally about 2m. However, the pile head displacement ranged from 1m to 1.2m [case 3].

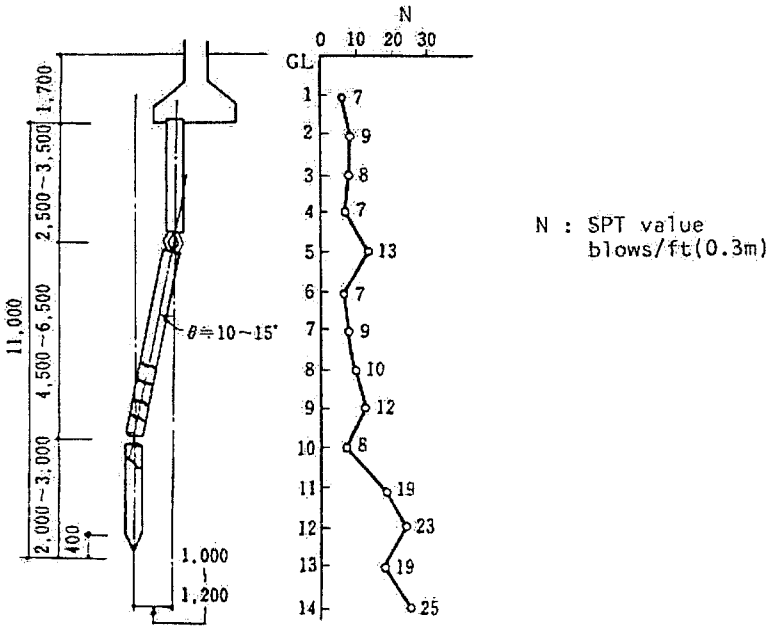

Figure 4.1. Damage to RC piles of the NHK-building, Niigata, 1964 (Kawamura et al., 1985), [case 3]

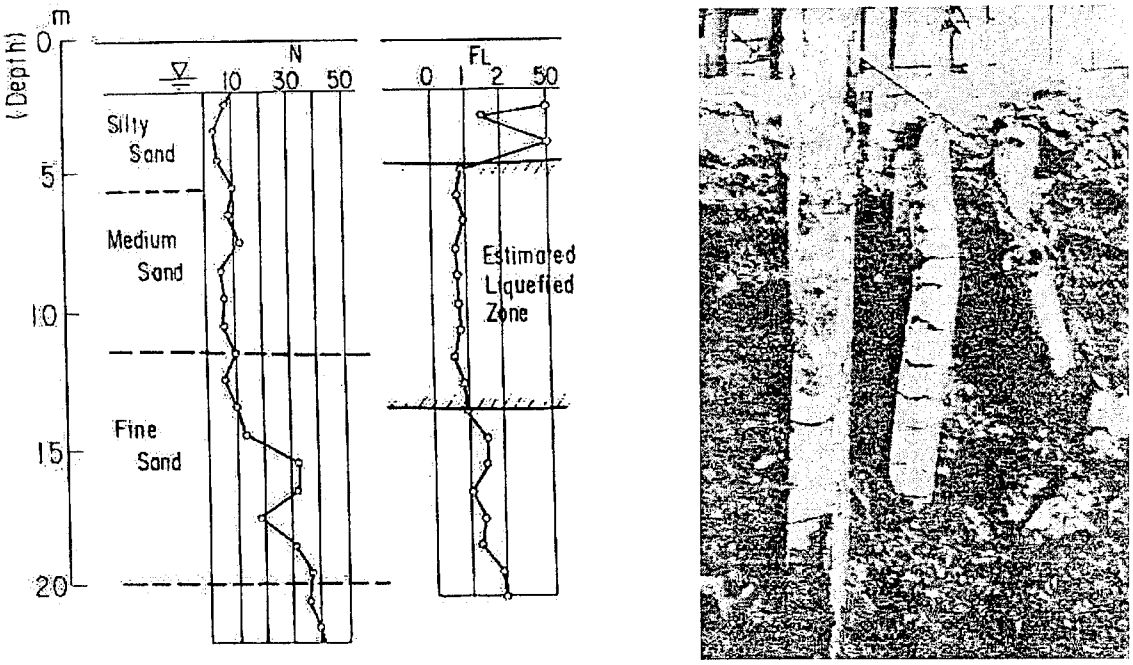

Figure 4.2. Ground conditions and damage to the piles at the Hotel Niigata building. (Kawamura et al., 1985), [case 4].

As in the case of the NHK building, the building of Hotel Niigata was in operation for 23 years after the earthquake despite the fact that the foundation piles were severely damaged. The N_{SPT} blowcounts at the Hotel Niigata were less than 10 down to 13m depth. The surface layer was composed of non-liquefiable silty sand (Figure 4.2). The precast concrete piles of diameter D=0.35m appeared to have horizontal cracks extending through the whole cross-section. The ground around the building was displaced by 4-5m due to lateral spreading (Kawamura et al., 1985). [case 4].

Close to the NHK building, the Hokuriku 10-story building was founded on precast concrete piles having diameter D=0.4m and length L=12m. The ground in the area surrounding the building moved 2m. However, no displacement or tilting of the building took place. The fact that the building efficiently resisted the lateral spreading was due to the large number of piles driven at close distance from one another. The dense arrangement of the piles densified the soil. Two factors helped improve the behavior of the building: the existence of a 6-7m basement, and that the bored piles, constructed at the perimeter of the building to support the excavation during construction, remained in place after completion (Yoshimi, 1990). No damage to the piles was reported. [case 5].

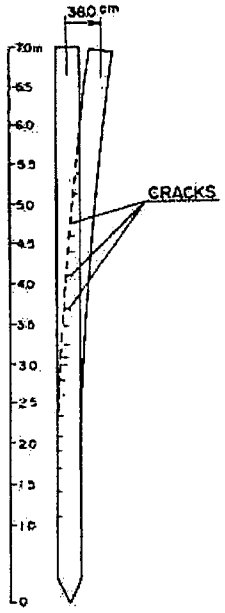

Figure 4.3. Bending cracks on concrete piles of a railway bridge in Niigata, 1964 [case 6].

A railway bridge supported by two piers standing on piles collapsed after a pile head displacement of 0.38m. The concrete piles had a diameter of 0.3m and a length of 7m. After the earthquake, the piles were extracted from the ground, revealing horizontal cracks along the entire length of the piles (Figure 4.3). The cracks, caused probably by the bending moment caused by the permanent head displacement, occurred on one side only. [case 6]

The NFCH building, a 3-story reinforced concrete structure was founded on Reinforced Concrete (RC) piles. The soil profile consisted of a loose sand (N_{SPT} < 10) overlying the bearing substratum (dense sand). The top 2m of the loose sand layer was not susceptible to liquefaction, since the sand was above the water table. Two piles of diameter D= 0.35m

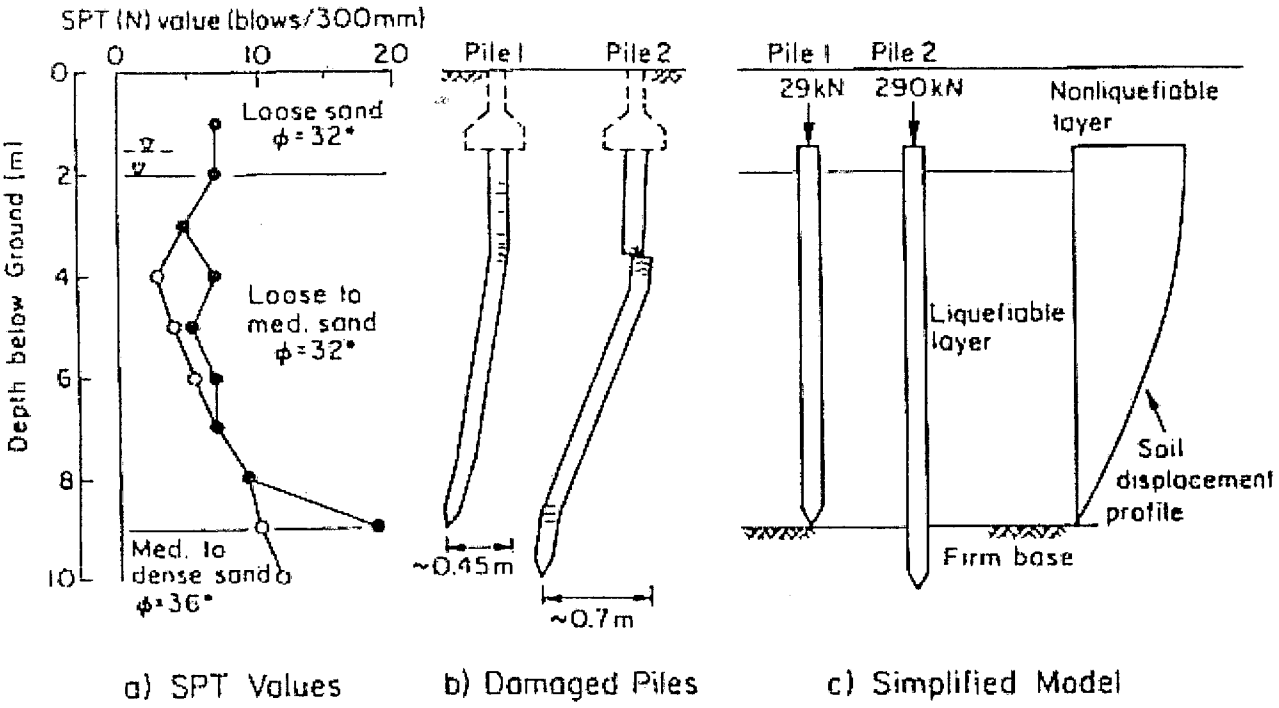

Figure 4.4. Soil conditions and observed pile deformation at NFCH building, Niigata 1964 (after Chaudhuri et al., 1995). [cases 7 and 8]

were fully excavated and examined. One pile (L=9m, pile 2 in Figure 4.4) was embedded into the bearing stratum by approximately 1m, while the tip of the other pile (pile 1; L=7m)

was right above the dense sand layer. Both piles showed damage 2m below the pile head, and approximately 1m below the liquefiable and non-liquefiable soil interface. However the 7m long pile (Pile 1) had horizontal cracks that appeared only on one side, while the 9m pile (Pile 2), which was embedded in the bearing stratum, suffered severe cracking and breakage (Chaudhuri et al., 1995). Additionally, the 9m long pile was damaged at the depth of the loose sand-bearing stratum interface. The permanent displacement of the pile heads induced by lateral spreading was 0.45m and 0.7m for pile 1 and pile 2, respectively. Chudhuri et al. (1995), after performing numerical analyses concluded that liquefaction led to the reduction of the subgrade reaction of the loose sand layer by a factor of 0.02-0.03 of the original value. [cases 7 and 8].

It must be noted that, during the Niigata, 1964, earthquake, buildings supported by friction piles suffered larger damage than buildings supported by end bearing piles; the damage was in the from of severe settlement and tilting. The liquefaction caused a reduction of the friction between the loose sand and the pile and resulted in a significant loss of the pile bearing capacity.

Tokachi-Oki earthquake, 1968

Circular horizontal cracks appeared on precast RC piles supporting a railway bridge. The diameter of the piles was 0.4m and their length ranged for 19 to 32m. The damage was due to lateral movement of the very soft cohesive soil (N=0) extending from the ground surface to a depth of 10m. The permanent displacement of the pile heads was 0.76m. The peak ground acceleration measured in the area was 0.23g. No cracks appeared in areas where the permanent displacement was less than 0.2m (Mizuno, 1987). [case 45]

Miyagiken-Oki earthquake, 1978

The Maruyoshi 3-story RC building was supported by concrete reinforced, precast hollow cylindrical piles (Figure 4.5). The outer diameter of the piles was 0.25m, the thickness of the concrete was 0.05m, and the length of the piles was 5m. The piles were surrounded by a 4m thick layer formation of soft clayey material with $N_{SPT}< 5$, and their tip was embedded in a layer of sand and gravel with $N_{SPT}> 40$. The undrained compressive strength of the clay materials was q_u= 50kPa and the elastic modulus, E= 8.6MPa. The internal friction angle of

the sand (bearing stratum) was ϕ=42° and the elastic modulus E= 62.8MPa. During the earthquake, the peak horizontal ground acceleration at the site inside the Sendai city was approximately 0.3g. After the earthquake, an investigation using phenolphthalein as a tracer revealed that the failure patterns developed during the seismic event and not during pile driving. Only a group of 6 piles of the building's foundation were examined after excavation. Due to the significant inclination of the dense sand layer that underlies the soft clay, the length of the piles ranged from 9m to 18m. Cracking occurred in all piles and along the entire length of the piles, with a maximum crack width of 3.6mm (the larger crack occurred

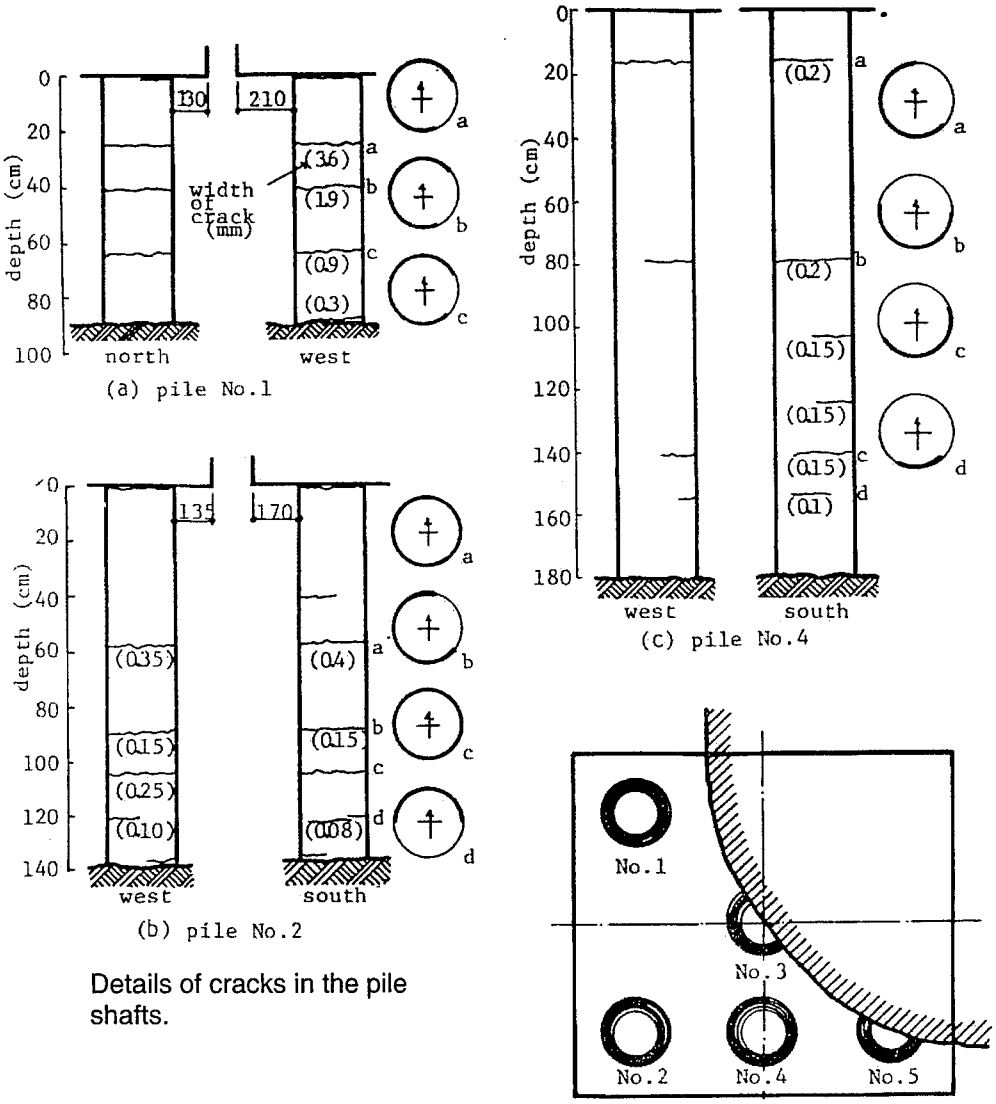

Details of cracks in the pile shafts.

Figure 4.5. Damage to piles of Maruyioshi building, Niigata (after Kishida et al.). [case 11]

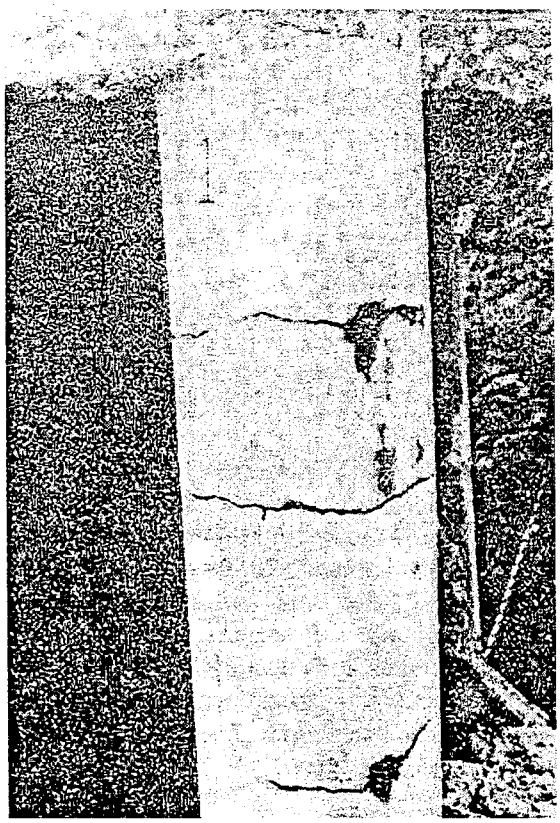

Figure 4.6. Bending cracks on piles of Maruyioshi building, Mihyagiken-Oki, 1978 (after Kishida et al.,1980). [case 11]

Figure 4.7. Crush of the autoclaved high strength concrete piles of Sendai building, Miyagiken -Oki (after Kishida et al.) [case 12]

in the shorter pile, which is placed in the corner of the examined group). The average crack width did not exceed 0.2mm. According to Kishida et al. (1980), the analysis of the Maruyoshi building case suggests that the inertial force due to the response of the superstructure was the major cause of the damage and that the piles would not have suffered any damage if the peak ground acceleration had been limited to 0.1g. (Kishida et al. (1980). [case 11]

Another structure damaged after the Miyagiken-Oki, 1978, earthquake was the 11-story Sendai municipal apartment building. The high strength concrete piles supporting the building were completely crushed at their pile heads (Figure 4.7). The failure of the piles resulted in tilting of the building, which was demolished and reconstructed after the earthquake. (Kishida et al. (1980). [case 12]

Mexico City earthquake, 1985

Most of Mexico city is covered by clayey deposits with water content up to 400% and N_{SPT} = 0. CPT investigations carried out after the earthquake yielded cone penetration resistance of about q_c= 0.5MPa. The 1985 earthquake imposed a maximum ground acceleration of up to 0.2g at sites located in the lake zone III (SCT), where the soil profile is composed of older lake deposits down to a depth ranging from 20 to 40m. Generally, in Mexico City end-bearing piles performed satisfactorily. Friction pile foundations suffered two types of failure: a) sudden settlement or b) permanent tilting and collapse. The first type was observed in the case of a 10 story building supported by piles with diameter 0.3 to 0.6m and 28m long. In another case, a building founded on 0.4m-diameter, 22m-long piles, tilted due to inertial moments and collapsed, pulling the piles out of the ground. The short piles of this foundation were working below their limit capacity under static conditions. According to Mendoza and Auvinet (1988), it is possible that the adherence between clay and pile was reduced during cyclic loading, leading to a reduction of the bearing capacity of friction piles. [case 13]

The head of the piles supporting a 16-story building were crushed and the steel was exposed. The building was sitting on the soft Mexico City clay layer with a thickness of 32.5m. The 36m long piles were embedded in the hard silty sand layer. The precast piles had rectangular cross-section with dimensions 0.3m x 0.4m. It should be noted that the slab where the piles were connected was on the ground surface and in some locations a little above it. At that shallow depth the piles experienced very large stresses due to the response of the superstructure (Ovando-Shelley et al., 1988). [case 14]

Loma Prieta earthquake, 1989

Piers consisting of pile bents supporting a highway bridge were crushed at the connection with the lateral beam. About 5m of the upper part of the piles were unsupported. The piles, having a diameter D = 0.38m, were embedded in soft cohesive soil. The peak ground surface acceleration at the site exceeded 0.2g. Due the response of the piles, a gap 60cm wide was formed between the piles and the cohesive soil, which indicates that the piles moved significantly. Investigators assessed that the piles were also cracked at depth (Iwasaki, 1990). [case 15]

Hyogoken-Nambu, Kobe earthquake, 1995

The Kobe earthquake was a unique case of earthquake induced damage to piles since all types and possible causes of damage were observed after this event. A dense infrastructure network, extending from the shallow and stiff deposits near the mountains to the thick liquefied reclaimed lands at the port of Kobe, was mostly supported on pile foundations. A large number of deep foundations was systematically investigated through either direct excavation and observation or borehole television systems lowered inside the piles. Non-destructive methods were also used such as velocity logging, impact wave and electromagnetic wave methods.

Railway bridges. Piles supporting the piers of the elevated bridge of Kobe Port -liner were found slightly cracked near the pile head. The reinforced concrete piles with diameter D= 1.5m and length 26m were embedded in a medium dense to dense sandy layer (N_{SPT} = 10-30) with 1.5m thick layers of clay. This formation was not liquefiable, [case 16]. Similar failure patterns were observed in the case of the Hankyou Railway bridge, although the 14m long piles with diameter 1.3m were embedded in a denser soil (N_{SPT} =20-40), [case 18]. Slight damage occurred to the superstructure (single pier and girder) of a Japanese Railway elevated bridge. However, after an investigation, the cast-in-place piles with diameter D= 0.6m appeared to be intact, [case 17]. The railway bridge piers that were damaged were located in an area with shallow and stiff soils where the acceleration was close to 0.82g.

Kobe line, Hanshin Expressway. A bridge pier of the Hanshin Expressway was founded on cast-in-place piles, having a diameter D = 1m and a length L = 14m. Cracks occurred near the pile head with a width of about 2mm. The concrete was not crushed and the reinforcement did not buckle. No damage occurred to the superstructure (single pier and girder). The foundation did not suffer severe settlements, pile body failure, or failure of the reinforcement. The soil was relatively stiff, similar to the soil at the Hankyu railway bridge. From loading tests (axial and lateral) it was found that despite a stiffness degradation at the top of the piles, the bearing capacity and the horizontal resistance of the piles were not affected significantly. However the test loads were applied statically. The actual strength of the concrete was f_c=41.7MPa, while the strength of the steel was f_s=367.9MPa (Okahara et al., 1996). [case 19]

Wangan line, Hanshin Expressway. The Wangan line was constructed on reclaimed land that was liquefied during the earthquake, and lateral spreading shifted piers and the surrounding grounds towards the waterfront. The 14 meter thick reclamation stratum was underlaid by a soft alluvial clay layer with N_{SPT} less than 6. The embedment length of the reinforced concrete piles inside the stiff sandy substratum ranged from 7 to 12m. Within a depth of 5 m below the pile cap, there were cracks with a width of 1 to 4mm. The total crack width in this area was 8.6mm, equivalent to a width of 1.7mm/m. Cracks appeared in the piles inside the clay layer and concentrated near the interface between the clay and the sand or between the clay and the reclamation soil; the cracks had a width of 0.3 to 1mm. In cases were the reclaimed land was better compacted (N_{SPT} up to 20), the cracking near the pile head was less dense (Okahara et al., 1996). [case 20]

No. 5 Bay Route, Hanshin Expressway. Pier 211 was only 30m from the quaywalls. The cast-in-place concrete piles had a diameter of 1.5m and were 34m long. Excavation around the pile heads revealed several vertical and horizontal cracks a few millimeters wide down to a depth of 1m from the pile head. Cracks were also detected down to a depth of 23 to 24m. The density of cracking showed a peak right above the interface between liquefiable reclaimed land (20m thick) and a soft silt layer 15m deep (6cracks/2m), and right above the interface between a stiff sand layer (bearing stratum) and a ductile sandy silt at 25m depth (5cracks/2m). The pile top was rigidly plugged into the foundation slab providing a fixed connection. The severe cracking (0-3m depth) might have been induced by the high inertial forces during intense shaking rather than by lateral spreading. Near the interface between the stiff sand and the silt, the cross sectional area of the reinforcement was reduced; this may be an extra factor for the damage that occurred at this depth, (Ishihara, 1997), [case 21]

Buildings in Port and Rokko island. Port and Rokko are two artificial islands constructed by deposing reclaimed land (mainly granular material) on the seabed. Lateral spreading due to liquefaction occurred in both artificial islands because of the loose state of the fill deposit (N_{SPT}< 10). Relative displacement between the pile top and the bottom exceeded 30cm and imposed a shear strain larger than 2%. This caused failure right below the pile cap and right above the stiff bearing layer. A four story building supported by prestressed concrete (PC) piles settled and tilted towards the sea. Excavation around the pile heads

revealed compressional and shear failures on the sea side with minor flexural cracks on the opposite side. The peak ground acceleration at the reclaimed land site did not exceed 0.33g, due to the deamplification effect caused by liquefaction; (Tokimatsu et al., 1996), [case 22]

Two buildings in Port island away from quaywalls. The two buildings were about 260m from the nearest quaywall. Thus, lateral spreading was insignificant at that distance and it was not the cause of failure. In one of the two piles investigated under building D (Pile 1; figure 4.8), dense cracking appeared few meters below the pile head. Horizontal cracks occurred also near the silty clay-liquefied fill interface. However some cracks occurred in the middle of the loose fill and soft clay layers. The second pile (Pile 1) had no cracks below the fill. The damage was located below the cap and in the middle of the liquefied fill layer (yielding moment 180KNm). This might be due to the fact that the fill layer, at a depth of 10m, shows an increase of stiffness (non liquefiable). No damage appeared to the piles of the second building (building C in figure 4.8.), which had prestressed piles 0.5m of diameter with steel jacket on the upper 8m; (Fujii et al, 1998), [case 23,24]

Permanent deformation of steel pipe piles. Steel pipe piles in Port island, with a diameter of 0.4 to 0.5m and 42m length, penetrated the liquefiable fill material (18m thick) and the soft silty clay layer (14m thick) down to the stiff gravelly sand substratum. Ground shaking and liquefaction were accompanied by lateral spreading, which resulted in a permanent head displacement of 0.34m. The residual deformation, probably due to local buckling occurred 15m from the pile head, which coincided with the location of the liquefied fill-soft silty clay layer; (Oh-Oka et al., 1998), [case 25].

Building on reclaimed land. The building located in Fukaehama was placed 350m from the nearest quay wall. The piles had a diameter of 0.45m and a length of 18m. Dense cracks of small width (7cracks/2m) on the one side of the pile appeared at a depth of 3-6m. A large circular crack occurred at a depth of 8.5-9.5m (liquefiable layer- silt clay interface) (Figures 4.9 and 4.10). The yield moment of the pile was 216kNm at a curvature of $0.012m^{-1}$ and the

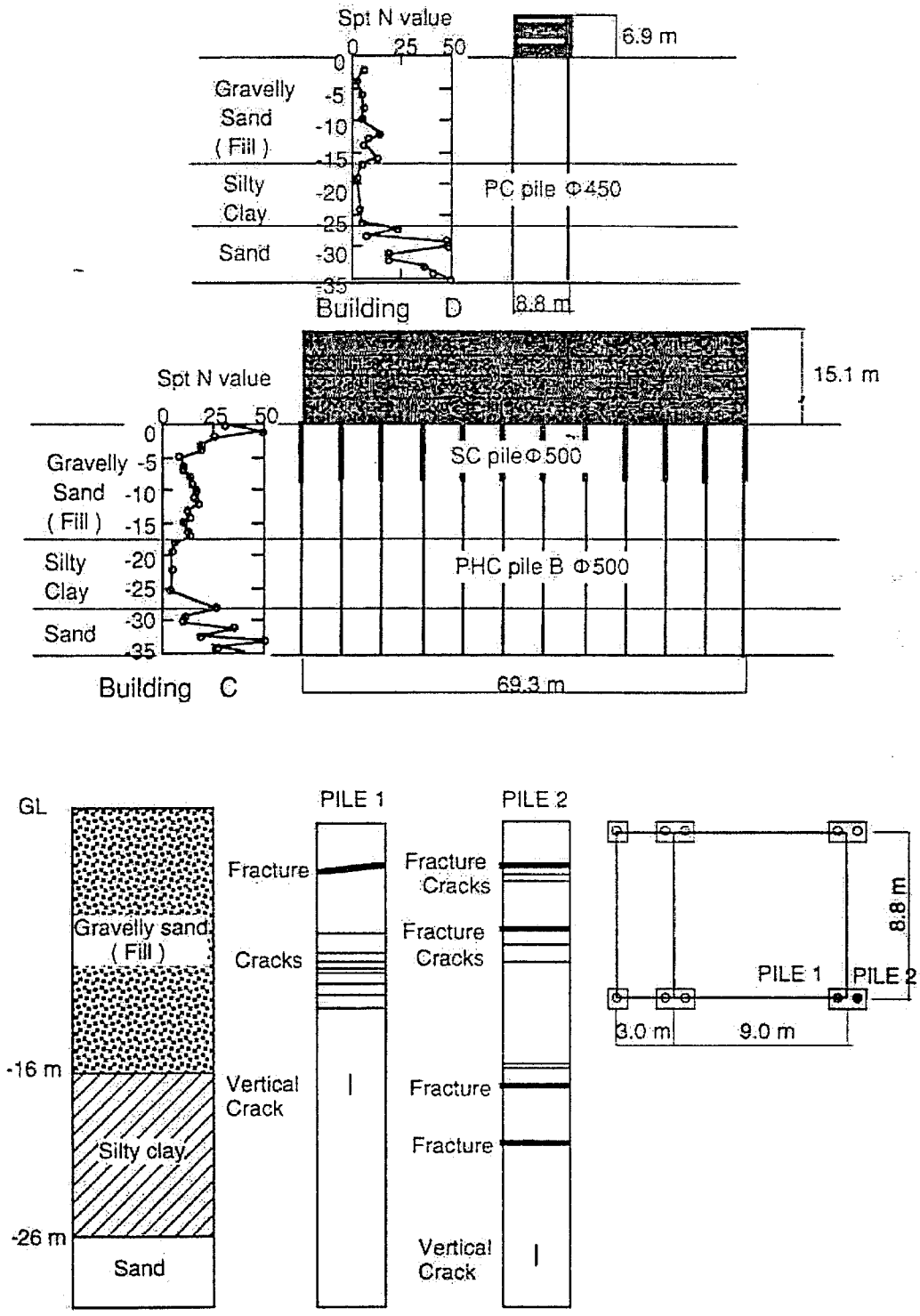

Figure 4.8: Damage to piles of buildings on port island, Kobe (after Fujii et al., 1997), [cases 23, 24]

crushing moment was 232kNm at a curvature of 0.022m^{-1}. Analyses performed showed that if the horizontal loads to the pile head from the superstructure had not been applied, the shear stresses at the pile head would had been less than half. However, the bending moment would had been almost of the same magnitude; (Fujii et al., 1998), [case 26].

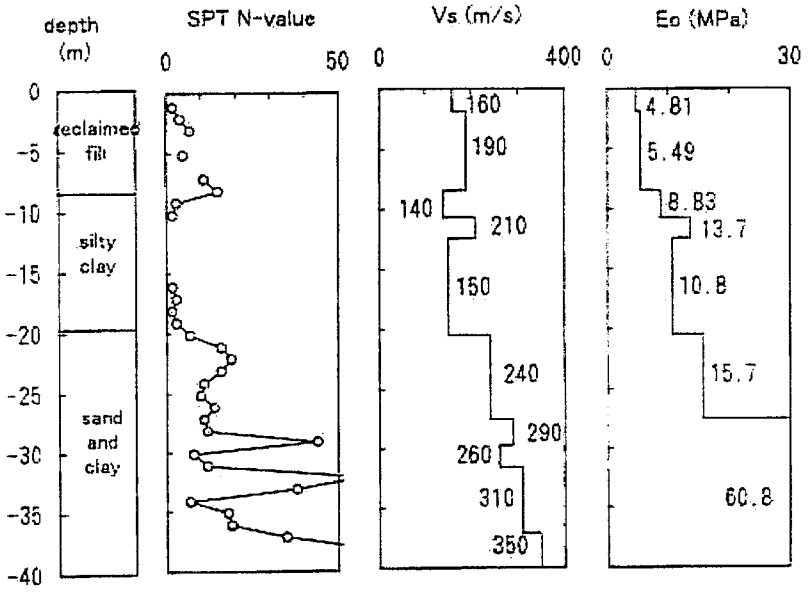

Figure 4.9. Soil profile under building on reclaimed land, Kobe (after Fujii et al.,1998); [case 26]

Buildings in Higaishinada-ku. Severe shear failure took place at a depth of 4.5m on piles supporting a three story building, on the sea side. The precast concrete (PC) piles had a length of 17m, and penetrated to the stiff gravely sand substratum. At a depth of 9m, near the interface between liquefiable and natural soil deposits, cracks formed on both sides of the pile. (Tokimatsu et al., 1996), [case 27]

Higashinada sewage treatment plant. The fill layer 12m-15m thick under the sewage treatment facilities was not improved during construction. It was estimated that about 44% of the piles surveyed under the sedimentation and aeration tank had been damaged at the depth of the contact between the liquefiable layer and a soft clayey deposit. At a depth of 3m from the head, the PC piles, of diameter 0.4m and length 23m, suffered overall breakage. Cracking occurred at a depth corresponding to the bottom of the liquefiable layer. Cracks at 3m depth were more than 10mm wide; (Nakayama et al., 19980), [case 28].

Buildings over alluvial fans. Numerous multi-story buildings sitting on alluvial fans suffered severe damage. Pile heads were crushed due to shearing and compression generated by the superstructure's inertial loads (Figures 4.11 and 4.12). In these cases there was no liquefaction and the failure was induced possibly by the pile-soil-building response and the

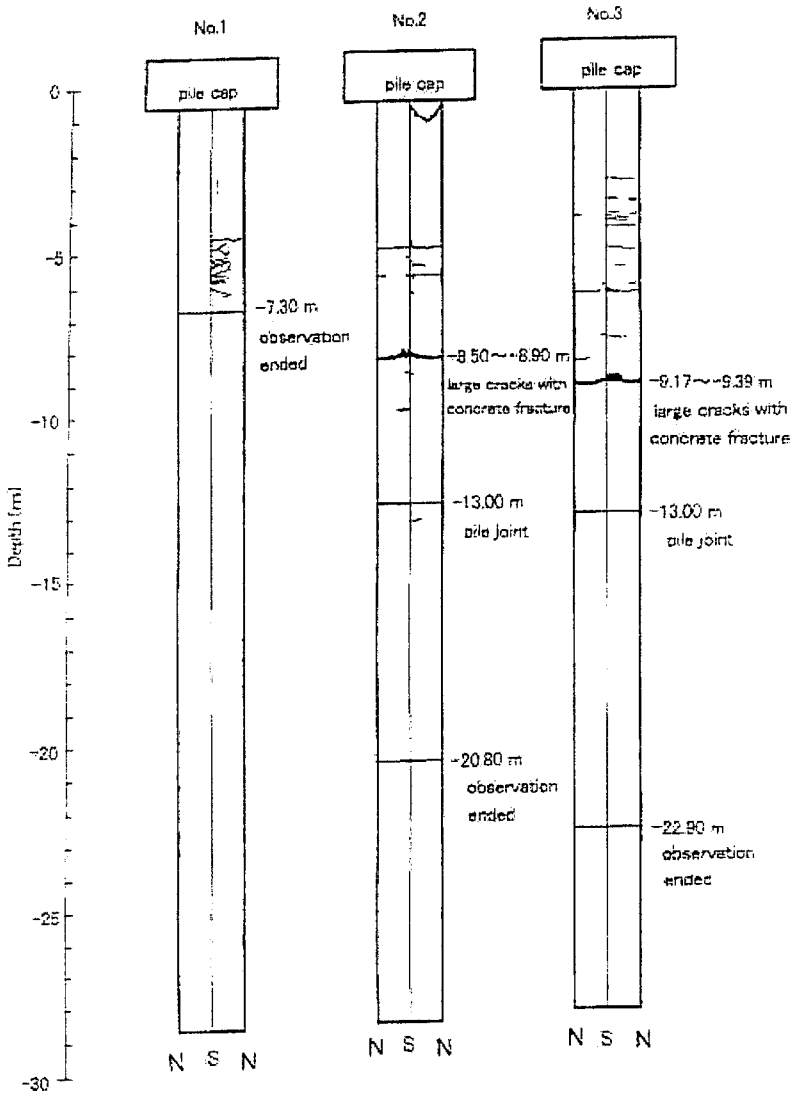

Figure 4.10. Pile damage on building sitting on reclaimed land, Kobe (after Fujii et al.,1998). [case 26]

different stiffness of the supporting layers. Unfortunately, several of these cases were not well documented and could not be included in the processed database; (Tokimatsu et al., 1996).

Buildings in Ashiyahama. Although excavated pile heads appeared sound, integrity sonic tests suggested that the piles of a school building had been damaged at depths between 6 and 15m, just above the interface of liquefiable-non liquefiable layers. The head of the PC piles was displaced by 0.8m while the displacement of the surrounding soil was 1.6m; (Tokimatsuet al., 1996), [cases 29,30]. The buildings of a waste disposal facility suffered minor or no damage. However, the cast-in-place piles with diameters 1.0-1.2m (Figure 4.13) were severely cracked (cracks more than 10mm wide) near the pile head and near the interface of liquefiable (loose sand) - non liquefiable layers (soft silty clay) at about 10m depth; (Tokimatsu et al., 1996), [case 31].

LPG storage facilities at Mikagehama Island. The large LPG storage tank No.101, founded on cast-in-place piles 1.1m of diameter and 27m long, did not suffer any significant settlement or tilting, despite liquefaction and lateral spreading in the sand fill layer. Although the tank was located only 30m from the revetment line, the piles suffered no damage because they were embedded about 6m in an unliquefiable stiff layer. The tank and the installations founded on piles that had a length less than 20m (RC and PC), suffered severe tilting. Revetments and quay walls moved laterally 1 to 2m seawards. Ground displacement due to lateral spreading and due to the movement of quay walls was observed at a range of 100-200m from the waterfront. Two smaller tanks, only 20m from the quaywalls suffered significant damage. The piles (20m long) of the tank TA 107 which was closer to the quay walls showed dense horizontal cracks (1crack/0.2m) along the inside wall, while the piles of TA 106 had less intense damage. The cracks developed predominantly at a depth between 5m and 10m, almost in the middle of the liquefied soil stratum which was 17m thick. The pile head moved about 50cm towards the sea. The damage investigation survey stopped at 10m depth due to technical reasons; (Ishihara, 1997), [cases 32, 33, 34, and 35].

Buildings in Fukaehama. A 5 story building was founded on PC piles with steel jacket that extended down to 6m depth. The pile diameter was 0.5-0.6m and the length was 33m. The thickness of the reclaimed land at the site was 10m, while the soft clayey layer extended

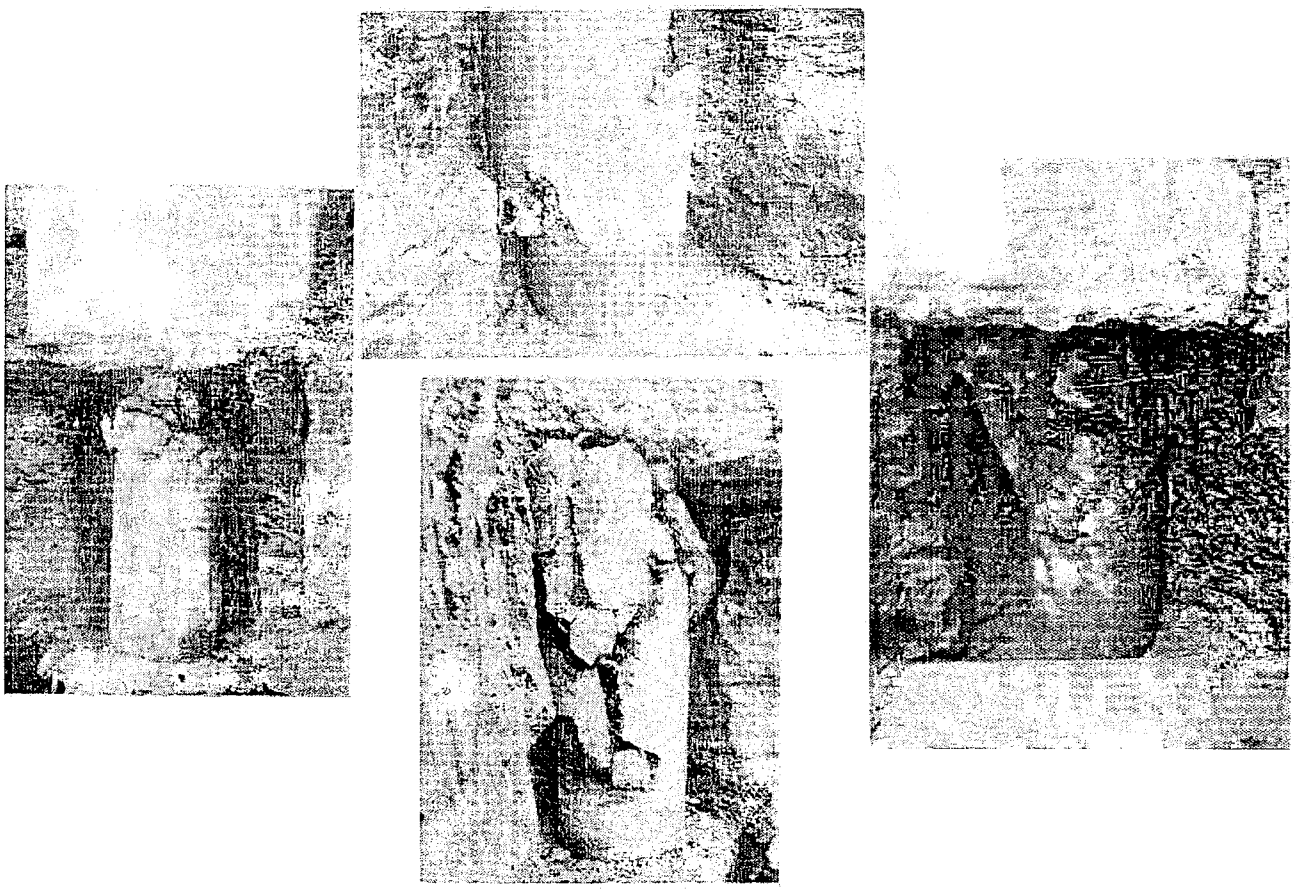

Figure 4.11. Compression and/or shear damage of pile heads in Takatori, Kobe, due to inertial loads applied by the 12-story superstructure. (after Mizuno, 1996)

Figure 4.12. Crushed pile head in building under alluvial fan, Kobe (after Tokimatsu et al., 1996).

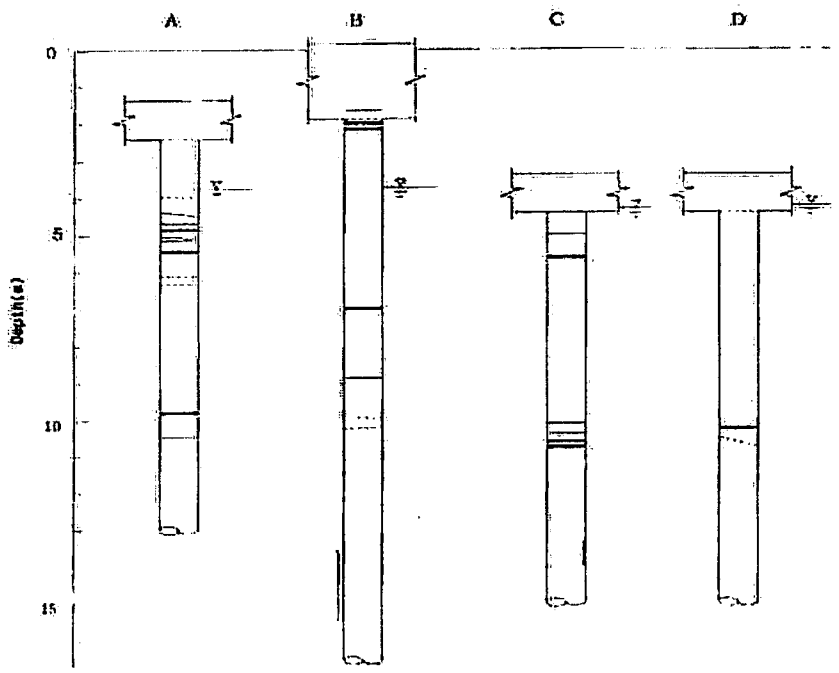

Figure 4.13. Damage of cast-in-place piles in Ashyihama, Kobe (after Mizuno, 1996). [case 31]

down to 23m. The damage was limited only to the liquefied fill-soft clay interface in the form of few horizontal cracks. The same type of piles with the same geometry were installed on a nearby building. Despite the absence of a superstructure, damage occurred near the interface between liquefied fill-soft clay. The pile heads in both cases were not displaced; (Tokimatsu and Asaka, 1998), [cases 36, 37]. Prestressed concrete piles (D=0.4m and L-20m) of a 3-story building suffered dense cracking at the interface between liquefied fill and soft silty clay, as well as at the middle of the liquefied layer; (Tokimatsu et al., 1997). Numerical analyses suggested that the response of the superstructure alone (no ground response) was not capable of generating the failure of the pile observed at the loose sand-soft clay interface; (Figure 4.14), [case 38].

Buildings in areas other than Port or Rokko island. Buildings supported on end bearing piles tilted because of shear failure near the pile head due to the overturning moment imposed by the superstructure. Buildings supported on friction piles suffered from tilting and significant settlement, due to bearing capacity failure caused by soil liquefaction. In Fukuehama, steel piles appeared to have tilted a little but minor damage occurred at the

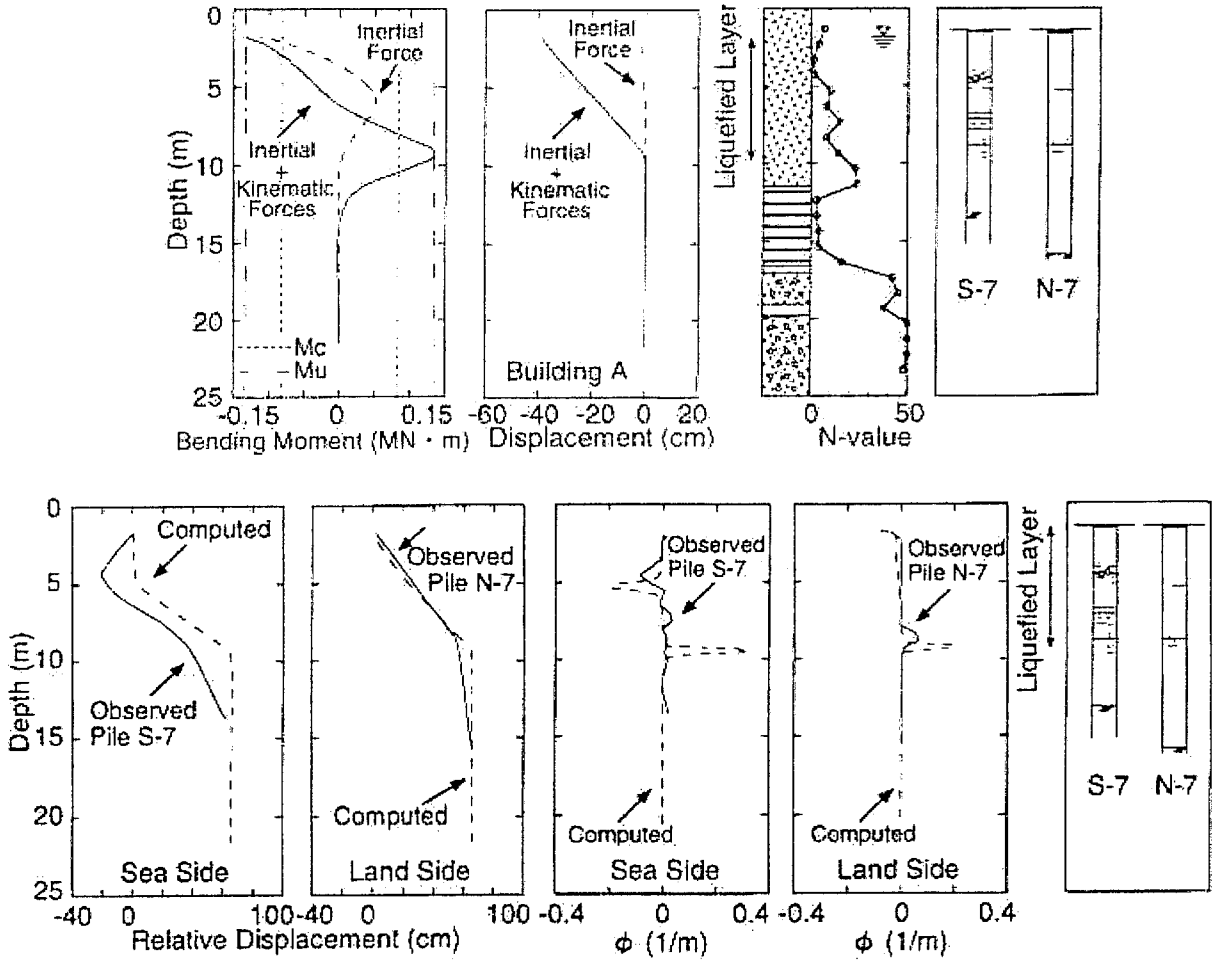

Figure 4.14. Numerically computed and observed displacement, bending moment and curvature of the piles of the building in Fukaehama, Kobe, (after Tokimatsu et al., 1997). [case 38]

connections between the pile cap and the pile head. However, steel pipe piles performed better than concrete piles because of their ductility; (Tokimatsu et al. 1996), [case 39]. A building under construction suffered dense cracking of its cast-in-place piles, especially near the pile head, although the diameters of the piles ranged from 1.2-1.7m; (Figure 4.15.). Some cracks appeared at the interface between liquefied sandy fill and soft silty clay. The lateral spreading of the ground surrounding the building reached 2.5m. However the pile head was displaced by only 0.9m; (Tokimatsu and Asaka, 1998), [case 40].

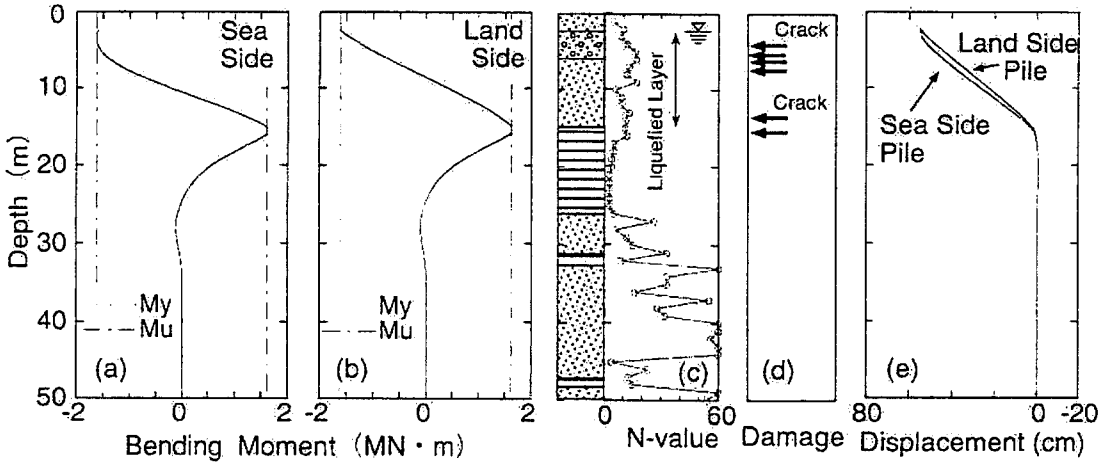

Figure 4.15. Soil profile, bending moment, displacement profile and damage on piles of a building under construction, Kobe (after Tokimatsu and Asaka, 1998). [case 40]

Freezer warehouse. This structure was located on reclaimed land when liquefaction took place. Cracks of maximum width 1mm appeared 30cm below the PC pile top, (Figure 4.16). The directionality of the damage was not clear and the permanent lateral displacement insignificant. The pile failure was probably caused by vibration rather than lateral spreading. The pile investigation did not extend in depth; however numerical analyses suggest that the cracking took place also near the interface between the liquefiable and the non-liquefiable layers, (Figure 4.17). The cracking moment of the piles was approximately 100kNm; (Fujii et al., 1996), [case 41].

Revetment on the Kanzaki River. Revetment in Osaka was founded on precast concrete (PC) friction piles having diameter of 0.35m and length of 7m. The soil profile consisted of a 4.3m thick layer of alluvial loose sand under a layer of 5.3m thick. During the earthquake, liquefaction and lateral spreading of the loose sand layer occurred. As a consequence, the revetment settled and tilted by 2 to 3 degrees. Horizontal cracks formed near the pile head with a density of 7-9 cracks/meter; [case 42].

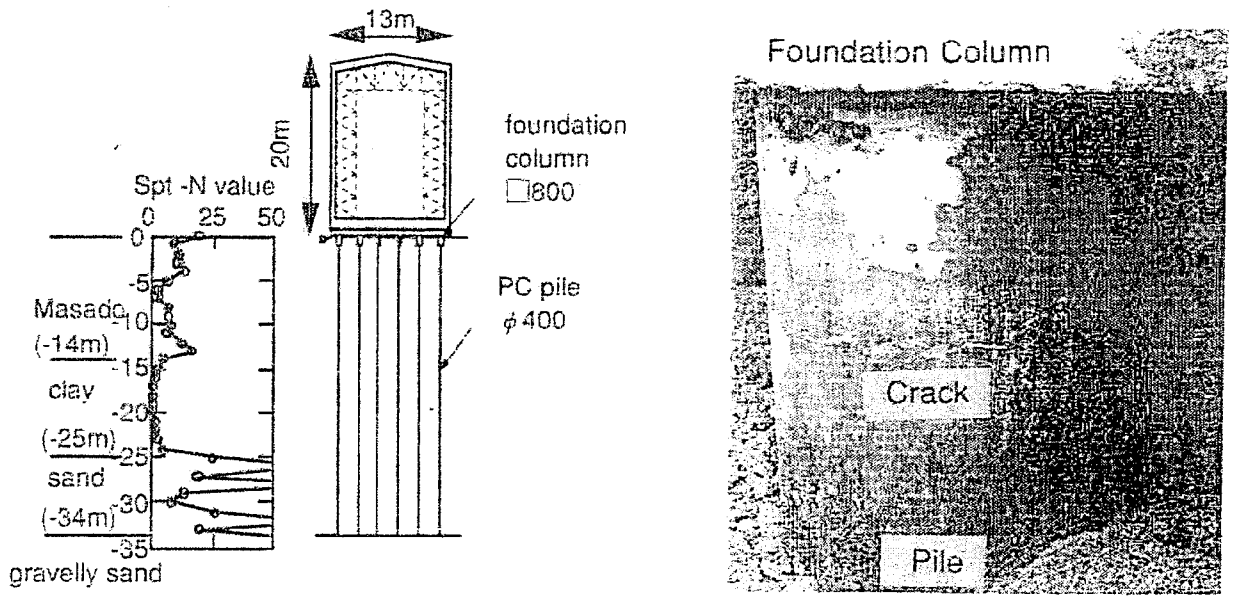

Figure 4.16. Soil profile, structure and damage on pile foundation of freezer warehouse, Kobe (after Fujii et al., 1996). [case 41]

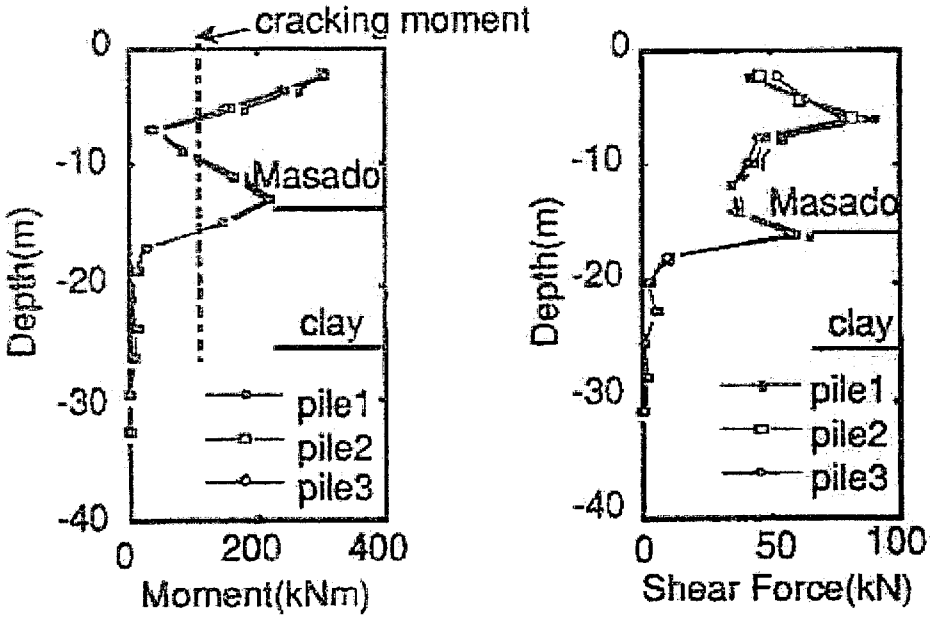

Figure 4.17: Moment and shear force calculated form numerical analysis on piles of freezer warehouse, Kobe (after Fujii et al., 1996). [case 41]

It should be noted that not all cases of pile damage are reported in the literature. Apparently undamaged foundations are not investigated due to lack of interest. There are many examples of foundations near damaged piles that were in the same ground conditions and had similar dimensions but experienced insignificant or no damage. Even piles in the same pile group suffered different degrees of damage. This is indicated by the research of Matsui and Oda (1996) and Okahara et al. (1996) who collected a large amount of information on the foundation of the piers of highway bridges. On the Kobe Route most of the piles investigated were undamaged and only 16% suffered slight cracking. The severe and heavy damage was concentrated on soft soils or on reclaimed lands due mainly to liquefaction and/or lateral spreading rather than to seismic motion. The occurrence of damage is strongly sensitive to local site conditions and to the applied loads. The data collected is useful to give an indication of under what conditions a pile might be susceptible to damage. The field cases presented above combined with the database of Mizuno (1987) [cases 43 to 59] are summarized in the following tables.

Case No.	Case	Pile Type	Superstructure	Diameter (m)	Length (m)	Type of soil	Soil properties	Seismic acceleration	Damage	Cause of damage	Head permanent disp. (m)	Free Field residual disp. (m)
1	Niigata, 1964	Steel	Bridge	0.6/12mm thick	25	Sand Coarse-Fine	Coarse (0-19m) N=4-11 / Fine (19m-) N=30	0.16g-0.19g	Local buckling / residual bending 6m above pile tip	Liquefaction/Ground shaking		2
2	Niigata, 1964	RC precast	Building	0.6	10	Clay (0-10m)/Sand (>10m)	Clay N=2-7/ Sand N=20	0.16g-0.19g	Cracking / crushing / exposure of steel	Liquefaction/Ground shaking		
3	NHK, Niigata, 1964	RC precast	4-story building	0.35	12	Loose Sand (0-10m)/Sand	Loose sand N=5-10/ Sand N=19-25	0.16g-0.19g	Cracking / crushing / exposure of steel	Liquefaction/ Lateral spreading	1.1-1.2	2
4	Hotel Niigata , Niigata, 1964	RC precast	Building	0.35	?	Silty Sand (0-6m)/Loose Sand (6m-12m)/Sand (>12m)	Silty Sand N=5-10/Loose Sand N=6-10/Sand N=10-40	0.16g-0.19g	Horizontal and oblique cracks	Liquefaction/ Lateral spreading		2
5	Hokuriku, Niigata, 1964	RC precast	10-story building	0.4	12	-	-	0.16g-0.19g	No damage			2
6	Niigata, 1964	RC precast	Railway bridge	0.3	7	-	-	0.16g-0.19g	Bending cracks along the entire length at only one side	Liquefaction/ Lateral spreading	0.38	

Table 4.1. Summary of cases of earthquake induced damage to piles including information about pile type and geometry, soil conditions, ground motion amplitude, type and cause of damage. Note: RC=Reinforced Concrete pile, PC=Prestressed Concrete pile, PHC= Prestressed High strength Concrete pile, AC=Autoclaved Concrete pile.

Case No.	Case	Pile Type	Superstructure	Diameter (m)	Length (m)	Type of soil	Soil properties	Seismic acceleration	Damage	Cause of damage	Head permanent disp. (m)	Free Field residual disp. (m)
7	NFCH, Niigata, 1964	RC precast	RC Building- pile2	0.35	9	Cemented Sand (0-1.8m)/Loose Sand (1.8m-8m)/Sand (>8m)	Loose Sand N<10/ Sand N=10-25	0.16g-0.19g	Cracks and breakage 3m below head and int. liq. no liq.	Liquefaction/ Lateral spreading	0.7	
8	NFCH, Niigata, 1964	RC precast	RC Building- pile1	0.35	7	Cemented Sand (0-1.8m)/Loose Sand (1.8m-8m)/Sand (>8m)	Loose Sand N<10/ Sand N=10-25	0.16g-0.19g	Cracking 3m below head	Liquefaction/ Lateral spreading	0.5	
9	Niigata, 1964	PC	2 story building	0.3	10	Clay (0-10m)/Sand (>10m)	Clay N=2-7/ Sand N=20 -27	0.16g-0.19g	Cracks / crushed head / exposure of steel	Liquefaction/Ground shaking		
10	Tokachi-Oki, 1968	RC precast	Railway bridge	0.4	19-32		N=0 (0-10 or 25m)/ N=11-34 (10-25m)/ N>50 bearing	0.23g	Horizontal cracking	Lateral spreading in soft coh. soil	0.76	
11	Maruyoshi Building, Miyagiken-Oki, 1978	PC	Three-story Building	0.25/50mm thick	5	Clay (0-4.5m)/Sand (>4.5m)	Clay qu=0.52KPa/ Sand N=40	0.3g	Horizontal cracks	Ground response		
12	Sendai Building,Miyagiken-Oki, 1978	AC	Eleven-story Building	?	?	Clay (0-4.5m)/Sand (>4.5m)	Clay qu=0.52KPa/ Sand N=41	0.3g	Head crushed /exposure of steel	Ground response/inertial forces		
13	Mexico, 1985	RC pre-bored square	16 story building	0.3x0.4	36	silt crust (0-2.5m)/ Clay (2.5-32.5m) / Sand (>32.5m)	silt crust N=5-10/ Clay N=0/ Silty Sand N=50	0.2g	Head crushed /exposure of steel	Ground respons/ inertial forces		

Table 4.1. (continued)

Case No.	Case	Pile Type	Superstructure	Diameter (m)	Length (m)	Type of soil	Soil properties	Seismic acceleration	Damage	Cause of damage	Head permanent disp. (m)	Free Field residual disp. (m)
14	Mexico, 1985	RC precast	8 story building	0.4	22	silt crust (0-2.7m)/ Clay (2.7-33.5m) / Sand (>33.5m)	silt crust N=5-10/ Clay N=0/ Silty Sand N=50	0.2g	Overturning / piles pulled out	Ground response/ Inertial forces		
15	Loma Prieta, 1989	RC cast-in-place	Bridge	0.38	?	Soft cohesive soil		0.2-0.25g	Crushed/crack at depth	Ground response/Lateral spreading		
16	Railway bridge, Port-Liner Kobe, 1995	RC	Railway bridge	1.5	26	sand/layers of clay (1.5m thick)	N=10-30 (sand) N=5-15 (clay)	0.83g	Almost cracked	Ground response		
17	Railway bridge, JR-Tokaido, Kobe, 1995	RC cast-in-place	Railway bridge	~0.6	?	Silt and Sand	N=5~10-(0-5m) N>20 (5-20m)	0.82g	None	-		
18	Railway bridge, Hankyu R., Kobe, 1995	RC cast-in-place	Railway bridge	1.3	14	Fine-Coarse sand/layers of clay (1.5m thick)	N=20-40 (sand) N=5-15 (clay)	0.81g	Horizontal cracking	Ground response		
19	Kobe line, Hanshin Expressway, Kobe, 1995	RC	Elevated highway pier	1.0	14	Fine-Coarse sand/layers of clay (1.5m thick)	N=20-40 (sand) N=5-15 (clay)	0.79-0.81g	Minor bending cracking	Ground response		
20	Wangan line, Hanshin Expressway, Kobe, 1995	RC	Elevated highway pier	1.5	27	Reclamation (0-10m)/Clay (10-18m)/Sand (>18m)	Re. N=30/Clay N<5/ Sand N=15-50	<0.7g	Serious horizontal and oblique cracking	Ground response/Liquefaction		

Table 4.1. (continued)

Case No.	Case	Pile Type	Superstructure	Diameter (m)	Length (m)	Type of soil	Soil properties	Seismic acceleration	Damage	Cause of damage	Head permanent disp. (m)	Free Field residual disp. (m)
21	No. 5 Bay Route, Hanshin Expressway, Kobe, 1995	RC cast-in-place	Elevated highway pier	1.5	34	Reclamation (0-20m)/Silt-Silty Sand (20-27m)/Gravel-Sand (>27m)	Re. N=15/Silt N<10/ Sand N=20-50	0.33g	Dense horizontal and oblique cracking	Liquefaction/ Lateral spreading	0.62	1
22	Port Island, Kobe, 1995	PC	Four-story building	0.4	30	Reclamation (0-18m)/Silt (18-25m)/Gravel-Dense Sand (>25m)	Re. N=10-40/Silt-Silty sand N<5/ Sand N=20-50	0.35g	Bending and shear cracking/ Head crushed	Liquefaction/ Lateral spreading		
23	Port Island, Kobe, 1995	PC	2-story building	0.45	35	Reclamation (0-16m)/Silty Clay (16-26m)/Dense Sand (>26m)	Reclamation N=5-25/Silty ClayN<5/Dense Sand 10-50	0.35g	Horizontal cracking	Ground response/Liquefaction	0.3	
24	Port Island, Kobe, 1995	PC-Steel jacket top 8m	4-story building	0.5	35	Reclamation (0-16m)/Silty Clay (16-28m)/Dense Sand (>28m)	Reclamation N=8-30/Silty ClayN=5/Dense Sand 10-50	0.35g	No damage			
25	Port Island, Kobe, 1995	Steel pipe	2-story building	0.4-0.5	42	Reclamation (0-15m)/Silty Clay (15-28m)/ Sand (>28m)	Reclamation N=8-30/Silty ClayN=5/Dense Sand 10-50	0.35g	Permanent deformation at 15m		0.34	
26	Building on reclaimed land, Kobe, 1995	PC	3-story building	0.45	28	Reclamation (-9m)/Silty Clay (9-20m)/Sand and Gravel (>20m)	Reclamation N=0-15/Silty Clay N<4/Sand an clay N=5-50	0.42g	Bending and shear cracking	Liquefaction/Ground shaking	0.25-0.3	1
27	Higaishinada-ku, Kobe, 1995	PC	Three-story building	-	17	Reclamation (0-9m)	-	0.33g	Bending and shear cracking / head crushed	Liquefaction/ Lateral spreading	0.3	

Table 4.1. (continued)

Case No.	Case	Pile Type	Superstructure	Diameter (m)	Length (m)	Type of soil	Soil properties	Seismic acceleration	Damage	Cause of damage	Head permanent disp. (m)	Free Field residual disp. (m)
28	Higashinada, Kobe, 1995	PC	Sewage treatment plant facilities	0.35-0.4	23	Reclamation (0-10m)/Clay (10-18m)/Sand and gravel (>18m)	Reclamation N=10/Clay N-4/Sand and gravel N=24-40	0.39g	breakage at 3m/ horizontal cracking at fill-clay interface	Liquefaction/ Lateral spreading	0.2>	2.0-3.0
29	Ashiyihama, Kobe, 1995	PC	School building	-	30	Sand (0-15m)/ Clay (15-20m)/Gravely Sand (>20m)	Sand N=5-20/ Clay N<5/Gravely Sand N=20-50	0.33g	Horizontal cracking	Liquefaction/ Lateral spreading	0.8	1.5
30	Ashiyihama, Kobe, 1995	PHC	School building	0.45	32	Sand (0-15m)/ Clay (15-20m)/Gravely Sand (>20m)	Sand N=5-20/ Clay N<5/Gravely Sand N=20-50	0.33g	Cracked at 8m/ broken at 16m	Liquefaction/ Lateral spreading	0.8	1.5
31	Ashiyihama, Kobe, 1996	RC cast-in-place	Waste disposal-four story building	1.0-1.2	30	Sand (0-10m)/ Silt (10-13m)/Sand-Clay(13-18m)/ Sand (>18m)	Sand N=3-20/ Silt N=2-8/Clay N=8/Gravely Sand N=10-50	0.33g	Dense horizontal cracks / oblique cracks	Liquefaction/ Lateral spreading	0.57	1.2-1.6
32	Mikagehama Island, Kobe, 1995	RC cast-in-place	LPG Tank	1.1	27	Fill (0-14m)/ Silty Clay (14m-18m)/ Sand (>18m)	Fill N<10/ Clay N<3/ Sand N=10-50	0.33g	Small horizontal cracks under slab	Liquefaction/ Lateral spreading	0.7	1 to 2m
33	Mikagehama Island, Kobe, 1995	RC / PC	LPG srorage yard facilities	0.3-1.1	5.0-2.5	Fill (0-14m)/ Silty Clay (14m-18m)/ Sand (>18m)	Fill N<10/ Clay N<3/ Sand N=10-50	0.33g	Sank/ severe titling	Liquefaction/ Lateral spreading		
34	Mikagehama Island, Kobe, 1995	RC precast	LPG Tanks	0.3	20	Fill (0-17m)/ Sandy Clay (17m-18m)/ Sand (>18m)	Fill N<10/ Clay N=15/ Sand N=15-50	0.33g	Dense horizontal cracks at 5-10m	Liquefaction/ Lateral spreading	0.5	1 to 2m

Table 4.1. (continued)

Case No.	Case	Pile Type	Superstructure	Diameter (m)	Length (m)	Type of soil	Soil properties	Seismic acceleration	Damage	Cause of damage	Head permanent disp. (m)	Free Field residual disp. (m)
35	Mikagehama Island, Kobe, 1995	PHC	4-story building	0.35	25	Fill (0-14m)/ Clay (14m-17m)/ Sand (>17m)	Fill N<10/ Clay N=5-10/ Sand N=10-50	0.33g	Horizontal cracking at head and fill-clay interface	Ground response/Liquefaction	0.36	
36	Fukuehama, Kobe, 1995	PHC/ steel jacket till 6m	5-story building	0.5-0.6	33	Fill (0-10m)/ Clay (10-14m/17-23m)/ Sand (14-17m/>23m)	Fill N<10/ Clay N<4/ Sand N=5-50	0.33g	Horizontal cracks at fill-clay interface	Ground response/Liquefaction		
37	Fukuehama, Kobe, 1995	PHC/ steel jacket till 5m	under construction	0.4-0.5	33	Fill (0-14m)/ Clay (14m-24m)/ Sand (>24m)	Fill N=0-15/ Clay N<4/ Sand N=10-50	0.33g	Horizontal cracks at 8m depth (liq-no liq interface)	Ground response/Liquefaction		
38	Fukuehama, Kobe, 1995	PC	3-story building	0.4	20	Fill (0-12m)/ Clay (12m-17m)/ Sand (>17m)	Fill N=0-20/ Clay N<5/ Sand N=40-50	0.33g	Cracking at head and middle to bottom liq. layer	Liquefaction/ Lateral spreading	0.8	2
39	Fukuehama, Kobe, 1995	Steel pipe	2-story building	0.46/ 9.5mm thick	27	Fill (0-16m)/ Clay (16m-22m)/ Sand (>22m)	Fill N=3-22/ Clay N<5/ Sand N=20-50	0.33g	No damage		0.5	3
40	Kobe, 1995	RC cast-in-place	under construction	1.2-1.7	48	Fill (0-15m)/ Clay (15m-26m)/ Sand (>26m)	Fill N=5-20/ Clay N<5/ Sand N=10-50	0.3-0.4g	Dense cracking near pile head/ at liq-no liq	Liquefaction/ Lateral spreading	0.9	2.5

Table 4.1. (continued)

Case No.	Case	Pile Type	Superstructure	Diameter (m)	Length (m)	Type of soil	Soil properties	Seismic acceleration	Damage	Cause of damage	Head permanent disp. (m)	Free Field residual disp. (m)
41	Warehouse, Kobe 1995	PC	Freezer warehouse	0.4	34	Fill (0-14m)/Clay (14m-25m)/ Sand (25m-34m)/Gravel	Fill N=3-20/Clay N=2/ Sand N=10-50	0.38g	Horizontal cracking	Ground response/ liquefaction	minor	0.38
42	Kanzaki river, Kobe 1995	RC precast	Revetment	0.35	7 (friction pile)	Fill (0-4.3m)/Silty sand (4.3-8.6m)/ Silt	-	0.21-0.27g	Horizontal cracking at pile head / 7-9cracks/m	Liquefaction/ Lateral spreading		
43	Niigata, 1964	RC precast	3 story building	0.3	6			0.16g-0.19g	Cracks at pile head			
44	Niigata, 1964	PC	Bridge	0.6	10			0.16g-0.19g	Several bending cracks	Liquefaction/ Lateral spreading		
45	Tokachi-Oki, 1968	RC precast	2 story building	0.3	14			0.23g	Crushed head / compressional and shear failures	Ground response		
46	Miyagiken-Oki, 1978	AC	5 story building	0.6	12			0.3g	Head crushed / exposure of steel	Ground response/ Inertial forces		
47	Miyagiken-Oki, 1978	AC	12 story building	0.4	16			0.3g	Horizontal circular cracks at pile	Ground response/ Inertial forces		
48	Miyagiken-Oki, 1978	AC	14 story building	0.6	24			0.3g	Diagonal cracks / Head crushed/tendons failure	Ground response/ Inertial forces		

Table 4.1. (continued)

Case No.	Case	Pile Type	Superstructure	Diameter (m)	Length (m)	Type of soil	Soil properties	Seismic acceleration	Damage	Cause of damage	Head permanent disp. (m)	Free Field residual disp. (m)
49	Miyagiken-Oki, 1978	PC	4 story building	0.35	5			0.3g	Head crushed/tendons buckled outside	Ground response/ Inertial forces		
50	Miyagiken-Oki, 1978	AC	5 story building	0.4	7			0.3g	No damage			
51	Miyagiken-Oki, 1978	PC	4 story building	0.3	10			0.3g	Head crushed at 0.6m below slab	Ground response/ lateral spreading		
52	Urakawa-Oki, 1983	RC precast	3 story building	0.3	?			0.3g-0.5g	Head crushed/rebar exposed /hooks cutoff	Ground response/ Inertial forces		
53	Urakawa-Oki, 1983	Steel pipe	4 story building	0.4/ 9mm thick	6.0-20.0			0.3g-0.5g	No damage			
54	Nihonkai-Chubu, 1983	RC precast	1 story building	0.5	9.5			0.24g	Failure of pile head	Liquefaction/Ground response		
55	Nihonkai-Chubu, 1983	PC	Sheet pile quay	0.4	13			0.24g	Cracks at pile head	Liquefaction/Ground response		
56	Nihonkai-Chubu, 1983	Steel pipe	Caisson quay	0.5/ 9-12mm thick	18			0.24g	No damage/ pile permanent bending	Liquefaction/ Lateral spreading	0.5-0.8	

Table 4.1. (continued)

Case No.	Case	Pile Type	Superstructure	Diameter (m)	Length (m)	Type of soil	Soil properties	Seismic acceleration	Damage	Cause of damage	Head permanent disp. (m)	Free Field residual disp. (m)
57	Nihonkai-Chubu, 1983	RC precast	Bridge	0.5	8			0.24g	Horizontal/bending cracking	Liquefaction/Ground response		
58	Nihonkai-Chubu, 1983	RC precast	4 story building	0.3	?			0.24g	Horizontal cracks/ Head failure	Liquefaction/Ground response		
59	Nihonkai-Chubu, 1983	RC precast	1 story building	0.35	7			0.24g	Head failures / some concrete parts flanked out	Liquefaction/Ground response		

Table 4.1. (continued)

CHAPTER 5: ANALYSIS OF SEISMICALLY INDUCED DAMAGE TO PILES

The numerous field cases presented in the previous chapter and the Mizuno (1987) database indicate that pile foundations are highly susceptible to damage under the loads generated by earthquakes. Although Japan had several experiences with seismic damage to piles prior 1995, the Hyogoken-Nambu earthquake proved that the design of deep foundations was not appropriate. In this chapter, the information gathered from actual cases is categorized and compiled in attempt to identify the causes and their relation with the type and severity of earthquake induced damage.

Degree of damage and residual pile capacity

Most of the reported cases concern concrete piles, either reinforced or prestressed. Reinforced concrete has the disadvantage, compared to structural steel, of loosing progressively its strength and stiffness upon cyclic loading. After several strain reversals bending and shear cracks may intercross each other leading to a extensive disorganization of the material. Thus, the severity and extension of concrete cracking is of great importance for the integrity not only of the deep foundation but also of the entire structure. According to Matsui and Kazuhiro (1996) and Okahara et al. (1996), who studied the distribution of damage to pile foundations of elevated highways, pile damage can be categorized with respect to severity as follows:

a) **Severe:** Dense cracking all over the pile, concrete separation, buckling of rebars, discontinuity of pile shaft; these types of failure are usually accompanied by residual horizontal displacement or settlement of the superstructure.

b) **Heavy:** Dense cracking and concrete separation near the pile head and several bending cracks at other locations at depth. This type of damage is by residual horizontal displacement of the pile head.

c) **Light:** Some bending cracks near the pile head and possibly at other locations.

d) **No damage**: No damage or slight bending cracking.

The severity of damage on concrete piles seems to be directly associated with the capacity of the foundation and the functionality of the structure after the earthquake. Testing of damaged foundations in Kobe showed that lightly damaged piles maintain sufficient vertical and lateral load capacity. If the cracking becomes denser and shear failure appears near the pile head, the lateral stiffness of the pile is reduced significantly but it can still maintain adequate vertical capacity. If the pile is crushed, then the pile looses both vertical and horizontal capacity.

Cases such as the multi-story buildings in Niigata, 1964, show that it is possible for the pile foundation to be heavily damaged, while the superstructure is almost intact. However, existing cracks on the piles and the resulting loss of lateral stiffness may lead to a largely different behavior of the structure during a future seismic event. The reduction of total stiffness of the structure-foundation-soil system will result in higher natural periods and larger displacements. Total failure of the piles and collapse of the structure is possible if the diminished lateral capacity is not restored. Cracking also exacerbates the problem of corrosion of reinforcing steel. In case of a severely damaged foundation, where the superstructure has subsided, restoration is very difficult. Heavily damaged foundations may be restored by increasing the number of piles in order to provide the additional lateral resistance that was lost during the earthquake. Although lightly damaged foundations may maintain sufficient capacity, the reinforcing steel corrosion due to the presence of cracks remains an issue.

Causes of damage

The causes of earthquake-induced damage can be categorized as follows:

a) **Ground response:** motion imposed to the pile body due to the response of the surrounding soil that generates bending and shear stress in the pile.

b) **Inertial forces:** large axial and horizontal loads due to response of the superstructure, in addition to the loads applied by the surrounding soil.

c) **Liquefaction/Ground motion:** decrease of the soil stiffness in the liquefiable layer no significant lateral permanent displacement with significant loss of lateral support.

d) **Liquefaction/Lateral spreading**: significant residual stresses due to permanent head displacement.

Although, the most essential cause of damage is ground shaking, ground response loads, inertial forces from the superstructure and pile response in liquefiable layer, are viewed separately, since each one affects differently the type and degree of the pile damage.

Damage location

Our review and interpretation shows that, generally, pile failures take place first near the pile head, where bending moments and shear forces are maximum. However many cases show that large cracks may occur at (Figure 5.1):

a) pile locations near an interface between layers with large differences in stiffness
b) between liquefied and non-liquefied layers
c) location of the second largest moment
d) sections where the density of steel reinforcement is reduced (Matsui and Kazuhiro, 1996),

The damage at the interface between liquefiable and non-liquefiable layers and between soft and stiff layers has been extensively observed in Kobe, where structures were founded on the liquefiable reclaimed land (Matsui and Kazuhiro, 1996; Tokimatsu et al., 1996; Fujii et al., 1998; Nakayama et al., 1998), [cases 20 to 22, 26 to 38, 40 and 42 in chapter 4] and after the Niigata, 1964 earthquake (Tazoh et al., 1987, Mizuno 1987), [cases 1-9]. The relative stiffness between adjacent layers seems to have a great effect on the distribution of strain along the pile. The damage tends to localize near the interfaces between soft and stiff layers since the strain concentrates at points of the soil profile where the difference of stiffness is high. The same mechanism is valid for the damage observed at the interface between liquefiable and non-liquefiable layers, even if their stiffness before the earthquake was similar. This is because during the earthquake the reduction of effective stress in the liquefied layer leads to a stiffness reduction that may range between 0.2 and 0.02 of the initial stiffness.

The second largest moment usually appears within the soft, loose, or liquefied layer. The formation of a plastic hinge at the top of the pile after the failure of the head and the

subsequent redistribution of bending moments creates new horizontal cracks at other locations.

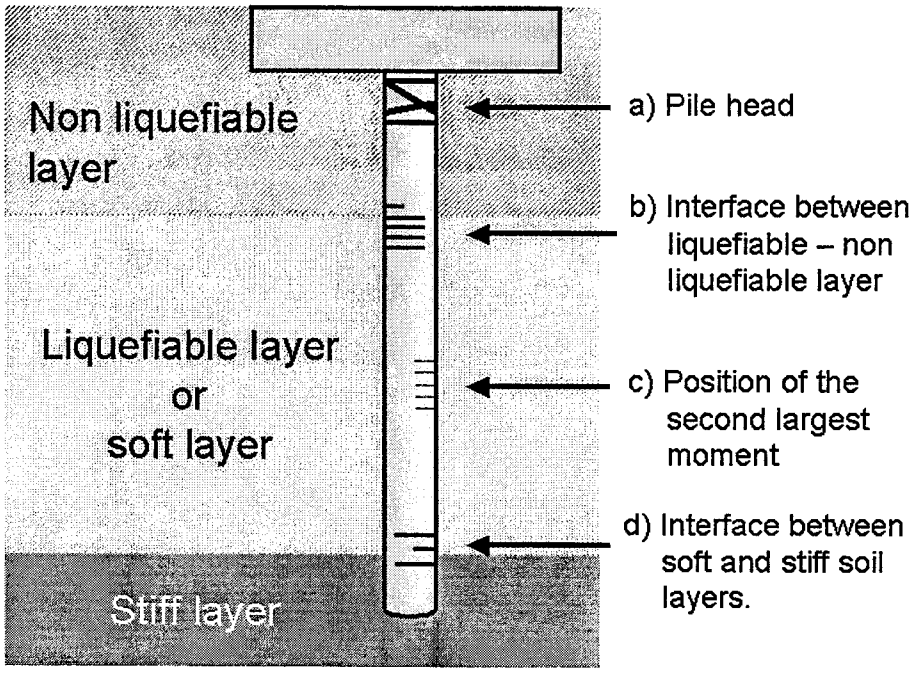

Figure 5.1. Pile locations most likely to sustain earthquake induced damage.

Effect of pile type to damage susceptibility

Figure 5.2 is a plot of the cases of Table 4.1, and shows the severity of damage versus the cause of damage. Cases with incomplete data or with an exceptional type of superstructure are excluded from Figure 5.2. The cases are sorted by the main cause of damage. In Figure 5.2, cases of steel piles and concrete piles with steel casing (SC) piles are circled to pinpoint their improved performance compared to that of reinforced concrete piles. The collected data shows that ground response without the presence of significant inertial loads can cause only light to heavy damage, usually horizontal cracks near the pile head and in some cases near the interface between soft and stiff soil layers. Reinforced concrete piles are highly susceptible to damage. However, it is often observed that SC piles significantly improve their performance even if the steel casing covers the pile only down to a certain depth, as reported by Tokimatsu et al. (1998) and Fujii et al. (1998) [cases 24, 27, and 37]. Steel pipe piles

behave well even in cases of liquefaction-induced lateral spreading because of their ductility. Few cases of local buckling are reported (Mizuno, 1987; Tazoh et al., 1987) [cases 1, 25, and 56]. It appears that failure of steel pipe piles is limited to cases of liquefaction and lateral spreading. There is no reported data of damage to steel piles due to ground response or inertial force. Furthermore, no clear distinction can be made with respect to the resistance to failure between cast-in-place, precast, or prestressed concrete piles.

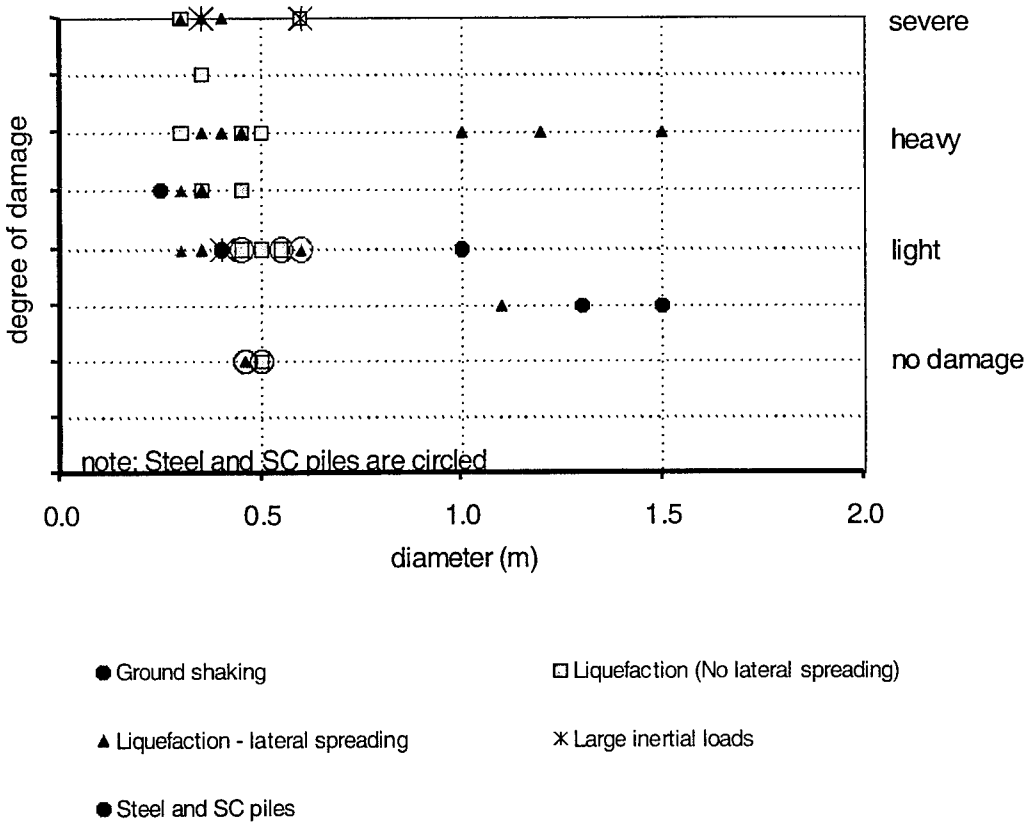

Figure 5.2. Degree of damage vs. pile diameter sorted by cause of damage.

Structures supported on friction piles in liquefiable layers may be subjected to tilting and significant settlement due to bearing capacity failure caused by soil liquefaction (Tokimatsu et al., 1996). Integrity of the piles themselves after liquefaction is not affected by the seismic loads since there is not adequate reaction from a liquefied soil to generate large stresses inside the piles. Friction piles should be avoided in cases where the soil deposit has a potential for liquefaction, and piles should be embedded into a stiffer non-liquefiable layer, even if the vertical loads are much smaller than the capacity provided by the stiff layer.

Liquefaction can produce pile failure due to the degradation of soil stiffness and loss of lateral support. Liquefaction without significant lateral spreading (less than 10-30cm) may cause less damage than lateral spreading with large head displacement. Lateral spreading imposes additional loading to the pile and may produce heavier damage in the form of diagonal cracks near the pile head and at the interfaces between liquefied and non-liquefied layers. Large axial and horizontal inertial loads coming from a tall superstructure can produce severe damage; crushing of the pile head or a combination of vertical and diagonal cracks are produced by the large axial inertial loads (Mizuno, 1987; Tokimatsu et al., 1996; Kishida et al., 1980).

Heavy damage in large diameter piles occurs mostly due to liquefaction. For piles with 0.5 m diameter or smaller, heavy or severe damage is caused by liquefaction with or without lateral spreading. However, if steel casing is used, the damage is light or there is no damage at all. In conclusion, the causes of damage can be ranked with increasing severity of damage as follows:

i) Ground response (light to heavy damage)
ii) Liquefaction/ Ground response (light to severe)
iii) Liquefaction/ Lateral spreading (light to severe)
iv) Large inertial loads (severe damage)

No distinct relations between diameter, pile slenderness (length/diameter), acceleration and the severity of damage could be established based on the data. However, a slight trend appears in that the susceptibility of damage increases decreasing available diameter. From the cases where the pile head displacement was measured, it can be concluded that permanent displacement is a critical factor of pile failure and the damage severity increases with the amount of residual displacement.

Finally, it is possible that the adherence between a soft clay deposit and the pile is reduced during cyclic loading; this may lead to a reduction of the bearing capacity of piles, as observed during the Mexico earthquake [cases 14]. Structures supported by these types of piles may suffer settlement and permanent tilting, and the piles may even be pulled out from

the ground. This effect is more critical in cases of tall structures where large inertial axial loads may be applied to the foundation.

Application to bridge pile foundations in Southern Indiana

Based on the established databases, pile damage can take place with or without liquefaction. The development of damage in cases without liquefaction requires the presence of significant peak acceleration at the ground surface (larger than 0.25g). In chapter 3, it was shown that the development of relatively large accelerations is possible in southern Indiana. The peak horizontal ground acceleration calculated from the ground response analysis for a Wabash Valley Fault System earthquake can range between 0.12g and 0.53g, with an average of 0.33g, and is comparable to the peak accelerations at the sites where damage to foundations has been reported. However, piles of bridge structures seem to be less susceptible to severe damage because this type of structure transmits limited vertical inertial loads to the foundation. According to the site response analysis, an earthquake generated by the New Madrid seismic zone with peak accelerations around 0.16g is potentially dangerous to pile foundations only if the liquefaction potential is high.

The data presented in chapter 4 suggests that the relative stiffness between soil layers is of great importance for the pile behavior during an earthquake. In southern Indiana both soft clayey soils and loose liquefiable soils are present usually underlain by layers of dense sand. The large difference in soil stiffness between layers increases the damage potential if the pile penetrates into the dense and non-liquefiable layer. Bridge piers and abutments may be subjected to lateral spreading, since liquefied granular material next to rivers tends to move towards the waterfront.

According to data from the Indiana Department of Transportation H piles driven to bedrock and steel shell encased concrete piles are customarily used in the State. As observed in Kobe, 1995, steel piles and SC piles behave much better than reinforced and prestressed concrete piles. In cases where a bridge is supported by these type of piles, the damage potential is low. However, a detailed investigation should be required to assess the response of the piles for the specific soil conditions and superstructure characteristics.

To identify the effect of different pile types on damage susceptibility, numerical simulations of a single pile subjected to seismic loading are performed for a typical soil profile in southwestern Indiana. A three-dimensional finite element model has been set-up with ABAQUS (Hibbitt, Karlsson and Sorensen, Inc.) to analyze a single pile subjected to ground shaking and inertial loads from the superstructure. The model, which is shown in Figure 5.3, consists of a total number of 3040 second-order elements that represent the soil and the pile. At the lateral boundary, infinite elements are attached to the main model to allow outwards energy transmission during the dynamic analysis. A frictional interface is defined between the pile and the soil. The superstructure is modeled as a single degree of freedom oscillator (beam elements and a point mass) connected to the pile head through a layer of rigid elements. This allows for horizontal loads and moments from the superstructure to be transferred to the pile. Both soil and pile are modeled as elastic materials.

The site GiBL, next to the Wabash River (Figure 3.5) is chosen as a representative case for the performance and behavior of SEC piles. The structure at this site is a three span road bridge supported on piles. The piles have a diameter of 356mm (14in). The steel casing extends throughout the pile. The piles in this bridge are not driven down to bedrock since they reached refusal before that. The unfactored design load on each pile was estimated as 356kN. The pile has a length of 10m and belongs to a single row of piles supporting the abutment. The mesh has the following characteristics: the thickness of the mesh is H= 13.37m; the skin friction angle along the entire pile length is $\delta = 16.7^{\circ}$ ($\tan\delta=0.3$); the value of the superstructure mass is set to the axial pile load design of 356kN. The values of the elastic modulus E are 21.5GPa for concrete and 200GPa for steel. The soil profile is composed of silt and silty clay with very low N_{SPT} values, underlain by dense sand and gravelly sand, which is the bearing stratum. The elastic modulus for each layer of elements is determined by reducing the initial modulus E_o to the equivalent linear secant modulus according to the results of the SHAKE analyses for the same site and earthquake scenario. The E_o values are estimated based on the Imai and Tonouchi (1982) relationships. Rayleigh factors consistent with the peak damping ratio from the response analysis are used. By making this consideration, despite the soil linearity assumed in the numerical model, the ground response is similar to that computed by SHAKE near the peak acceleration values.

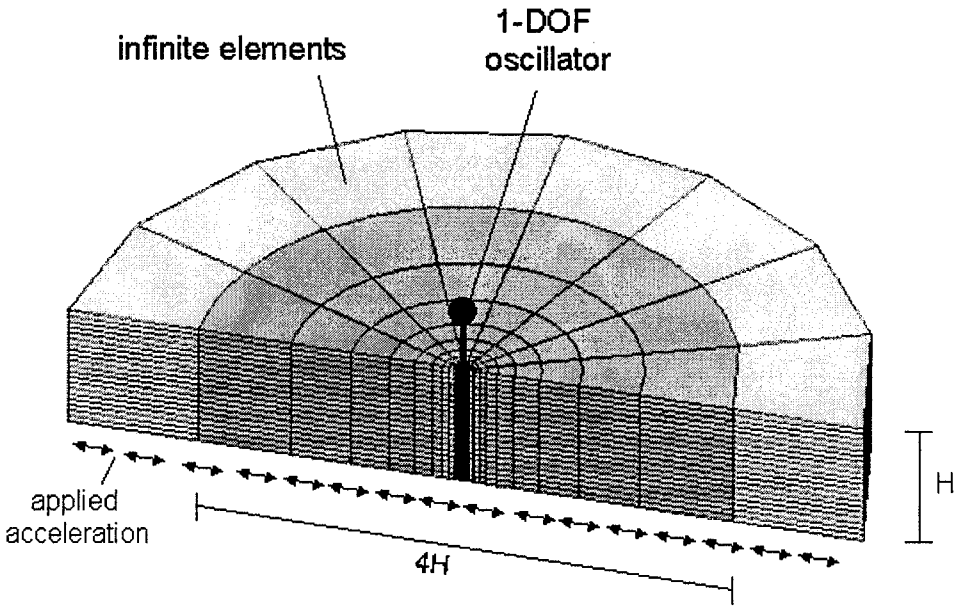

Figure 5.3. Mesh used in finite element method analyses.

Two runs are performed: (1) for a SEC piles with a steel shell 1in thick; and (2) for a reinforced concrete pile having the same diameter. This is done to observe the effect of the steel casing. The pile is analyzed for a Wabash Valley fault system earthquake scenario because it is the most critical (see chapter 3). The results are summarized in Figure 5.4. The bending moment is computed by integrating the axial stress at each layer of elements.

For the SEC pile, the maximum bending moment, 207.7kNm, occurs at the pile head and corresponds to a maximum tensile stress in the concrete equal to $\sigma_{t,max}$= 4.91MPa. Assuming a concrete tensile strength f_{ct}=2.4MPa (f_c=3000psi), the induced tensile stress is capable of initiating limited cracking in the concrete near the pile head.

For the concrete pile, the skin friction angle is set to be $\delta = 21.8^\circ$ ($\tan\delta$=0.4). The maximum bending moment is located at the pile head. It has a magnitude of 101.4kNm, and is smaller than the SEC pile (Figure 5.4). However, the corresponding maximum tensile stress in the concrete, $\sigma_{t,max}$= 19.1MPa, is much larger than the assumed concrete tensile strength. The results show that a SEC pile would sustain less damage than a reinforced concrete pile.

The practice of using steel H piles and steel encased concrete piles in bridge foundations in southern Indiana reduces the potential of heavy damage due to major seismic events. Although our analysis shows that larger moments may be developed in a SEC pile than in a concrete pile, the stresses in the concrete are smaller. Steel casing concrete piles seem to be a efficient method for earthquake resistant pile foundations, but additional detailed work is required on this subject.

Effect of steel casing thickness and effect of pile cap on pile performance

In the previous section, two cases of a single pile embedded in the soil profile GiBL have been examined, one of a reinforced concrete pile and one of steel encased concrete pile (SEC) with casing thickness of 1" (2.54cm). Additional analyses of a single pile with the same length (10m) and diameter (0.356m) embedded in the same soil profile (GiBL) are performed for several values of the casing thickness in order to obtain a better insight into the effect of steel casing on the performance of concrete piles.

Figure 5.5 shows the maximum bending moment and maximum axial stress in the pile for different steel casing thickness, ranging from 0.203" to 1'. It can be observed in the figure that as the steel thickness increases, the bending moments decrease up to a thickness of 0.5 inches, and then increase for larger steel thicknesses. However, the maximum stress in the pile increases with decreasing the steel thickness. In fact, the beneficial effects of the casing appear at thicknesses greater or equal than 0.31". The positive effect that one might expect by adding steel to the pile is counterbalanced by the higher stresses that this creates. The reason for higher bending moments for thicker steel casings is the change of stiffness of the soil-structure system as more steel is added. As the thickness of the casing is increased, the natural period of the system is reduced, the response of the superstructure is increased, and thus the inertial loads from the superstructure to the pile are increased. For small casing thickness, the stress relief to the pile concrete due to the steel in the pile's composite cross-section is counterbalanced by the increased inertial loads from the superstructure. For large casing thickness, the positive effect of increasing the steel section compensates for the increase of bending moments due to the increase of stiffness. The results show that the overall stiffness of the system is very sensitive to the steel added. In actual cases this may

not be so because of the pile cap, that has been neglected in the above analyses. As the pile tries to displace and rotate, the pile cap has to follow; however, the soil under the pile prevents or at least restrains such movements. The introduction of the pile cap into the model increases the rocking (rotation around an axis parallel to the ground) stiffness of the soil-pile structure system, and thus decreases the sensitivity of the system's natural period to the pile stiffness and thus to the increase of stiffness due to the casing.

A series of analyses are performed in order to identify the effect of the pile cap. The pile cap stiffness depends on the geometry of the pile cap and on the properties of the soil layers near the surface. However, the actual stiffness introduced by the pile cap may be diminished because of construction details or because of connection details between the pile and the cap. Also, the rocking stiffness changes with the amplitude of the rotation of the cap because of the reduction of the soil's shear modulus with deformation or because of a possible separation between the cap and the underlying soil.

An estimation of the pile rocking stiffness is made based on the research of Dobry and Gazetas (1986). The distance between piles is 6ft and the width of the cap is 2.9ft. Thus, the portion of the cap that corresponds to each pile is a rectangular parallelogram of length L=1.83m (6ft) and width B=0.88m (2.9ft), with a circular whole in the middle (the area occupied by the cross-section of the pile head) of radius R=0.178m. The small strain rocking stiffness around the long direction can be calculated as:

$$K_{\theta x} = S_{rx} \frac{G}{1-\nu} (I_x)^{0.75} - \frac{8GR^3}{3(1-\nu)} \qquad (5.1)$$

where G is the shear modulus of the soil underneath the cap, ν the Poisson's ratio, $S_{rx} = 3.2$ and $I_x = \frac{1}{12} L B^3$. For a soil shear modulus G= 115MPa with Poisson's ratio 0.33, the small strain rocking modulus is $K_{\theta x}$= 97.94MNm. The rocking modulus is probably smaller due to the non-linear behavior of the soil and the poor connection between the pile head and the pile cap. Two scenarios are analyzed, (1) $K_{\theta x}$= 97.94MNm (i.e. full stiffness) and (2) rocking modulus reduced to one half, i.e. $K_{\theta x}$= 48.97MNm. The pile cap is introduced into the finite element model as a rotational spring attached to the connection between the SDOF oscillator

and the pile. The contribution of the pile cap to the horizontal stiffness of the system and to damping of the cap motion are neglected.

Results are presented in Figures 5.6 through 5.9. The introduction of the pile cap decreases significantly the moments that the superstructure applies to the pile head. Figures 5.6 and 5.7 show that, for a given cap rocking stiffness, the moments at the pile head increase as the casing thickness increases. This is because as the difference between the pile stiffness and the cap stiffness is reduced, the portion of the inertial loads taken by the pile gets larger. What is interesting is that as the thickness of the steel casing increases, the stresses in the pile increase.

Figures 5.8 and 5.9 illustrate the effect of the rocking stiffness of the pile cap. As the rocking modulus increases, the bending moments decrease and, consequently, the stresses in the pile decrease. In general, the soil-pile-structure system plus the cap has a low natural period that results in high inertial loads; however the period of the system is almost independent of the stiffness of the pile. As a consequence, the tensile stresses in the pile during the seismic event decrease as the thickness of the steel casing increases. Thus, the presence of steel casing in these analyses is beneficial.

In the case of the GiBL site, the largest load to the pile is produced by the response of the superstructure and affects the upper part of the pile down to a depth of approximately 2.5m. Most of the damage is likely to occur within this depth. The moments produced at larger depths originate from the response of the soil surrounding the pile and are much smaller than the moments developed near the pile head. Deep moments increase as the pile stiffness increases (i.e. as the casing thickness increases), since the imposed displacements to the pile by the ground do not change much for the cases analyzed. In most cases, steel casing reduces stresses on both upper and lower parts of the pile.

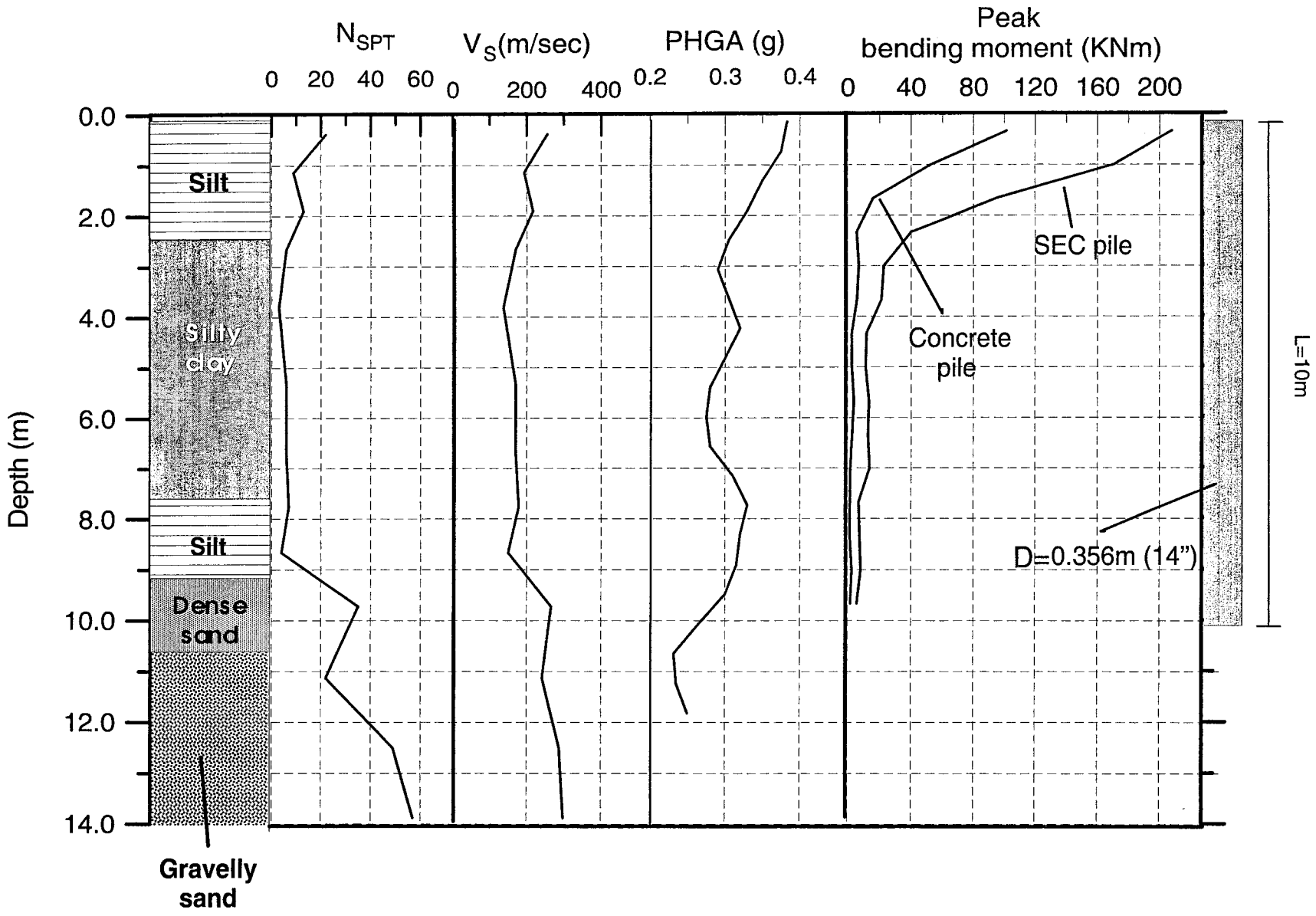

Figure 5.4. Soil profile, peak horizontal accelerations and peak bending moment for 10m long concrete and steel casing concrete (SEC) piles at site GiBL for a WVFS earthquake scenario.

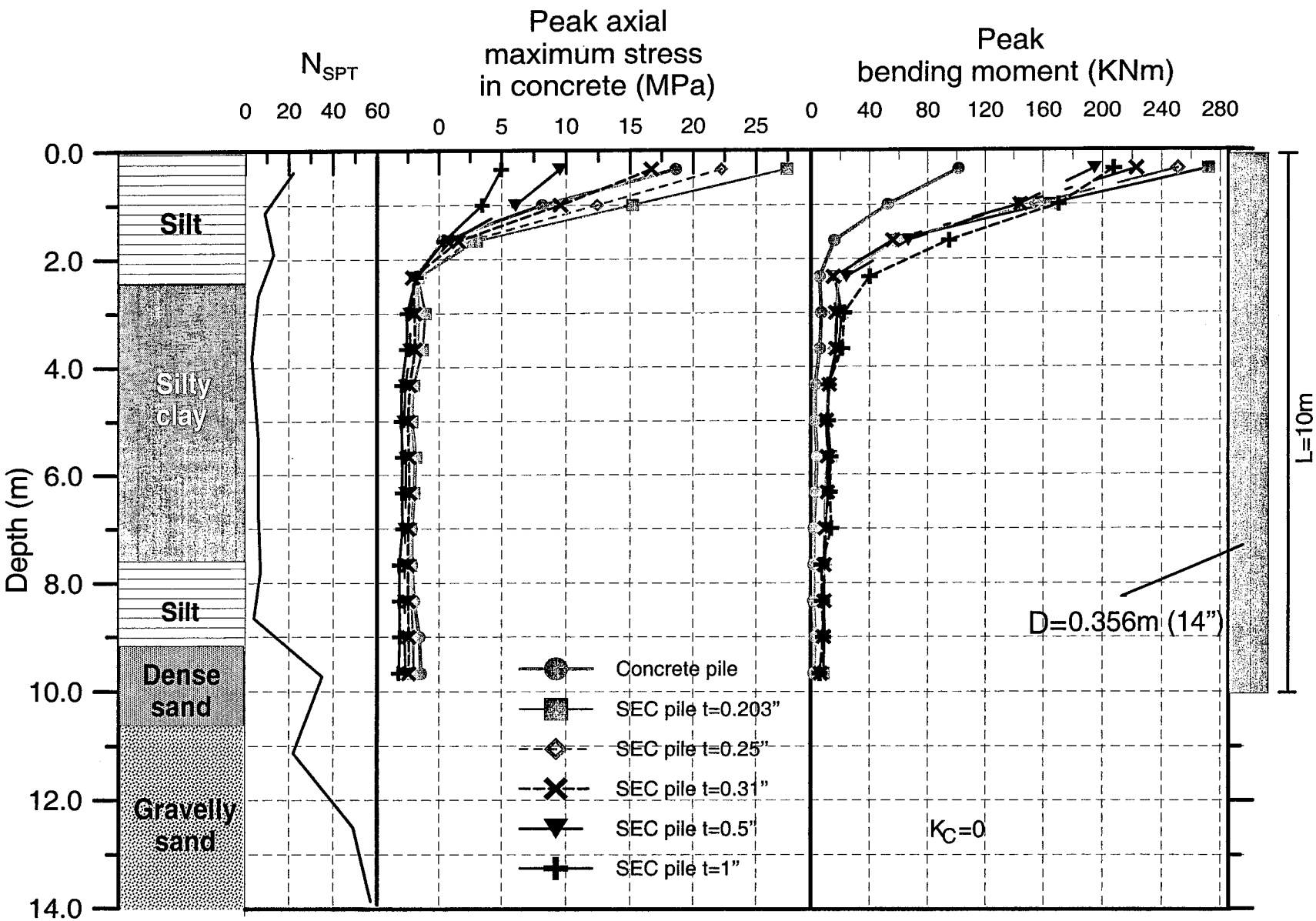

Figure 5.5. Soil profile, peak axial maximum stress in concrete and peak bending moment for 10m long pile at site GiBL for a WVFS earthquake scenario for various steel casing thicknesses and neglecting the pile cap.

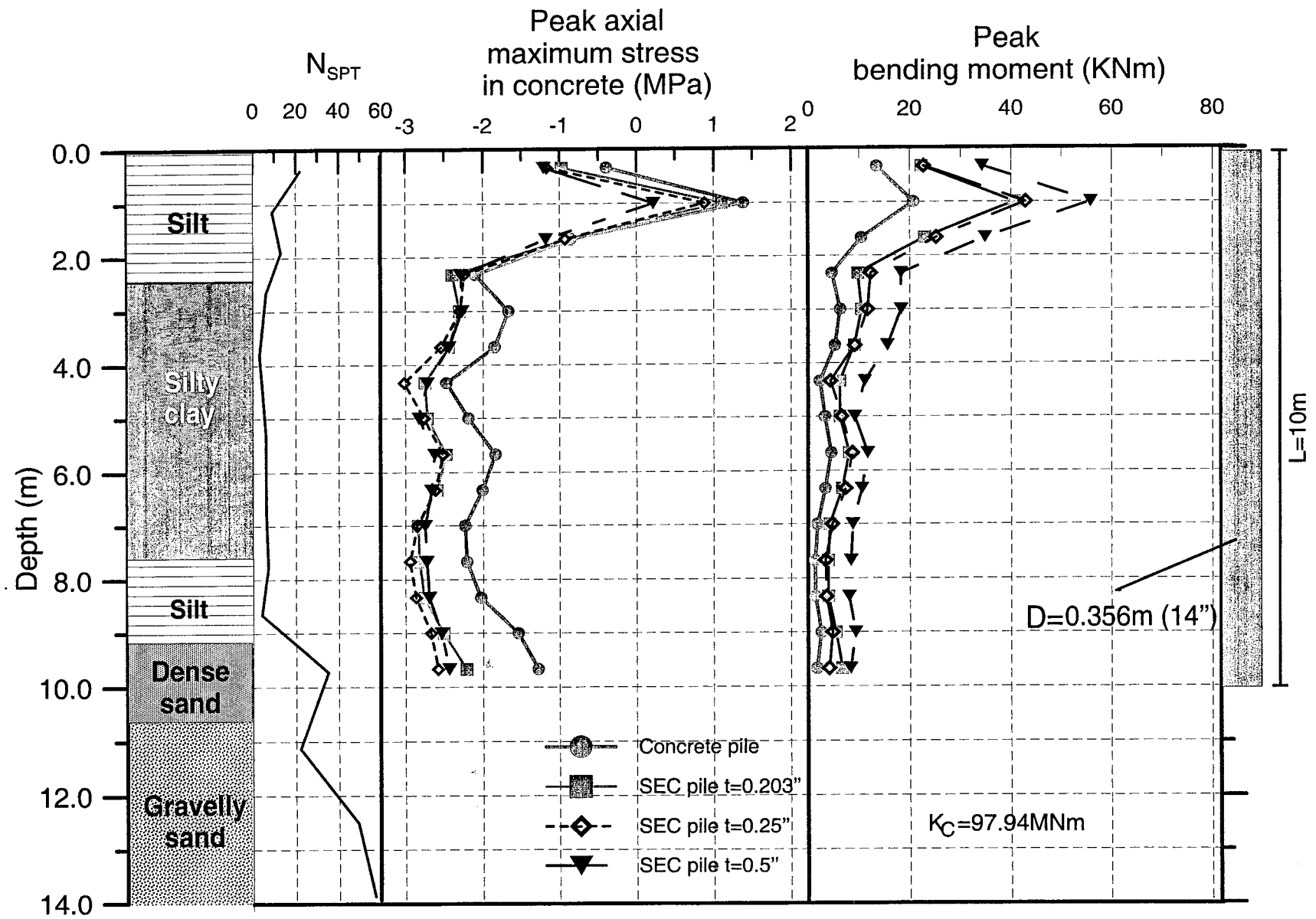

Figure 5.6. Soil profile, peak axial maximum stress in concrete and peak bending moment for 10m long pile at site GiBL for a WVFS earthquake scenario for various steel casing thicknesses and pile cap rocking stiffness 97.94MNm.

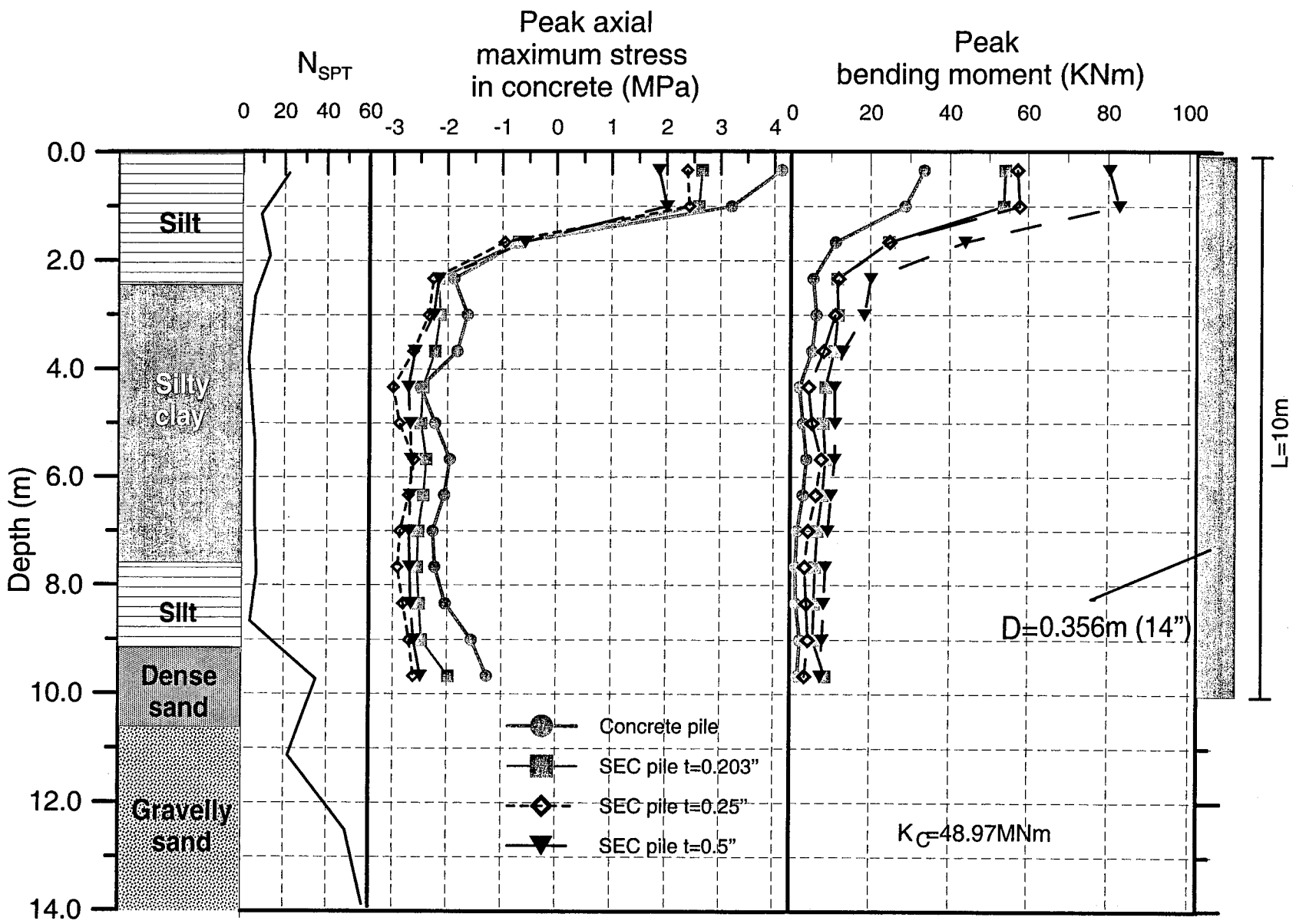

Figure 5.7. Soil profile, peak axial maximum stress in concrete and peak bending moment for 10m long pile at site GiBL for a WVFS earthquake scenario for various steel casing thicknesses and pile cap rocking stiffness 48.97MNm.

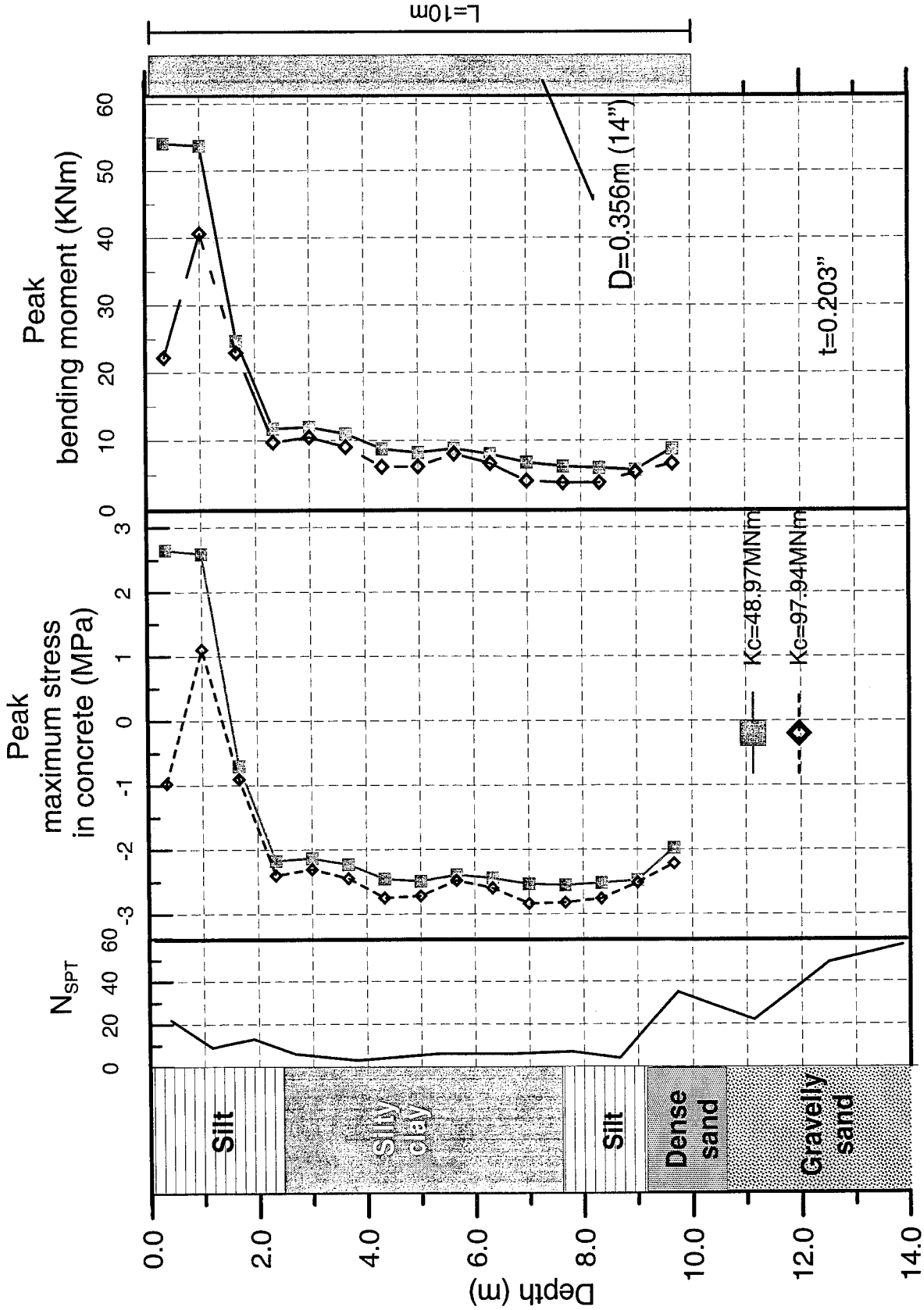

Figure 5.8. Effect of cap rocking stiffness on the response the 10m long SEC pile with steel casing thickness of 0.203" at site GiBL for a WVFS earthquake scenario.

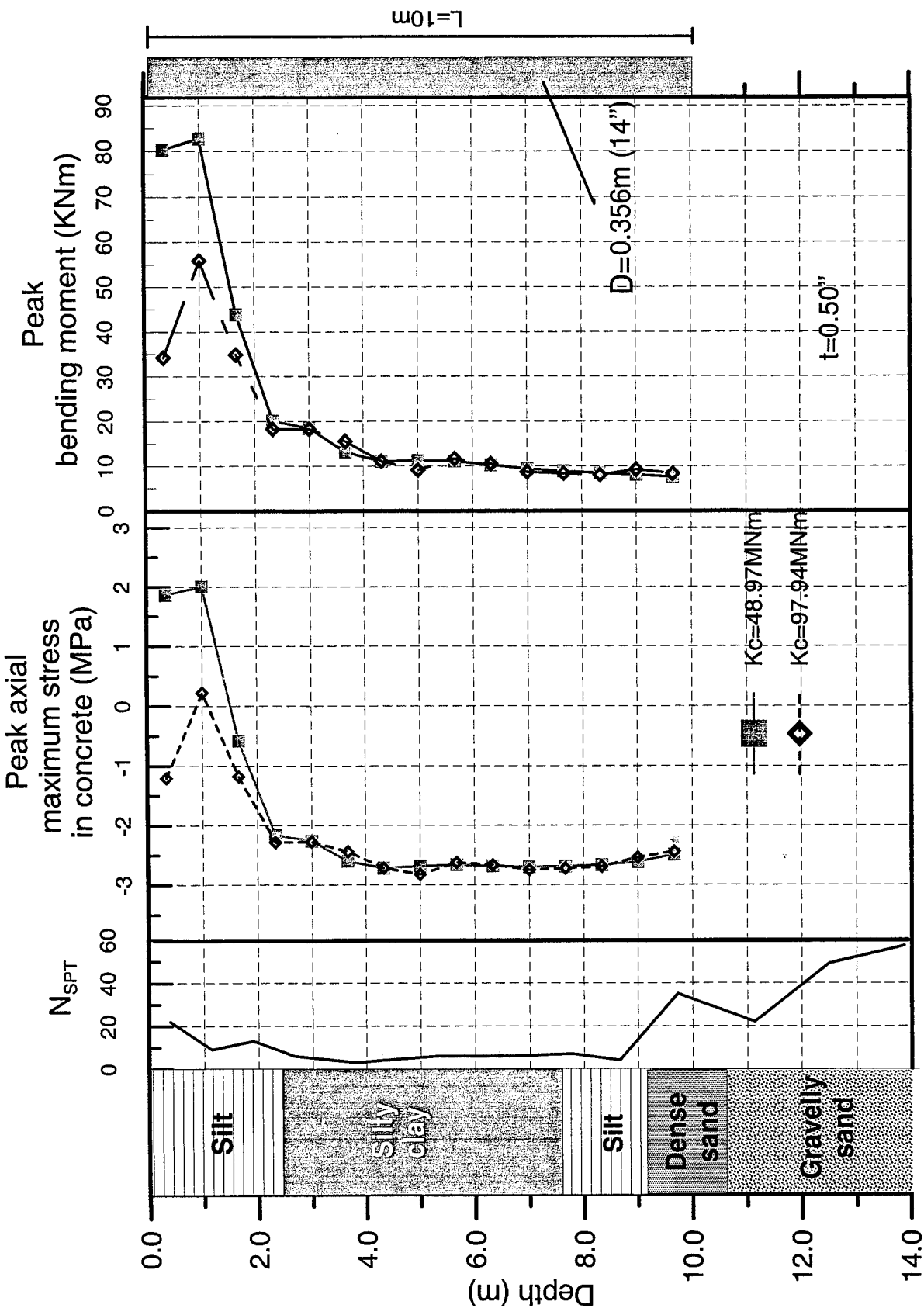

Figure 5.9. Effect of cap rocking stiffness on the response the 10m long SEC pile with steel casing thickness of 0.50" at site GiBL for a WVFS earthquake scenario.

CHAPTER 6: RECOMMENDATIONS

Results from the ground response and liquefaction potential studies presented in chapter 3 are combined with the data and findings from the literature survey presented in chapters 4 and 5. A number of conclusions and recommendations are presented in this chapter. For clarity they have been divided in two groups: (1) Recommendations; and (2) Observations and Findings. In the first group, results that have a direct application and implementation to design and construction are incorporated; in the second group, general theoretical results and observations are included. While all conclusions and recommendations are equally important, this classification is intended to provide additional insight to the conclusions reached.

Recommendations

(1) Local site conditions have a significant effect on ground accelerations and on the peak acceleration at the ground surface. The ground accelerations at the base rock are amplified in most of the sites examined in this study. The amount of amplification depends on the natural period of the soil profile and on the origin of the earthquake. This study reinforces previous conclusions in that the ground response is highly sensitive to local soil conditions. The methodology required to identify structures that require site-specific analysis is beyond the scope of this project. It should be determined either as part of the "Criteria for Selection of Primary Routes for the State of Indiana", or in a subsequent study.

(2) Site-specific studies of deep foundations should include ground response analyses. The amplitude of the input rock acceleration can be estimated using a deterministic approach with appropriate attenuation relationships such as the one considered in this study or using the peak ground acceleration on rock provided by the USGS in the seismic hazard maps. The USGS approach can be used for routine design; the deterministic approach should be used when the earthquake parameters fall outside the USGS scope (e.g. different seismic source, earthquake magnitude, etc.). The soil shear wave velocity V_s is best obtained from direct in situ measurements; there are a number of techniques than can be used for this purpose, such as seismic cross-hole or seismic down-hole tests. As an alternative, SPT and CPT tests can also be used because of the large body of past experience with these tests; although the

SPT and the seismic CPT test provide less accurate measurements than the seismic tests, they have the advantage that they can be performed rapidly and they provide penetration resistance with depth that can be correlated to parameters other than V_s, such as strength and index properties.

(3) Site-specific analyses must take into account the inertial loads from the superstructure as well as the deformation of the pile due to the response of the surrounding soil. If the soil profile contains soil layers that are liquefiable, a detailed analysis should be required to address the safety of the foundation if liquefaction occurs. Recommendations to the designer should be included in the body of the report.

(4) Small diameter ($D < 0.6$ m) concrete piles should be avoided in Southern Indiana.

Observations and Findings

(1) Soil liquefaction is possible even in the case of an earthquake originating in the more distant New Madrid Seismic Zone. This is consistent with evidence of paleoliquefaction as a result of prehistoric earthquakes. Given that pile foundations are susceptible to severe damage in cases of liquefaction and lateral spreading, the effects of these phenomena should be investigated on bridge foundations relying on piling. Lateral spreading is likely to occur in most of the bridges crossing rivers in southern Indiana due to the possible inclination of the ground surface and to the presence of liquefiable non-liquefiable layers sloping towards the river.

(2) Ground accelerations higher than 0.25g are capable of producing damage to concrete piles with diameters ranging from 0.3 to 0.6 m if no liquefaction occurs. Damage to large diameter piles ($D > 0.6$ m), in the absence of liquefaction, is reported only when the peak ground acceleration (PGA) exceeds 0.7g. Thus, it may be concluded that in southern Indiana, where the estimated PGA is less than 0.7g, large diameter concrete piles at sites with low liquefaction potential are unlikely to suffer damage.

(3) The practice in Indiana of installing steel piles reduces significantly the potential of damage to the piles during an earthquake, especially in sites where liquefaction or lateral spreading are not likely to occur. SEC piles appear to have also a beneficial effect, although this observation is based on a limited number of cases and more investigation is required to draw a more definite conclusion.

(4) For existing concrete pile foundations that are susceptible to heavy or severe damage, excavation and placement of a steel jacket on the upper part of the pile can be considered as a retrofitting and strengthening technique. The thickness of such a casing, as well as the necessary length should be determined on a case-by-case basis. However, the effect of steel casing on the performance of SEC piles needs to be investigated in detail to verify the findings of the present study. Moreover, the installation of additional piles connected to the superstructure by expanding the pile cap can be applied in southern Indiana. The additional piles must be capable of sustaining the earthquake loads efficiently. Specific retrofit treatment is outside of the scope of this study. It should be evaluated either as part of the "Criteria for Selection of Primary Routes for the State of Indiana", or in a subsequent study.

(5) The conclusions from this investigation rely on a number of assumptions concerning the magnitude and probability of occurrence of an earthquake from the Wabash Valley Fault System or from the New Madrid Seismic Zone. The results suggest that an earthquake from the Wabash Valley Fault System (WVFS) is the most critical for Southwestern Indiana. As a consequence, the ground accelerations found in this research are higher than the accelerations currently considered for design in this region. However, it is not the goal of this project to determine what accelerations should be taken for design in Indiana. It is recommended that further research should be undertaken to determine such accelerations.

LIST OF REFERENCES

Atkinson G. and M. Boore [1987]. "Stohastic Prediction of Ground Motion and Spectral Response Parameters at Hard-Rock Sites in Eastern North America". Bulletin of the Seismological Society of America, Vol. 77, No. 2, pp. 440-467.

Atkinson G. and M. Boore [1990]. "Recent Trends in Ground Motion and Spectral Response Relations for North America". Earthquake Spectra, Earthquake Engineering Research Institute, Vol. 6, No. 1, pp. 15-32.

Atkinson G. and M. Boore [1995]. "Ground Motion Relations for Eastern North America". Bulletin of the Seismological Society of America, Vol. 85, No. 1, pp. 17-30.

Atkinson G. and M. Boore [1997]. "Some Comparisons Between Recent Ground-Motion Relations". Seismological Research Letters, Vol. 68, No. 1, pp. 24-40.

Boore, D. and W. Joyner [1991]. "Estimation of Ground Motion at Deep-Soil Sites in Eastern North America". Bulletin of the Seismological Society of America, Vol. 81, No. 6, pp. 2167-2183.

Campbell, K. [1981]. "A ground motion model for the central United States based on near-source acceleration data". Earthquakes and Earthquake Engineering--Eastern United States [proceedings], Ann Arbor, Michigan, Vol. 1, pp. 213-232.

Chaudhuri, D., S. Toprak and T. D. O'Rourke [1995]. "Pile response to lateral spread: a benchmark case". Lifeline Earthquake Engineering, Proceedings of the Fourth U.S. Conference, American Society of Civil Engineers, New York, pp. 755-762.

Dahle, A., H. Bungum, L. Kvamme [1990]. "Attenuation Models Inferred from Intraplate Earthquake Recordings". Earthquake Engineering and Structural Dynamics, Vol. 19, pp. 1125-1141.

Dobry, R. and G. Gazetas [1986]. "Dynamic Response of Arbitrary Shaped Foundations". Journal of Geotechnical Engineering, ASCE, Vol. 112, No. 2, pp.109-154.

Finn, W. D. L., T. Thavaraj and G. Wu [1996]. "Seismic Analysis of Pile Foundations: State-of-Art". Proceedings, Eleventh World Conference on Earthquake Engineering, Elsevier Science Ltd. Paper No. 2073.

Fujii, S., N. Isemoto, Y. Satou, O. Kaneko, H. Funahara, T. Arai, K. Tokimatsu [1998]. "Investigation and Analysis of a Pile Foundation Damaged by Liquefaction during the 1995 Hyogoken-Nambu Earthquake". Special Issue of Soils and Foundations, Japanese Geotechnical Society, pp. 179-192.

Fujii, S., M. Cubrinovski, K. Tokimatsu and H. Tadashi [1998]. "Analyses of Damaged and Undamaged Pile Foundations in Liquefied Soils during the 1995 Kobe Earthquake". *Geotechnical Earthquake Engineering and Soil Dynamics III*, Geotechnical Special Publication 75, ASCE, Reston, Virginia, Vol. 2, pp. 1187-1198.

Fujii, S., H. Funahara and J. Yamaguchi [1996]. "Numerical Analysis of Damaged Piles due to Soil Liquefaction during Hyogoken-Nambu Earthquake". Proceedings, Eleventh World Conference on Earthquake Engineering, Elsevier Science Ltd. Paper No. 329.

Green, R. K., J. I. Sun, H. M. Lelio, R. C. Quittmeyer, T. C. Statton and T. L. Cooling [1991]. "Development of Probabilistic Seismic Hazard Map for Evaluating the Seismic Vulnerability of Bridges in Illinois". Proceedings of the Fourth International Conference on Seismic Zonation, Earthquake Engineering Research Inst. Vol. II, Oakland, California, pp. 761-768.

Hwang, H. and J-R. Huo [1997]. "Attenuation relations of ground motion for rock and soil sites in eastern United States". Soil Dynamics and Earthquake Engineering, Elsevier Science, Vol. 16, pp. 363-372.

Imai, T. and K. Tonouchi [1982]. "Correlation of N-value with S-Wave Velocity and Shear Modulus". Proceedings of the 2nd European Symposium on Penetration Testing, Amsterdam, pp.57-72.

Ishibashi, K. and X. Zhang [1993]. "Unified dynamic shear moduli and damping ratios of sand and clay". Soils and Foundations, Vol. 3, No. 1, pp. 1129-1143.

Ishihara, K. [1997]. "Geotechnical Aspects of the 1995 Kobe Earthquake". Terzaghi Oration, Proceedings of the 14th International Conference on Soil Mechanics and Foundation Engineering, Hamburg.

Iwasaki, T. [1990]. " Summary Report on the Loma Prieta Earthquake of October 17, 1989". Proceedings of the 22nd Joint Meeting of the U.S.-Japan Cooperative Program in Natural Resources Panel on Wind and Seismic Effects, National Inst. of Standards and Technology, Gaithersburg, Maryland, pp. 363-374

Johnston, A. [1989]. "Moment Magnitude Estimation for Stable Continental Earthquakes". Seismological Research Letters, Vol. 60. No. 1, pp.13.

Karube, D. and K. Makoto [1996]. "Geotechnical aspects of the January 17, 1995 Hyogoken-Nambu earthquake: Damage to Foundations of Railway structures". Special Issue of Soils and Foundations, Japanese Geotechnical Society, pp. 201-210.

Kawamura, S., T. Nishizawa, T. Wada [1985]. "Damage to Piles due to Liquefaction Found by Excavation Twenty Years after Earthquake". Nikkei Architecture, Tokyo, Japan, pp. 130-134.

Kayabali, K. [1993]. *Earthquake Hazard Analysis for the City of Evansville, Indiana.* Ph.D. Thesis, Purdue University, West Lafayette, IN.

Kishida, H., H. Hanazato and S. Nakai [1980]. "Damage of reinforced precast concrete piles during the Miyagiken-oki earthquake of June 12, 1978". Proceedings of the Seventh World Conference on Earthquake Engineering, Vo. 9, Istanbul, pp. 461-468.

Matsui, T. and K. Oda [1996]. "Geotechnical aspects of the January 17, 1995 Hyogoken-Nambu earthquake: Foundation Damage of Structures". Special Issue of Soils and Foundations, Japanese Geotechnical Society, pp.189-200

M. Mendoza and G. Auvinet [1988]. "The Mexico Earthquake of September 19, 1985 - Behavior of Building Foundations in Mexico City". Earthquake Spectra, Vol. 4., No. 4, pp. 835-851.

Mizuno, H. [1987]. "Pile Damage during Earthquake in Japan (1923-1983)". *Dynamic Response of Pile Foundations*, Geotechnical Special Publication, No. 11, ASCE, pp. 53-78.

Mizuno, H., M. Iiba, T. Hirade [1996]. "Pile Damage during 1995 Hyougoken-Nambu Earthquake in Japan". Proceedings of the Eleventh World Conference on Earthquake Engineering, Elsevier Science, paper No. 977.

Nakajima, H., H. Hayashi, K. Kosa [1996]. « Experimental study on the bearing capacity of cast-in-place concrete piles damaged by the Hanshin earthquake". Proceedings of the 28th Joint Meeting of the U.S.-Japan Cooperative Program in Natural Resources Panel on Wind and Seismic Effects, National Inst. of Standards and Technology, Gaithersburg, Maryland, pp. 441-449.

Nakayama, M., H. Masui and S. Yanagihara [1998]. "Analysis of Pile damage in Higashinada Sewage Treatment Plant during the Hyogoken-Nambu Earthquake". Proceedings, Third China-Japan-US Trilateral Symposium on Lifeline Earthquake Engineering, Kunming, China, pp. 189-195.

Nuttli, O. W. [1982]. "The Earthquake Problem in the Eastern United States". Journal of the Structural Division, ASCE, Vol. 108, No. ST6, pp. 1302-1312.

Nuttli, O. W. and R. B. Herrmann [1984]. "Ground Motion of Mississippi Valley Earthquakes". Journal of Technical Topics in Civil Engineering, 110(1), pp. 54-69.

Obermeier, S. F. [1998]. "Liquefaction evidence for strong earthquakes of Holocene and latest Pleistocene ages in the States of Indiana and Illinois, USA". Engineering Geology 50, pp. 227-254.

Obermeier, S. F. and E. C. Pond [1999]. "Issues in Using Liquefaction Features for Paleoseismic Analysis". Seismological Research Letters, Vol. 70, No. 1, pp. 34-58.

Oh-Oka, H., M. Fukui, M. Hatanaka, J. Ohara, S. Honda [1998]. " Permanent Deformation of Steel Pipe Piles Penetrating Compacted Fill at Wharf on Port Island. Special Issue of Soils and Foundations, Japanese Geotechnical Society, pp. 147-162.

Okahara, M., M. Nakano and Y. Kimura [1996]. "Analysis of Damaged Foundations of Highway Bridges in the 1995 Hyogo-ken Nambu Earthquake". Wind and Seismic Effects, Proceedings of the 28th Joint Meeting of the U.S.-Japan Cooperative Program in Natural Resources Panel on Wind and Seismic Effects, National Inst. of Standards and Technology, Gaithersburg, Maryland, pp. 205-222

Ovando-Shelley E., M. Mendoza and M. Romo [1988]. "The Mexico Earthquake of September 19, 1985 - Deformability of Mexico City Hard Deposits Under Cyclic Loading". Earthquake Spectra, Vol. 4., No. 4, pp. 753-769.

Sasaki, Y., J. Koseki, K. Shioji, M. Konishi, Y. Kondo, T. Terada [1997]. "Damage to Higashinada sewage treatment plant by the 1995 Hyogoken-Nambu earthquake". Seismic Behavior of Ground and Geotechnical Structure, Balkema, Rotterdam, pp. 297-298

Seed, H. B., K. Tokimatsu, L. F. Harder and R. M. Chung [1985]. "Influence of SPT Procedure in Soil Liquefaction Resistance Evaluation". Journal of Geotechnical Engineering, ASCE, Vol. 111, No. 12, pp. 1425-1445.

Tamura, C. [1985]. "Outline of Damages from Nihonkai Chubu Earthquake of 1983". Civil Engineering in Japan, 24, pp. 149-171.

Tazoh, T., K. Shimizu and T. Wakara [1987]. "Seismic Observations and Analysis of Grouped Piles". *Dynamic Response of Pile Foundations*, Geotechnical Special Publication, No.11, ASCE, pp. 1-20.

Tokimatsu, K., and A. Yoshiharu [1998]. "Geotechnical aspects of the January 17, 1995 Hyogoken-Nambu earthquake: Effects of Liquefaction-Induced Ground Displacements on Pile Performance in the 1995 Hyogoken-Nambu Earthquake". Special Issue of Soils and Foundations, Japanese Geotechnical Society, pp. 163-177.

Tokimatsu, K., M. Mizuno and M. Kakurai [1996]. "Geotechnical aspects of the January 17, 1995 Hyogoken-Nambu earthquake: Building Damage Associated with Geotechnical Problems". Special Issue of Soils and Foundations, Japanese Geotechnical Society, pp. 219-234.

Tokimatsu, K., H. Oh-Oka, K. Satake, Y. Shamoto, Y. Asaka [1998]. "Effects of Lateral Ground Movements on Failure Patterns of Piles in the 1995 Hyogoken-Nambu Earthquake". *Geotechnical Earthquake Engineering and Soil Dynamics III*, Geotechnical Special Publication 75, ASCE, Reston, Virginia, Vol. 2, pp. 1175-1185.

Tokimatsu, K. and Y. Asaka [1998]. "Effects of Liquefaction-Induced Ground Displacements on Pile Performance in the 1995 Hyogoken-Nambu Earthquake". Special Issue of Soils and Foundations, Japanese Geotechnical Society, pp. 163-177.

Wheeler, R. and A. Johnston [1992]. " Geologic Implications of Earthquake Source Parameters in Central and Eastern North America". Seismological Research Letters, Vol. 63, No. 4, pp. 491-514.

Yasue, T., T. Iwasaki, Y. Sasaki, H. Asanuma, T. Nakjima [1983]. "Report of the Urakawa-oki earthquake of March 21, 1982". Wind and Seismic Effects, Proceedings of the 14th Joint Panel Conference of the U.S.-Japan Cooperative Program in Natural Resources, U.S. National Bureau of Standards, Washington, D.C., pp. 325-342.